BRIDGE APPROACH SLAB ANALYSIS AND DESIGN INCORPORATING ELASTIC SOIL SUPPORT

A Thesis presented to

the Faculty of the Graduate School

at the University of Missouri-Columbia

In Partial Fulfillment

of the Requirements for the Degree

Master of Science

---

by

SHUANG MA

Dr. Vellore S. Gopalaratnam, Thesis Supervisor

DECEMBER 2011

The undersigned, appointed by the Dean of the Graduate School,

have examined the dissertation entitled

BRIDGE APPROACH SLAB ANALYSIS AND DESIGN INCORPORATING ELASTIC SOIL SUPPORT

Presented by

Shuang Ma

A candidate for the degree of

Master of Science

And hereby certify that, in their opinion, it is worthy of acceptance.

_____

Professor Vellore Gopalaratnam

_____

Professor P Frank Pai

_____

Assistant Professor Sarah L. Orton

ACKNOWLEDGEMENTS

First and foremost, I am heartily thankful to my advisor, Dr. Vellore S. Gopalaratnam, who has given me invaluable guidance throughout my graduate studies. Without his instruction and encouragement, I would not have learned the art of studying, researching and teaching through my unique experience as an international graduate student in the United States.

I would like to acknowledge Missouri Department of Transportation, the Department of Civil and Environmental Engineering at the University of Missouri-Columbia, National University Transportation Center and Missouri University of Science and Technology for the funding on this project and on my graduate studies. I would also like to acknowledge Prof. Ganesh Thiagarajan, Sheetal Ajgaonkar and Reza Ghotbi from the University of Missouri-Kansas City for their cooperation and efforts to fulfill this task.

I would like to thank Dr. P Frank Pai and Dr. Sarah L. Orton for serving on my thesis committee and their suggestions are very helpful

I would like to thank all my fellow students, especially group members Manikya B. Gudimetla and Ravi Sankar Chamarthi who have shared with me an eagerness to learn, collaborate and make progress.

Finally, I give deep gratitude to my parents, my sister and my fiancé for their everlasting love and support throughout my life.

LIST OF CONTENTS

LIST OF TABLES

LIST OF FIGURES:

BRIDGE APPROACH SLAB ANALYSIS AND DESIGN INCORPORATING ELASTIC SOIL SUPPORT

Shuang Ma

Dr. Vellore S. Gopalaratnam, Thesis Supervisor

ABSTRACT

The development of equations necessary for the analysis of finite bridge approach slabs (BAS) on elastic soil support is reported in this thesis. Results are compared for moments and shear forces governing the design for a wide range of values of soil elastic modulus ranging from dense sand to very loose sand. Results from systematic studies assuming wash out of soil support are also presented using a customized uniaxial finite-difference model. The influences of wash-out length and location have been discussed. Moreover, the functions of sleeper slab at the pavement end of the conventional design are studied. It is replaced by a modified end-section reinforcement detailing to provide enhanced local two-way action, providing increased flexural rigidity in the direction transverse to the traffic direction. An Excel-based VBA program is developed for application of designing bridge approach slab incorporating partial elastic soil support. Additionally, a biaxial finite-difference model is developed using MATLAB for better understanding the performance of BAS in both longitudinal and transverse directions. Results from uniaxial and biaxial solutions are compared and discussed. Initial construction cost of this new design alternative is computed and presented to demonstrate that the BAS designed with consideration of elastic soil support results in a cost-effective design. Life cycle costs too are competitive if only agency costs are included, for rural traffic demands, this design is the most cost-effective alternatives among those considered.

CHAPTER 1 INTRODUCTION

1.1 Motivation for the Project

A bridge approach slab is the transition component between bridge and pavement. The bridge end is supported on the abutment which in turn is supported on hard rock bed while pavement lays on the shallow foundation on the natural embankment. The settlements of the two different supporting systems can be largely different causing potential problems in the performance of the bridge approach slab.

Figure 1-1 Bridge and bridge approach slab

Problems have been reported in field observations for many years. Drivers experience a bump when they exit many bridges because the slab does not allow smooth transition as intended. As the curvature of slab changes, the slope difference between bridge deck and the slab is inevitable. The settlement of embankment soil beneath the slab is

another potential problem. Since geographic characteristic near bridges often make soil more saturated than normal, inefficient drainage may cause large water pressure in embankment and washout of soil as well. Along with the consolidation of foundation soil, settlement will increase in time. It aggravates the bump and also causes undesirable cracking in the bridge approach slab.

Millions of dollars are spent yearly on repairs to lift slabs, reinforce soil embankments, seal cracks, and replace drainage systems. Traffic is stopped during this construction, which adds to the total cost of bridge approach problems. Missouri Department of Transportation initiated this project to optimize the design of bridge approach slabs and develop cost effective solutions to this problem.

1.2 Significance of the Investigation

Conventional design of typical bridge approach slabs which Missouri and other states follow simulates a strip of slab as a simple supported beam at the bridge abutment end and pavement sleeper slab end without considering soil support between the two ends. It is a conservative design based on assumption that soil beneath slab does not make any contribution to support the slab or that all of soil is washed away due to erosion. Since soil is not accounted in design, the requirements for embankment condition usually vary from state to state based on local experience. Although the fact that embankment condition plays an important role is well known, few states have implemented the soil supported approach slab into design, and there has been an

alarming lack of research on finding an effective design method for approach slabs incorporating soil support.

This thesis gives solutions incorporating a combination of structural, geotechnical and hydrological aspects necessary to adequately address the bridge approach problems of design. This thesis researched alternatingly to develop an indirect solution to the "bump" problems from a structural perspective. The relation between soil condition and design forces of approach slab are established herein and utilized to demonstrate the superiority of bridge approach slabs (BAS) designed incorporating soil elastic soil support. Even with significant soil washout, this thesis' design is cost effective compared to all the current alternatives.

For design engineers, this thesis offers a user-friendly MS Office Excel-based design aid that directly and quickly incorporates elastic soil support while designing BAS.

1.3 Objectives

The main goal of this thesis is to develop an optimized structural design method for bridge approach slab incorporating elastic soil support. The detailed objectives are as follows:

1. **Develop the analytical model of the optimized BAS incorporating soil support.** Through derivation from governing differential equation, develop an analytical model of BAS with continuous elastic soil support under symmetric load configurations. Discuss the correlation between soil stiffness, slab geometry, internal forces and required reinforcement with data gathered from analytical solutions.

2. **Investigate BAS subjected to potential soil washout and settlement of pavement end support.**

Apply finite difference method on the uniaxial bending model of BAS using Excel to make implementation of the model user friendly. Investigate effects of soil washout by changing defined variable length of washout, location of washout and location of tandem, followed by deriving general influence charts of soil conditions and internal forces of BAS. Develop solutions that allowed for the potential settlement (yielding) of the sleeper slab at the pavement end.

3. **Conduct the finite element analysis of biaxial bending of the BAS.**

For a better understanding the actual stress state in BAS, conduct the analysis of biaxial bending of BAS using MATLAB-based finite element program with a view to compare it to results from the uniaxial bending solutions observed earlier. Study the results from the biaxial analysis and results that change the internal forces in the approach slab.

4. **Implement the analysis procedure into practical design in a user-friendly interface.**

Develop Excel VBA program that contains the comprehensive design procedure for easy implementation of the design of soil supported BAS including parametric washout studies as well.

1.4 Thesis Organization and General Approach

Chapter Two covers a comprehensive literature review including reviews of projects from states' "Departments of Transportation" and public domain reports, papers and technical notes.

Chapter Three focuses on the analytical solution for finite and infinite length slabs subjected to symmetrical uniform distributed load and concentrated load obtained using AASHTO BAS design guidelines.

Chapter Four describes the use of finite difference method both for uniaxial bending and biaxial bending solutions. Finite size models were developed to study unsymmetrical soil conditions like existing voids under the slab near the abutment and also pavement end support condition. Excel worksheet with VBA program embedded and MATLAB program were utilized to conduct exhaustive case studies. Investigation of variations in deformation patterns, internal moments and shear forces, and type of pavement end support is carried out.

Chapter Five includes a cost analysis of bridge approach slabs. Chapter Six includes conclusions from thesis research while addressing limitations and possible future work.

CHAPTER 2 BACKGROUND INFORMATION AND LITERATURE REVIEW

Previous researchers have completed numerous studies about how to improve performance of bridge approach slabs identifying many problems identified with BAS performance. Briaud (1997) estimated $100 million is expended for annual repairs on bridge approach slabs by DOTs nationwide. Many state DOTs have devoted effort to improving approach slabs for better management of transportation.

2.1 Performance of Bridge Approach Slab

The primary purpose of using approach slabs is to provide a smooth ride at the transition region of bridge and pavement, according to 81% of the respondents from state DOTs in a survey conducted by Hoppe (1999). The survey also revealed that reducing impact on backwall and enhancing drainage control ranked second and third in importance when it came to discussing BAS advantages, while BAS disadvantages included high initial construction cost, maintenance related costs due to settling, staged construction and increased construction time.

Although a bridge approach slab is supposed to be a smooth transition slab, it does not perform like that especially with age. It is frequently observed that passengers feel uncomfortable when they drive through the end of bridge or “bump” zone. This has been attributed to differential settlements between abutment on the pile and pavement on the natural foundation. In turn, the bump has been said to cause differential

settlement by increased impact loads on the bridge deck. The bump is due to an abrupt change in slope. Under a severe condition, it can also be a threat to driver's lives rather than a merely uncomfortable experience. About 25% of bridge approach slabs suffer from the bump problem according to a report by Briaud (1997). In a drive-by survey by Long (1998) in Illinois, a significant differential movement was observed on 27% of 1181 approaches. In the Hoppe survey (1999), more than half of the respondents believed that differential settlement brings serious maintenance problem. To evaluate bump performance of bridge approach slabs, some criteria have been established. Long (1998) suggests a settlement less than 50 to 75 mm or a slope less than 1/200 of approach slab can satisfy riding comfort for new construction, while remedial measures should be taken when the gradient is equal to or greater than 1/100 to 1/125. Zhang's (2007) research shows that allowable slope of approach slab should be determined considering running speed of vehicles and length of slab. In a comprehensive study in Iowa by White (2007), an International Roughness Index and profile measurements were employed to evaluate the riding quality of approach slab, which showed a two times higher IRI value at approach transition than on the adjacent pavement.

Besides bump problem, cracks are often observed at bridge approach slab sites, causing another concern about workability. New Jersey reported severe transverse structural cracking existing on a number of approach slabs under heavy impact load and inadequate soil condition, as reported by Nassif (2003). Chen (2006) conducted a failure analysis for Texas DOT and observed a severely cracked approach slab and

ruptured MSE wall that was leaking embankment sand. James(1990) stated that cracking is frequently observed on backwalls of concrete reinforced abutment in Texas.

2.2 Reasons for Failure of Bridge Approach Slab

Previous investigations into bridge approach slabs highlight it as a complicated problem related to soil condition, drainage issues, abutment type, expansion joints and pavement. In a Washington State Transportation Center report written by Kramer (1991), differential settlement was cited as the most common source of bridge approach problems. Differential settlement has many causes:

a) Compression of natural foundation soil which include primary consolidation, time-dependent secondary consolidation and creep under constant level of shear stress.
b) Compression of embankment soil that results from distortion movement or creep and volume change along with variation of density, gradation, plasticity and environment.
c) Local compression at bridge pavement interface which may be caused by inadequate compaction at abutment, bad drainage system, rutting/distortion of pavement, traffic loading like tire pressure, and thermal bridge movement when expansion joints do not perform their function well.

Similar findings were reported from a visual survey in Illinois carried out by Long (1998). He addressed six main causes of differential movement at bridge approach interface: 1) local compression or erosion of materials at the approach embankment-

abutment interface; 2) a broken approach slab; 3) compression of foundation soil; 4) compression or internal erosion of embankment soils; 5) poor construction grade control; 6) areal distortion of foundation soils caused by mine subsidence or other areal mechanisms.

Bump and differential movement do not exist because of only one factor. Most observed problems have causes that affect each other. For instance, erosion of embankment materials can lead to less support from soil and thus more settlement of bridge approach, while settlement further causes more local compression and washout. The research work reported by Briaud (1997) points out that the bump problem can be magnified by the following characteristics:

a) High embankment fill;
b) Pile supported abutment;
c) High average daily traffic;
d) Soft natural silt soil foundation;
e) Heavy rain storms;
f) Extreme freeze-thaw cycles;
g) Steep approach gradients

He also demonstrated that settlement of bridge approach slabs are mainly attributed to poor construction practices such as:

a) not compacting embankment fill well and not expecting compression of natural foundation;

b) providing inefficient drainage system causing voids to develop beneath the approach slab following washout of embankment fill;

c) not placing proper expansion joints which lead to abutment movement due to pavement expansion with increase in temperature.

The following schematic highlights explanation the observed problems and their possible causes in bridge approach slab.

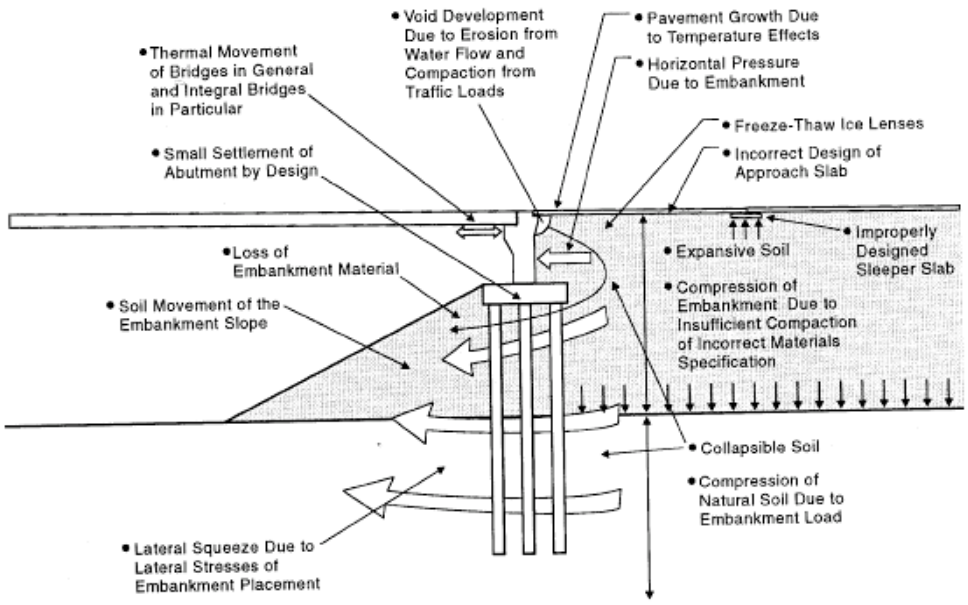

Figure 2-1 Cause of Bump at Bridge Approach Slab by Briaud (1997)

A report from Kentucky Transportation Center prepared by Dupont (2002) covering a review of reports and papers concurred with previous findings. The author conducted an evaluation of current practices related to settlement of bridge approach slab and divided them into five categories:

1) Approach embankment foundations
2) Approach embankment
3) Approach slab
4) Bridge abutment type
5) Approach drainage

Dupont (2002) states that foundation soil is the most important factor leading to settlement of bridge approach slabs and severe problems always occur at those sites with compressible cohesive soil like soft clay and silt clay which would exhibit a time dependent compression pattern. Embankment material also plays a key role, but the way of compaction will determine the settlement potential of the embankment. He mentioned that design of approach slab involves sufficient reinforcement and assumption of unsupported length to ensure the slab can undertake specific loads. And it is essential to develop effective drainage by not letting water seep between bridge slab and approach slabs; otherwise it will result in erosion of soil and void development.

Field investigation of bridge approaches (conducted by White (2007) and supported by Iowa DOT) revealed common mistakes in bridge approach practices. The observations includes: void development beneath bridge approach in one year of construction because of insufficient backfill moisture control followed by soil collapse; badly sealed joints by flexible foam and recycled tires leading to much less movement than the design width; poor water management and thus failure of slope protection and exposure

of H-pile; soil blocked by dry collapsed sub drains; asphalt overlays on approach slabs showing signs of distress and continued settlement.

2.2.1 Compression of Embankment and Foundation Soil

It is inevitable that foundation soil will endure consolidation before and after construction that includes initial and primary consolidation and secondary time-dependent consolidation/creep as well. In some situations, consolidation of foundation can be the major cause of BAS settlement. Long (1998) found that a 150mm to 220 mm displacement of an approach slab occurred one and a half years after it was built, which was believed to a consequence of problematic peat layer 12 m deep from top of embankment. Usually, surcharge is undertaken to initiate the major consolidation but secondary consolidation will still happen due to its natural properties.

The embankment/backfill material properties and size gradation are sometimes neglected in design and construction, leading to severe bump problems. From the test of soil boring carried out by Seo (2002) at two bridge sites in Texas, it was observed that embankment fill of sandy and silt clay, and clay resulted in poor performance of the approach slabs. On one bridge site, inadequate compaction was noticed due to human error. Abu- Hejleh (2006) found that compressive fill material like loose sand, organic and soft clay will exhibit a large deformation due to creep under vehicle load. . His studies also proved that a granular uniform fill material is susceptible to vibration-induced time dependent deformation. At the same time, it is known that well graded embankment with less fine sand will be resistant to soil washout. Hoppe (1999)

stated that the percentage passing No. 8 sieve should be limited to 60% so that soil erosion can be reduced. His argument also addressed that granular backfill can cause high soil collapse when the moisture ranges from 3% to 7% while porous material will not collapse at any moisture level. Therefore, moisture content should be specified when placing backfill material. However, it is a fact that soil near abutment will absorb more water than soil far away as stated by Seo (2002), leaving soil with high water content, low strength and high compressibility.

Moreover, Briaud (1997) considered the height of embankment as a critical factor in generating differential settlement. Seo (2002) concurred and expected that settlement of embankment is proportional to the height of embankment.

2.2.2 Expansion Joints and Growth of Pavement

Lenke (2006) conducted a field evaluation of 17 bridges in New Mexico and noted that several of them had poorly maintained expansion joints on the departure end of the bridges, which was believed to contribute to the bump. Mekkawy's (2005) studies brought out that insufficient sealed expansion joints can lead to soil erosion due to water infiltration.

James (1990) observed cracks and damage on the abutment wall and on the shoulder of bridge approach. His investigation proved the longitudinal growth of the reinforced concrete pavement attributes to observed distress. Two mechanisms were developed to explain the behavior of pavement: thermal ratcheting and chemical reaction. This was borne out by Chen (2006) who discovered that pavement constructed with siliceous

gravel is prone to severe cracks and spalling due to a higher expansion coefficient than that of limestone. He stated that if contraction/expansion is not well accommodated, the bridge approaches can exhibit significant cracking. Therefore, performance of bridge approach slabs is associated with expansion joints because of their function to release stress from the superstructure.

If the seal of an expansion joint is installed improperly or maintained infrequently, there is no room for structure to expand because of the debris collected in the joint (Ha, 2002). Therefore effectiveness is lost at the expansion joint as observed mostly in newly constructed bridges (Kramer, 1991).

2.2.3 Design of Approach Slab

Hoppe (1999) investigated that the typical size of the approach slab that most states use is 6.1 m (20 ft) long with a variation from 3 m (10 ft) to 12.2 m (40 ft) and 0.3 m (12 in) deep with a variation from 0.28 m (9 in) to 0.38 (15 in). Since there is no standard specification for bridge approach slab, the design often depends on local experience. BAS are almost always designed as a simply supported beam (one way slab finite strip analysis). A reasonable design approach that combines comprehensive survey of site, thorough understanding of soil conditions and empirical knowledge can mitigate bump and cracking.

A two-span approach slab in Texas was physically modeled using BEST devices by Seo (2002) and the result showed that settlement of a two-span slab was two times as high as that of one span under same condition. Dupont (2002) believed a longer

approach slab could minimize problems as the slope is decreased for same settlement. Nassif (2003) and Roy (2007) both addressed the importance of adequate thickness of the bridge approach slab in their studies. A thin approach slab with low capacity is more prone to cracking according to their investigations.

2.2.4 Drainage and Erosion

Mekkawy (2005) did an extensive field investigation in six Iowa districts to identify bridge approach slab problems. It was observed 40% of the inspected bridges had poor drainage and severe soil erosion due to ineffective sub drain and end drain systems and water infiltration through insufficiently sealed expansion joints. Water that seeps into embankment and abutment backfill can lead to washout of soil, and development of voids under slab as a sequence.

According to Long (1998), drainage is a major concern in maintenance which always affects bridge approach performance. Poor drainage in base course and upper embankment can not only undermine support of approach slab, but can also bring swelling or collapse as the soil volume changes due to freeze-thaw and excessive pressure to abutment backwalls. In his survey, water runoff was observed seeping into backfill and soil was washed through seams on the concrete slope facing.

Measures need to be taken to ensure better drainage. Hoppe's (1999) survey summarized typical provisions for drainage of bridge approaches in most states which include plastic drainpipes, weep holes in the abutment and use of granular, free-draining fill. Some states use geosynthetic material fabrics and geocomposite

drainage panels. Briaud (1997) suggested that surface water should be directed away from bridge joints, abutment areas and slopes. He also suggested design of separating pavement curb and wing wall so that water from pavement will not enter the joint between wing wall and edge of pavement. Furthermore, wrapping embankment using geotextile fabrics can reduce soil erosion and fines infiltration.

2.2.5 Abutment

Abutments are classified into two types based on connection between bridge slab, abutment and approach slab: 1) integral bridge abutment typically with doweled connection and 2) non-integral abutment with expansion joints (Roman, 2002). Integral abutment has a low construction and maintenance cost and is supposed to resist lateral forces caused by expansion of bridge deck and pavement. Non-integral abutment is subjected to drainage issues including proper sealing and maintenance of expansion joints. From the perspective of structural forms, Dupont (2002) summarized four types of BAS for non-integral abutments:

a. closed abutment with high wing wall subjected to high earth pressure,

b. perched or stub abutment with smallest resistance and least construction material,

c. spill-through abutment allowing transfer of lateral forces through columns, and

d. mechanically stabilized abutment constructed atop mechanically stabilized backfill.

Performance of bridge approach slab has also been attributed to the types of abutment. Puppala (2008) revealed Texas DOT attributes bump problem partly to inaccessibility to compact embankment near abutment based on years of experience with non- integral

abutments. In investigation conducted by James (1990), many bridges exhibited tilting and cracking at the abutment. His research shows distress of approach slab results from vertical movement, lateral movement and tilting of abutment. Soil erosion, swelling or settlement can generate forces and movement of abutment, resulting in rotation and cracks in abutment. Movement of the abutments has a direct impact on the adverse performance of the BAS.

2.3 Alternatives for Bridge Approach Slabs

Conventional bridge approach slabs currently used by most states has a constant thickness cast in place reinforced concrete slab. Due to high construction and maintenance cost, a number of different structural slabs have been investigated or examined to achieve better performance at lower cost.

1. Ribbed approach slab

Shi (2005) studied a stiffer slab also called ribbed approach slab under a prescribed settlement. The slab was 40 ft long and had three alternatives with different beam spacing which were modeled using finite element method to optimize the design. His research showed thickness of slab can be reduced in the design of ribbed slab compared to flat slab, saving construction material but increasing flexural stiffness. It was demonstrated that ribbed slab with beams spaced 32 ft apart is good for a small settlement while slabs with beam spacing at 12 ft and 16 ft have adequate strengths for larger differential movement.

2. Pile supported slab

Severe settlement of bridge approaches were frequently observed in southern Louisiana due to its poor geological characteristics. Foundation soil there primarily consists of soft compressive cohesive or loose granular soil and thick organic clay exists near ground surface. For the sake of gradual and smooth transition, bridge approach slabs are built on a set of piles with varying lengths. Settlement with longest pile near abutment was the smallest while that with shortest pile at pavement end was the largest. This provides for a smooth transition. Bakeer (2005) conducted a field evaluation on the performance of pile supported approach slabs. Differential settlement still exists mainly because of embankment-pile downdrag interaction and longer piles can be selected on a site-specific basis.

3. Precast prestressed approach slab

Iowa Department of Transportation experimented with a precast prestressed approach slab system on Highway 60 in 2006 to evaluate and demonstrate this potential solution for bridge approach. Merritt's (2007) report on the project included details of development, design, construction and field implementation. The major advantage of precast prestressed approach slab is rapid construction followed by improved durability, reduced slab thickness, and longer permissible slab lengths between expansion joints. For a site that has unpredictable soil condition and erosion, precast prestressed approach slab is superior because it is designed as an "approach bridge" that does not rely on soil support beneath the slab. This experimental study highlighted the adaptability in bridge construction of a precast prestressed approach slab.

4. Sloped approach slab

Wong (1994) brought up the sloped approach slab as a replacement for slabs constructed at a horizontal position to solve bump problem at bridge end. He found that constructing the slab at an angle to horizontal so that it slopes down beneath the pavement can provide gradual surface deformation, which was observed from a small scale experiment conducted in laboratory. For the three slabs with different slopes tested, a rapid change of deformation was observed. The horizontal slab deformed the most; the slab oriented at 5 degrees exhibited medium surface deformation; the sloped slab oriented at 10 degrees exhibited the least deformation. It was believed the gradual changing thickness of base course material under the approach slab had an effect on smooth profile under repeated vehicle loading.

5. Fiber-reinforced approach slab

Longitudinal and transverse cracks are often detected as a result of distress of bridge approach slab. To find out an alternative of reinforcement, a full size experiment including the performance of a bridge approach slab was conducted by Chai (2009). In addition to conventional steel reinforcement, a double-layer pultruded fiber-reinforced polymer grating and glass fiber-reinforced polymer rebars were used in cast-in-place approach slabs as a side by side comparison. Although cracks were observed on all three slabs, the fiber-reinforced approach slabs exhibited smaller deflections and larger stiffness even after part of the soil had been washed away.

2.4 Advanced Backfill Material

Yeh (1995) did a full scale test of performance of bridge approach slab with three different backfill materials in Colorado. It was observed flowfill material, which also called low-strength material, exhibited less movement and better ride than expanded polystyrene and structural backfill.

1. Controlled low-strength material (CLSM)

CLSM is a mixed material that combines Portland cement, fly ash and other cementitious material, aggregates, water and chemical admixtures, air-entraining agents and foaming agents. In NCHRP's report (2008), CLSM was recommended in construction of highway and bridge approach embankment as well. The significant benefit of CLSM is to use local material including by-product, however, the cost is higher when it serves as an alternate to embankment soil.

Flowability of fresh CLSM makes it a desirable material for abutment backfill at a low labor cost without much compaction. Only one hour is required for hardening to achieve prescribed compressive strengths. And due to low compressibility and ease construction, using CLSM as embankment of bridge approach offers an efficient method to minimize differential settlement and bump problems. (NCHRP, 2008)

2. Deep cement mixing

Deep cement mixing is a widely used effective way to treat soft clay by forcing cement mix deep into the soil to form a solid column foundation. Lin (1997) presented an implementation of using deep cement mixing on bridge approach embankment to reduce differential settlement. The test results showed a significant reduction of

settlement and lateral movement of soft clay, and a short construction time for cement mixing columns to reach full design length. Experiment in laboratory also indicated that strength of soil-cement mixture varies with water content of natural soil and cement powder is an effective strengthening agent when water content is high.

3. Mechanical stabilized earth

Oregon Department of Transportation conducted an implementation of geotextile reinforcement in bridge approach slab embankment as recorded and discussed by Groom (1993). Benefits like reducing water infiltration, improving surface quality, and retarding vegetation growth in cracks were expected.

In Colorado, there's a growing practice for MSE backfill for a lower cost alternative to flowable backfill. The idea is to build a wall that can restrain lateral and vertical movement of backfill and form a gap between backfill and abutment, and eliminate pressure on abutment due to variation of soil. Geofabric material is used to wrap around the back face of abutment and geogrid reinforcement is added to backfill soil to stiffen it, which is believed to reduce differential settlement of bridge approach slab. Porous material was also selected to fill in embankment at some sites because of its high resistance to wetting induced softening/collapse and erosion. (Abu-Hejleh, 2006)

2.5 Maintenance and Repair

Even for a thoughtful design of approach slab incorporating extensive investigation of foundation soil, well compacted embankment and backfill with fully equipped drainage system, frequently planned maintenance is necessary to mitigate or prevent differential

settlement and bump that might happen after construction. Maintenance activity may involve cleaning of expansion joints, drainage of water in structure and replacing of ruptured drain pipe. If severe movement occurs, lanes need to be closed as steps are taken to repair the approach slab. Kramer (1991) reported that asphalt overlay on the distressed approach slab to ensure a smooth ride and mudjacking to lift the slab back to position were the two commonly used measures. Other mitigation methods for settled or broken approach slab were summarized by Puppala (2008) that includes replacement of deteriorated slab by prefabricated slab, and pressure grouting under the slab using urethane injections.

CHAPTER 3 ANALYTICAL MODEL AND DESIGN IMPLEMENTATION OF BAS-ES

3.1 Analytical Modeling of the Bridge Approach Slab

Considering soil support, the design moment of approach slab can be reduced compared to original simple supported slab. It is necessary to study how much the soil affects design. Previous work has been done by Robison and Luna (2004), who employed the finite element model in PLAXIS involving four stages of construction and loading. Two layers of soil, one for consolidation and one for immediate deformation, are built with soil parameters changing all the time. The model was successfully used to compare with observed deformation of bridge A6031 and A5843 in Missouri. Cai et al (2005) developed a three-dimensional finite element model (see Figure 3-1) to analyze the performance of bridge approach slab considering the partial soil support under given embankment settlement. Differential settlement at the pavement end of approach slab is assumed along with the linear settlement of embankment.

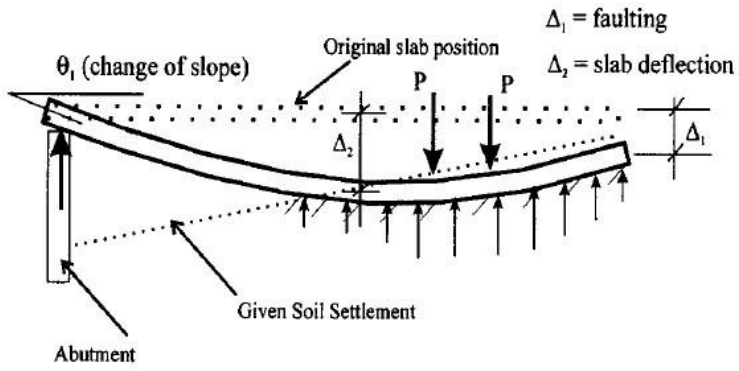

Figure 3-1 The finite element model of BAS under given embankment settlement studied by Cai et al (2005)

In this chapter, a strip of bridge approach slab is modeled as a simply supported beam with continuous soil support and no settlement at pavement end (see Figure 3-2). Solutions are obtained for settlement and internal forces. Additional variations on these primary design variables as well as more involved analytical models are discussed later in this thesis.

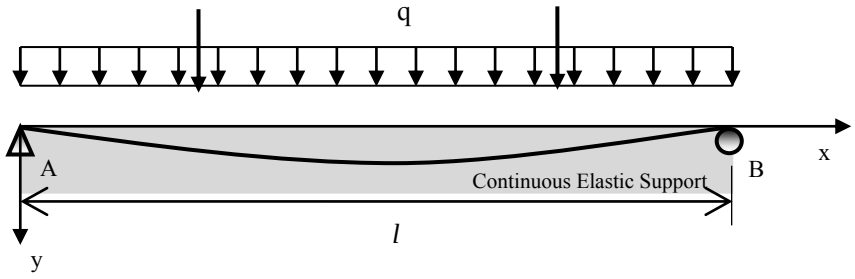

Figure 3-2 Diagram of BAS incorporating continuous elastic soil support

3.2 Governing Differential Equation and Homogenous Solution

The classical solution of a beam (a finite strip of a slab of unit width) on elastic support is developed here. This treatment is appropriate for the one-way bending dominant in the BAS. Consider a slab of an infinite length supported horizontally on an elastic medium (such as compacted fill of sand) and subjected to combinations of vertical concentrated forces and distributed forces (perpendicular to the axis of the slab), and concentrated moments. The action of these loads causes the slab to deflect, producing continuously distributed reaction forces, p (psi), due to the stiffness of the soil. It is assumed that these reaction forces are linearly proportional to the slab deflection, y (in)

and the elastic modulus of the soil (often also referred as soil modulus parameter, *k*, measured as psi/in or pci), i.e. $p = ky$. Consideration of the equilibrium of an infinitesimal length of the slab shown in Figure 3-3 allows derivation of the governing differential equation of the problem.

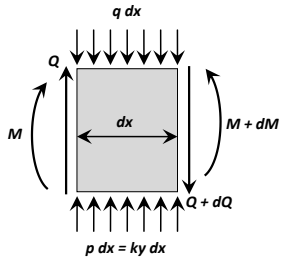

Figure 3-3 Equilibrium of an infinitesimal element from a slab on elastic support

From equilibrium of the vertical forces one can obtain:

$$\frac{dQ}{dx} = k\,y - q \qquad \text{(Eqn. 3-1)}$$

and, from the equilibrium of moment one can obtain:

$$Q = \frac{dM}{dx} \qquad \text{(Eqn. 3-2)}$$

Hence,

$$\frac{dQ}{dx} = \frac{d^2M}{dx^2} = k\,y - q \qquad \text{(Eqn. 3-3)}$$

Using the moment curvature relations, along with Eqns. 3-1, 3-2 and 3-3, one obtains the governing differential equation for a slab on continuous elastic support as:

$$EI\,\frac{d^4y}{dx^4} = q - k\,y \qquad \text{(Eqn. 3-4)}$$

where *EI* is the flexural rigidity of the slab. The homogeneous solution on Eqn. 3-4 (case where $q = 0$), can be obtained as:

$$y = Ce^{-\lambda x}(\cos\lambda x + \sin\lambda x) \qquad \text{(Eqn. 3-5)}$$

by making use of the observation that the deflection, y, is finite even as $x \to \infty$, and $(dy/dx)_{x=0} = 0$ (condition of symmetry), where,

$$\lambda = \sqrt[4]{\frac{k}{4EI}} \qquad \text{(Eqn. 3-6)}$$

Slab of infinite length subjected to concentrated force, *F*.*

Using the homogeneous solution one can readily obtain the deflection, moment and shear force solutions for a slab of infinite length subjected to a concentrated force, F (Figure 3-4)

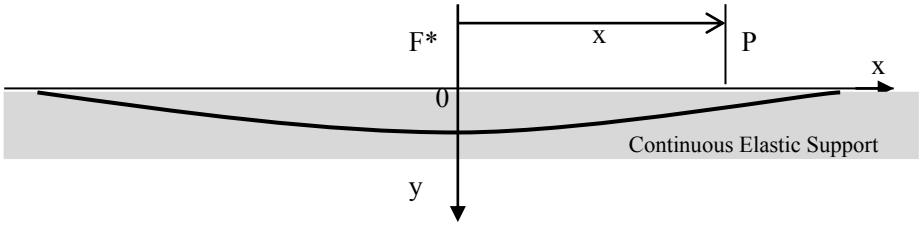

Figure 3-4 Slab of infinite length on continuous elastic support subjected to concentrated force F^*

For any point P ($x \geq 0$), the deflection, y, the slope, θ, the bending moment, M, and the shear force, Q for the case of loading shown in Figure 3-4 are given by:

$$\left.\begin{aligned} y &= \frac{F^*\,\lambda}{2k} C_{1,x} \\ \theta &= -\frac{F^*\,\lambda^2}{k} C_{2,x} \\ M &= \frac{F^*}{4\lambda} C_{3,x} \\ Q &= -\frac{F^*}{2} C_{4,x} \end{aligned}\right\} \qquad \text{(Eqn. 3-7)}$$

where,

$$\left.\begin{aligned} C_{1,x} &= e^{-\lambda x}(\cos\lambda x + \sin\lambda x) \\ C_{2,x} &= e^{-\lambda x}\sin\lambda x \\ C_{3,x} &= e^{-\lambda x}(\cos\lambda x - \sin\lambda x) \\ C_{4,x} &= e^{-\lambda x}\cos\lambda x \end{aligned}\right\} \qquad \text{(Eqn. 3-8)}$$

Slab of infinite length subjected to concentrated moment, *M*.*

Another fundamental solution that will be useful to determine bending moments in finite sized BAS, the case of an infinite slab on elastic support subjected to a clock-wise moment, *M** as shown in Figure 3-5.

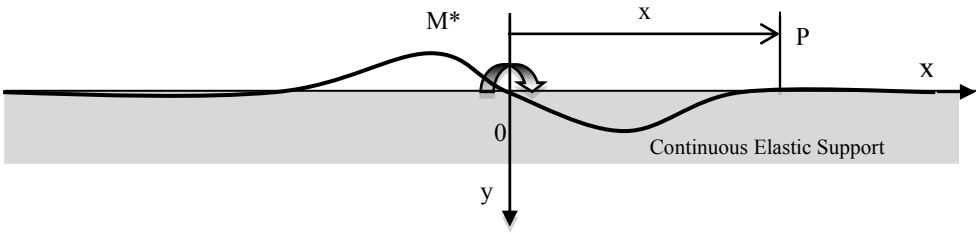

Figure 3-5 Slab of infinite length on continuous elastic support subjected to moment *M**

Again, for any point P ($x \geq 0$), the deflection, y, the slope, θ, the bending moment, M, and the shear force, Q for the case of loading shown in Figure 3-5 are given by:

$$\left.\begin{aligned} y &= \frac{M^*\lambda^2}{k}C_{2,x} \\ \theta &= \frac{M^*\lambda^3}{k}C_{3,x} \\ M &= \frac{M^*}{2}C_{4,x} \\ Q &= -\frac{M^*\lambda}{2}C_{1,x} \end{aligned}\right\} \qquad \text{(Eqn. 3-9)}$$

Where λ and $C_{1,x}, C_{2,x}, C_{3,x}, C_{4,x}$ are defined in Eqns. 3-6 and 3-8.

3.3 Customizing Solutions to Finite Length Slab to Prescribed Load Configurations

It is necessary to customize the classical fundamental solutions presented in Sections for finite lengths of slab and for loading configurations that simulate self-weight (slab dead load) and vehicular loads (lane, design truck and tandem loads) for computing the internal forces such as flexural moment and shear force in bridge approach slab on elastic soil support. This is necessary because in addition to satisfying the equations of equilibrium, the slab has to specifically satisfy the kinematic and static boundary conditions at its end supports as well. These exact solutions for finite length slabs will then be used in the design of BAS as shown in the design example in following Sections and also developing the user-friendly Excel file (BAS design incorporating Elastic Soil Support – BAS-ES) as a design aid. The file, which includes a Visual Basic program, provides users with a two-step procedure to analyze and design reinforced concrete BAS for flexure with checks on shear capacity, crack control, distribution and temperature and shrinkage steel requirements.

The solutions developed in previous sections satisfy the governing differential equation of the slab obtained from equilibrium considerations. Using the principles of superposition, any combination of particular solutions of the governing differential equation will also satisfy equilibrium. It then follows that any combination of the solutions, all of which satisfy equilibrium, can be made to satisfy kinematic and static conditions at specific points on the infinite slab (such as end supports). Using this

approach, solutions for finite slab lengths can be typically obtained in three steps for any given loading as described below.

(i) Using the solutions for an infinite slab (such as the ones presented in Eqns 3-7, 3-8, 3-9), the moments and displacements at the left (M_A and y_A) and right (M_B and y_B) supports of the finite slab can be computed.

(ii) The end reaction, P'_o, and moment, M'_o which act on both the left ($x=0$) and right ($x=l$) supports (for this, a symmetric loading problem) can be determined along with moments $-M_A$, and $-M_B$, and displacements $-y_A$ and $-y_B$ at the supports A and B. These end forces when added to the solutions from (i) above ensure simply supported slab-end fixity conditions ($M = 0$, and $y = 0$ at both the left and right supports of the slab of length l). It can be shown that the end reaction, P'_o, and moment, M'_o are given as:

$$\left.\begin{aligned} P_0 &= 4\lambda F_I\left[M_A C_{2,l} - 2\lambda^2 EIy_A(1+C_{4,l})\right] \\ M_0 &= 2F_I\left[-M_A(1+C_{1,l}) + 2\lambda^2 EIy_A(1+C_{3,l})\right] \end{aligned}\right\} \quad \text{(Eqn. 3-10)}$$

where the notation F_l represents:

$$F_I = -\frac{1}{C_{2,l}(1+C_{3,l}) - (1+C_{4,l})(1+C_{1,l})} \quad \text{(Eqn. 3-11)}$$

a. Finite length simply supported slab subjected to uniform load

Using the above approach of superposition, it is possible to obtain maximum moment and support reactions for a loading geometry shown in Figure 3-6.

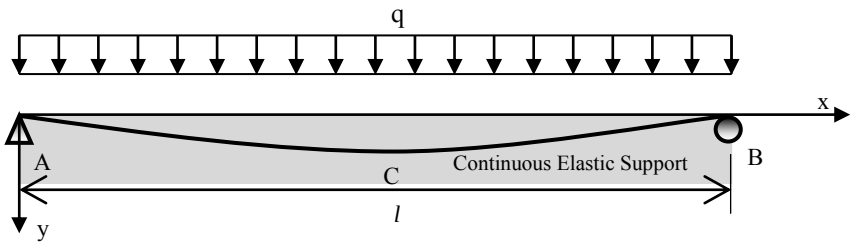

Figure 3-6 Simply supported slab of finite length on elastic support subjected to uniform load, *q*

The moment at the midspan, M_c ($x = l/2$) is given by:

$$M_c = \frac{q_0}{2\lambda^2} C_{2,\frac{l}{2}} + \frac{P_1}{2\lambda} C_{3,\frac{l}{2}} + M_1 C_{4,\frac{l}{2}} \qquad \text{(Eqn. 3-12)}$$

The reaction forces at the left and right supports are obtained as:

$$R_A = R_B = -\frac{P_1}{2} C_{4,l} - \frac{\lambda M_1}{2} C_{1,l} - \frac{P_1}{2} C_{4,0} + \frac{\lambda M_1}{2} C_{1,0} + \frac{q_0}{4\lambda}(C_{3,l} - 1) \qquad \text{(Eqn. 3-13)}$$

b. Finite length simply supported slab subjected to symmetric concentrated forces

Using the elastic superposition approach, it is possible to obtain maximum moment and support reactions for a loading geometry shown in Figure 3-7.

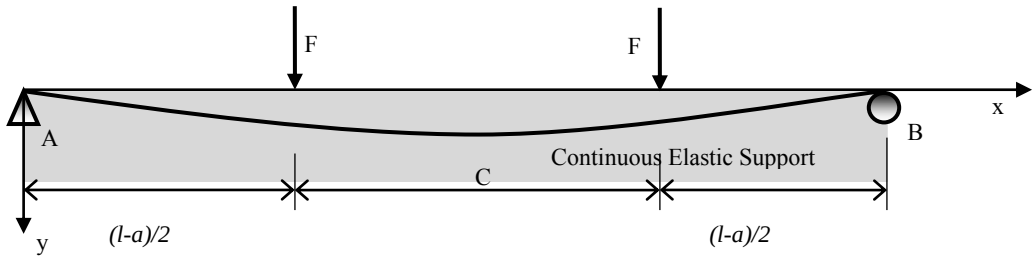

Figure 3-7 Simply supported slab of finite length on elastic support subjected to two symmetric concentrated forces, *F*

The moment at the midspan, M_c ($x=l/2$) is given by:

$$M_c = 2\left(\frac{P_0'}{4\lambda} C_{3,\frac{l}{2}} + \frac{M_0'}{2} C_{4,\frac{l}{2}} + \frac{F}{4\lambda} C_{3,\frac{a}{2}}\right) \qquad \text{(Eqn. 3-14)}$$

where $C_{3,\frac{l}{2}}, C_{4,\frac{l}{2}}$ and $C_{3,\frac{a}{2}}$ are constants defined in Eqn. 3.8 evaluated at *x = l/2, l/2* and *a/2,* respectively and,

$$R_A = R_B = \frac{P_0^{'}}{2}C_{4,x_1} + \frac{M_0^{'}\lambda}{2}C_{1,x_1} + \frac{F}{2}C_{4,x_2} + \frac{F}{2}C_{4,x_3} + \frac{P_0^{'}}{2}C_{4,x_4} - \frac{M_0^{'}\lambda}{2}C_{4,x_4}$$

(Eqn. 3-15)

where

$$x_1 = l, \quad x_2 = \frac{l+a}{2}, \quad x_3 = \frac{l-a}{2}, \text{ and } x_4 = 0$$

3.4 Summary of a Design Example with Soft Soil

A reinforced concrete bridge approach slab 38 ft. wide (for 2-12 ft lanes of traffic, assuming 4 ft wide inside shoulder and 10 ft wide outside shoulder) and 25 ft span assuming continuous elastic soil support is designed. It is assumed that the soil support is provided by weak “loose sand” with a soil modulus parameter, k, of 30 psi/in. Concrete with f'_c = 4,000 psi, E_c = 3,605 ksi and c = 150 pcf is used. Grade 60 conventional reinforcing steel is used. Loads considered include dead load, HL-93 lane load, truck load or tandem load (in this case, tandem load governs and hence is considered instead of the truck load). The design meets all current MODOT and AASHTO design specifications. The amount of reinforcement used for the design represents significant savings compared to the standard MoDOT BAS design as discussed. Detailed design example is covered in Appendix A.

Table 3-1 Details of reinforcement based on incorporating elastic soil support

Layer	Reinforcement
Top Longitudinal Bars	#5 @ 12”
Top Distribution Bars	#4 @ 12”
Bottom Longitudinal Bars	#6 @ 8”
Bottom Distribution Bars	#4 @ 12”

3.5 Observations on BAS Incorporating Elastic Soil Support

Figure 3-8 includes a plot of Strength I and Service I maximum bending moments as a function of soil elastic modulus, k (psi/in). A very wide range of k values relevant to Missouri conditions are plotted. A k-value of 20 psi/in represents loose submerged sand, while a k-value of 225 psi/in represents dense sand (above the water table). The figure shows maximum moment values for soil stiffness values up to 500 psi/in (very dense sand). It should be noted that the theory for BAS analysis incorporating continuous elastic soil support in the limiting case of k = 0 psi/in predicts Strength I and Service I maximum moments that are identical to the conventional simply supported analysis (Strength I moment of 959 k-in and Service I moment of 588 k-in for the geometric and loading parameters considered).

Figure 3-9 includes a plot of Strength I and Service I maximum shear forces as a function of soil elastic modulus, k (psi/in). It indicates same relationship between

maximum shear forces and soil modulus as that of maximum bending moments and soil modulus. When soil becomes stiffer, shear forces in approach slab can be greatly reduced.

Table 3-2 includes a comparison of the maximum moments for various support conditions for a 12” thick BAS and associate requirement of longitudinal flexural steel (bottom layer of steel in the longitudinal or traffic direction).

It is also interesting to observe that, when elastic soil support is considered as a basis for design, a reduction in slab thickness results in smaller required design moments. Table 3-3 lists maximum design moment and associated steel area required for two slab thicknesses (12” and 10”, with effective depths of 9” and 7”) for a range of soil elastic modulus. The reason for this result is the fact that lower slab flexural rigidity produces larger deflections and hence greater soil support. While one can take some advantage of this observation in optimizing design based on flexural strength, limiting serviceability parameters such as acceptable deflections and crack-widths may necessitate higher slab depths.

Based on the alternate analysis procedure presented in this document it is readily evident that the design moments and shear for a BAS can be significantly reduced even if the slab was assumed to be supported continuously on loose sand (i.e. BAS support does not need to come from a very stiff foundation).

The theory developed is based on well accepted principles of mechanics and the assumptions of elastic soil support are realistic and practically achievable. Ways to optimize BAS design to provide for reductions in initial cost as well as improve long-term performance through use of innovations in construction (improved quality control with precast slabs with cast-in-place topping of unreinforced or fiber reinforced concrete) and materials (use of hybrid reinforcement of conventional reinforcing steel with discrete steel fibers providing better crack control and improved impact and fatigue resistance) can be developed. This follow-up should allow, in addition to optimized initial design, improved attention to serviceability issues such as crack-control and durability. The BAS-ES approach in addition to initial cost reductions has the potential to offer innovations in BAS analysis and design.

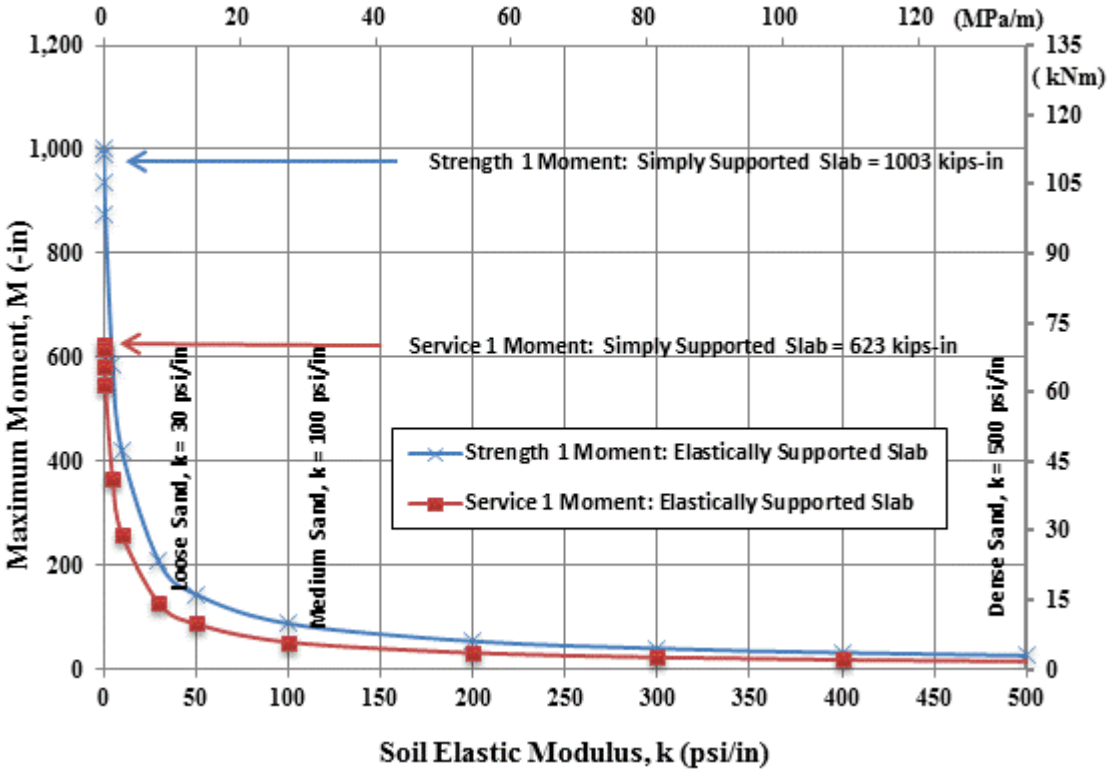

Figure 3-8 Plot highlighting influence of soil support on design moment, even considering a loose sand with k = 20 psi/in it is possible to reduce the design moment required by 75% (see also Table 3.1)

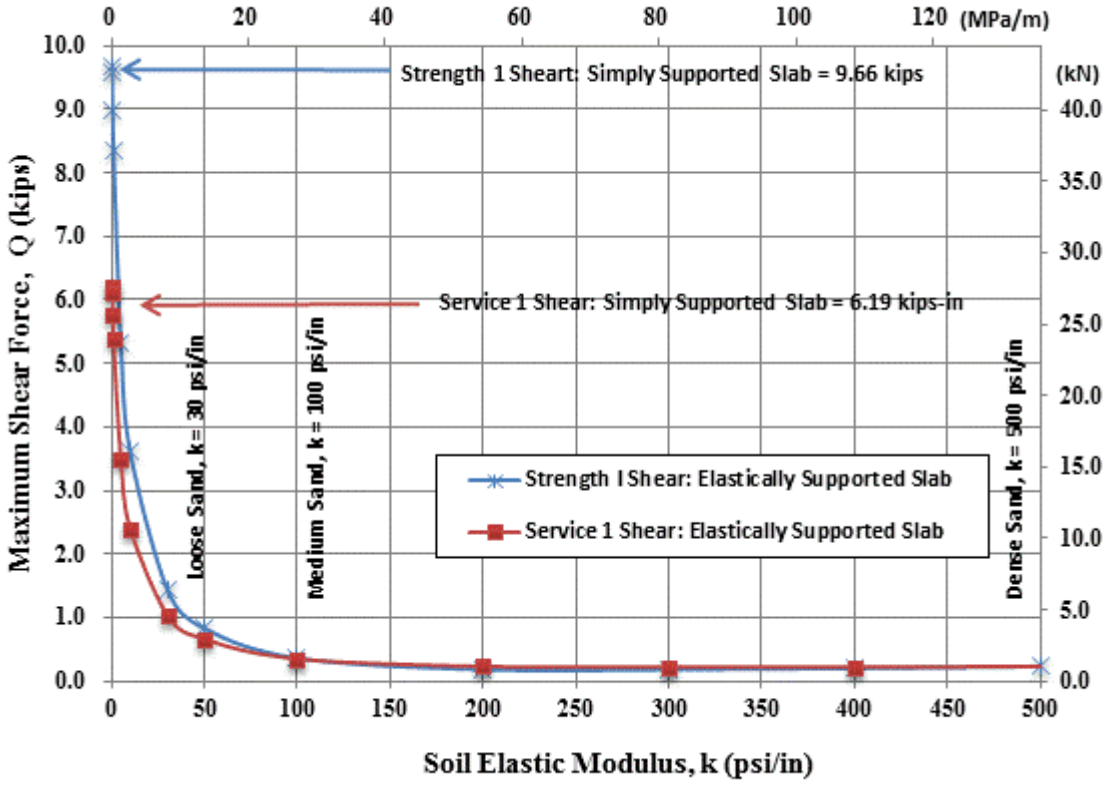

Figure 3-9 Plot highlighting influence of soil support on design shear force.

Table 3-2 Comparison of maximum design moment and corresponding area of flexural steel required for a 12” deep slab for various soil support conditions

Support Conditions	Soil Elastic Modulus (psi/in)	Maximum Moment (k-in)	Area of Steel Required (in^2)
Simply Supported	0	959	2.47
Elastically Supported Loose Sand	1	832	2.06
	5	548	1.26
	10	389	0.86
	20	254	0.55
	30	193	0.410
Elastically Supported Medium Sand	50	135	0.28
	80	97	0.20
	100	83	0.17
	150	63	0.13
	200	51	0.11
Elastically Supported Dense Sand	300	38	0.08
	400	30	0.06
	500	25	0.05

Table 3-3 Comparison of maximum factored design moment and corresponding area of flexural steel required for 12” and 10”deep reinforced concrete slab for various soil support conditions

Soil Elastic Parameter k (psi/in)	Slab Depth h (in), [d (in)]	Maximum Moment M (k-in)	Area of Steel Required (in^2)
Very Loose Sand 5	12 [9]	548	1.26
	10 [7]	411	1.25
Loose Sand 30	12 [9]	193	0.41
	10 [7]	129	0.35
Medium Sand 100	12 [9]	83	0.17
	10 [7]	57	0.15
Dense Sand 500	12 [9]	25	0.05
	10 [7]	14	0.04

3.6 User-Friendly Analysis and Design of BAS-ES Using Customized Excel Application

Customized solutions of finite length slab described earlier are used in the Excel-based Visual Basic design software for BAS using Elastic Soil Support (BAS-ES). Internal forces are computed for MoDOT prescribed bridge loading based on the mechanics model described in Figure 3-10. It shows a user-friendly front-end of BAS-ES that allows a two-step design process that meets all AASHTO and MoDOT specifications.

First, fill in the Input1 part with basic parameters describing soil condition, geometry and material of the bridge approach slab, and click on calculate tab. Then maximum internal moment and shear force for both strength limit and service limit will show in Output1. Second, provide detailed longitudinal and transverse reinforcement in Input2 and click on Check tab to ensure all the design checks satisfied. Reminders will show in Output2 if there's insufficient capacity and reinforcement steel need to be adjusted, either increase the number of bars or reduce the spacing of reinforcement. Multiple-trials are necessary to reach an optimum amount of reinforcement and Output2 area of main reinforcement steel can serve as a reference.

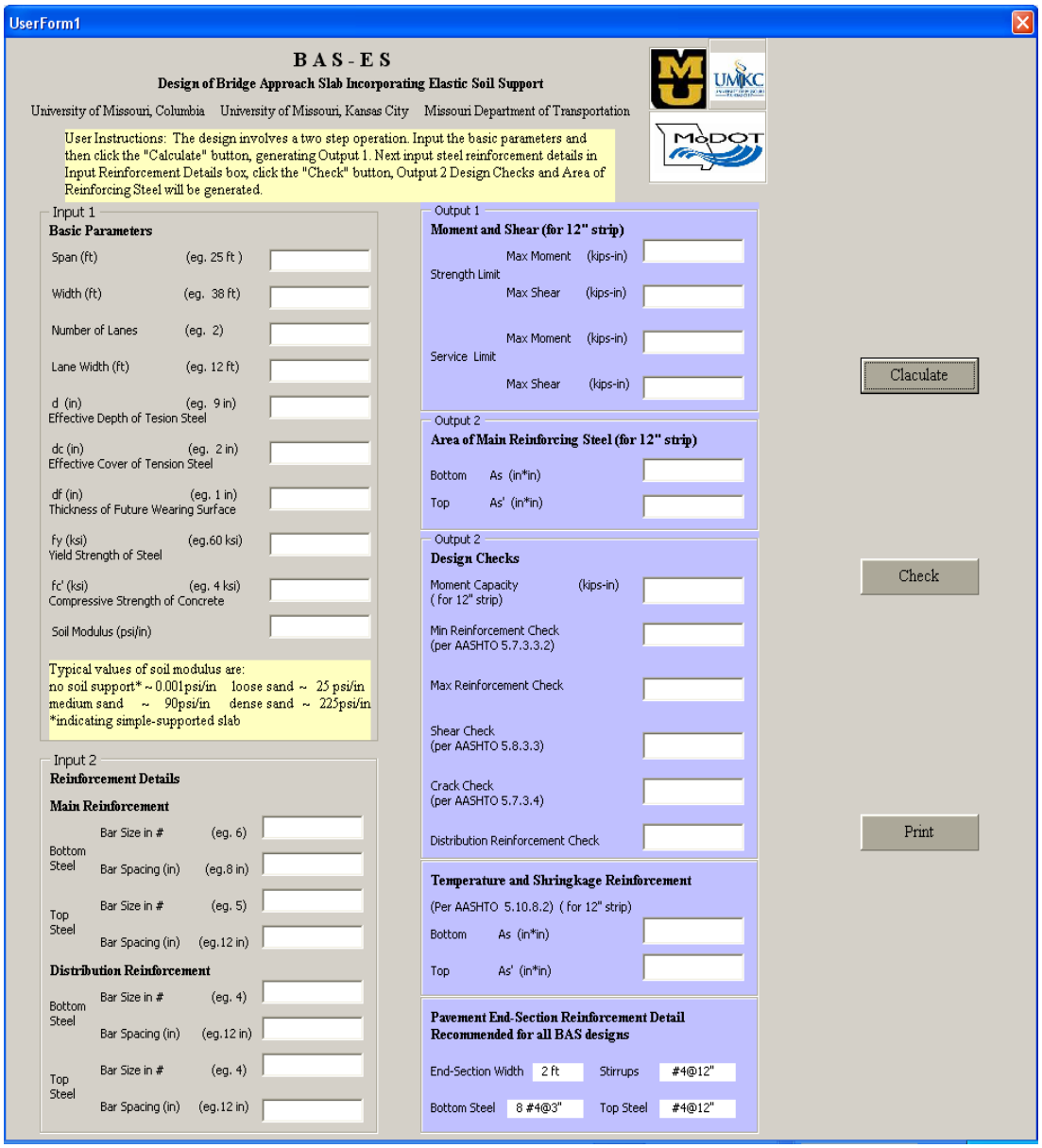

Figure 3-10 The user-friendly front-end of BAS-ES, the MS Excel-based Visual Basic software to design BAS incorporating elastic soil support

CHAPTER 4 ADVANCED FINITE DIFFERENCE MODELING OF BAS-ES

4.1 Introduction

A progressive study comprising four components detailing the application of finite difference method for bridge approach slab is reported in this chapter. In the first part, uniaxial bending model of beam is developed using an excel worksheet to investigate advanced cases of BAS incorporating elastic soil support and unsymmetrical loading configuration, followed by a systematic study of the effects of soil washout on performance of BAS. Washout length and location are the primary parameters studied. Then the second component details investigation of the uniaxial bending with modifications to the pavement end support. Settlement of the sleeper slab is studied in this second component of this chapter (yielding support versus nonyielding support). The third component, biaxial bending model of plate is developed using MATLAB with 2-dimensional loading of the BAS. Specific cases with soil washout and yielding pavement end support are solved using the biaxial model and discussed in detail. The fourth component includes a comparison between uniaxial and biaxial solutions with a view to validate the simpler uniaxial bending model for general design application.

4.1.1 Background of Washout Studies

One concern often expressed when assuming elastic soil support in the design of a slab-on-grade is the potential loss of soil support and void formation under the slab due

to consolidation, poor drainage or other similar hydraulic/geotechnical events. It is for this reason an analysis of the influence of potential washout on the maximum moments and shear developed in the BAS needs to be studied. The focus of the parametric study described here is: to determine maximum moments and shear forces in the elastically soil supported slab resulting from a partial or complete washout of soil beneath the slab. Consider the elastically supported BAS shown in Figure 4-1. Partial washout of the soil support (washout length, L, unshaded portion beneath BAS) and location of the washout from the bridge abutment end (left-end), b (to the left-end of the washout region) are considered for a uniformly loaded slab. By varying L from 0' to the total length of the slab (25' for standard MoDOT BAS), one can validate maximum moments and shear forces for the "completely supported BAS" (BAS-ES per the design approach proposed here) to a "simply-supported BAS" (standard MoDOT BAS design approach). One can also study the influence of the location of the washout by varying "b" from 0' to desired lengths (based on washout length L used) to investigate the influence of washout exhaustively.

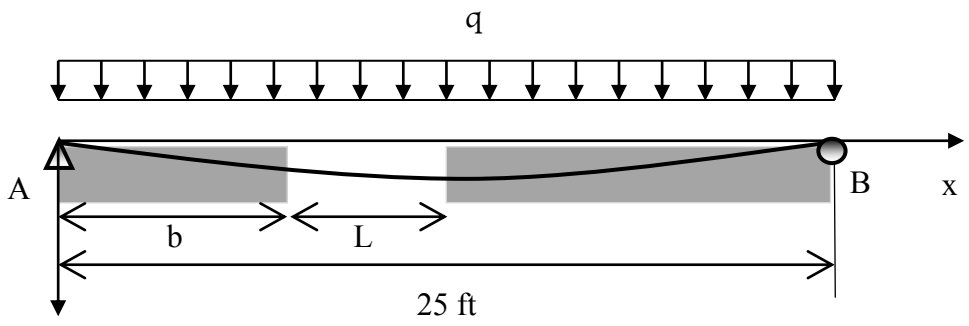

Figure 4-1 Simply-supported slab subjected to uniformly distributed load, q, showing soil wash-out (unshaded region of length L) and partial soil support (shaded regions)

4.1.2 Uniaxial Finite Difference Model of BAS-ES with Partial Soil Washout

A finite difference model of the BAS-ES was developed to study the influence of washout length and location on maximum moments and shear developed in the slab. The model uses the finite strip method (1' or 12" width strip transverse to traffic direction) of one-way bending of slab as is the current practice on design of BAS. The governing differential equation of a beam on elastic foundation is solved numerically using the finite difference approach. The finite difference approach allows a very elegant way of developing approximate solutions to the complicated problem of "beam on elastic foundation with washout". Instead of solving an ill-posed 4th order non-linear differential equation, the finite difference approach facilitates deflection solution using a system of linear algebraic equations. The solution involves the discretization of a 12" width strip of the BAS into finite length elements along the length of the slab (traffic direction). In the solutions described in this section, the 25 ft. slab length has been discretized into 50 elements, each of length, h = 0.5 ft (6"). The governing differential equation (GDE) for the problem is applied at each node of the model (51 nodes for the 50 element model -- minus the two end nodes that are considered fixed supports – resulting in 49 nodes for GDE application). At each node the GDE of the beam on elastic support is given by Eqn. 4-1:

$$EI\,\frac{d^4 y_i}{dx^4} = q_i - k\,y_i \qquad \text{(Eqn. 4-1)}$$

The fourth derivate of the deflection, *y*, is represented using finite difference operators by

$$\frac{d^4 y_i}{dx^4} = \frac{y_{i+2} - 4y_{i+1} + 6y_i - 4y_{i-1} + y_{i-2}}{h^4} \qquad \text{(Eqn. 4-2)}$$

where the subscript *i* refers to the *i*th node in the discretization and y_i is the vertical deflection of the *i*th node.

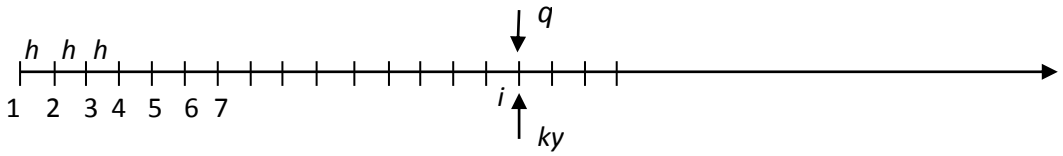

Figure 4-2 Finite length elements with distributed load, *q*, and soil pressure, *ky*, on the nodes

Therefore, for the internal nodes (49 in this example), one can establish the relationship:

$$y_{i+2} - 4y_{i+1} + (6 + \frac{kh^4}{EI})y_i - 4y_{i-1} + y_{i-2} = \frac{q_i h^4}{EI} \qquad \text{(Eqn. 4-3)}$$

For the uniform dead load and lane load q; $q_i (2 \le i \le 50) = q$;

For the concentrated tandem load F, acting on any node n, it is possible to establish an equivalent distributed load, assuming the concentrated force is distributed over one element: $q_i = \frac{F}{h}$, $q_{i+1} = q_{i-1} = 0$;

For the nodes within the washout region, the soil modulus k is set to 0. Nodes at the boundaries of the washout region use a soil modulus value of one-half the actual soil modulus. For nodes outside the washout region (i.e. soil supported regions) the actual soil modulus is used.

Using 50 elements to discretize the BAS along its length, a 49 by 49 matrix can be built as shown in Eq. 4-4 (based on the analytical development described in Eqs. 4-1, 4-2, 4-3);

$$\begin{bmatrix} 5+\frac{kh^4}{EI} & -4 & 1 & 0 & 0 & \dots & 0 & 0 & 0 & 0 & 0 \\ -4 & 6+\frac{kh^4}{EI} & -4 & 1 & 0 & \dots & 0 & 0 & 0 & 0 & 0 \\ 1 & -4 & 6+\frac{kh^4}{EI} & -4 & 1 & \dots & 0 & 0 & 0 & 0 & 0 \\ 0 & & & & & & 0 & 0 & 0 & 0 & 0 \\ 0 & 0 & & & & & & 0 & 0 & 0 & 0 \\ \dots & \dots & \dots & & & & & \dots & \dots & \dots & \\ \dots & \dots & \dots & \dots & & & & & \dots & \dots & \\ 0 & 0 & 0 & 0 & 0 & & & & & 0 & \\ 0 & 0 & 0 & 0 & 0 & \dots & 1 & -4 & 6+\frac{kh^4}{EI} & -4 & 1 \\ 0 & 0 & 0 & 0 & 0 & \dots & 0 & 1 & -4 & 6+\frac{kh^4}{EI} & -4 \\ 0 & 0 & 0 & 0 & 0 & \dots & 0 & 0 & 1 & -4 & 5+\frac{kh^4}{EI} \end{bmatrix} \times \begin{pmatrix} y_2 \\ y_3 \\ y_4 \\ y_5 \\ \vdots \\ \vdots \\ \vdots \\ \vdots \\ y_{47} \\ y_{48} \\ y_{49} \\ y_{50} \end{pmatrix} \begin{pmatrix} q_2 \\ q_3 \\ q_4 \\ q_5 \\ \vdots \\ \vdots \\ \vdots \\ \vdots \\ q_{47} \\ q_{48} \\ q_{49} \\ q_{50} \end{pmatrix} \frac{h^4}{EI}$$

(Eqn. 4-4)

The above system of linear algebraic equations can be used to solve for the nodal displacements, y_i, which can then be used to establish nodal moment and shear force values using the finite difference operators for the second and third derivatives as shown in Eqn. 4-5 and 4-6, respectively.

$$M_i = -EIy_i'' = -EI\,\frac{y_{i+1} - 2y_i + y_{i-1}}{h^2} \qquad \text{(Eqn. 4-5)}$$

$$Q_i = -EIy_i''' = -EI\,\frac{y_{i+2} - 2y_{i+1} + 2y_{i-1} - y_{i-2}}{2h^3} \qquad \text{(Eqn. 4-6)}$$

The finite difference solution thus obtained can be used to exhaustively develop shear and moment diagrams due to the critical combinations of self-weight, lane load, truck and tandem loads in addition to variations in the washout parameters, L (washout

length) and b, (washout location). The finite difference solutions represent numerical approximation of the exact closed-form solutions to the GDE of the problem and as such are prone to errors that can typically be minimized with finer discretization. The 50 elements discretization used in obtaining the results discussed here has been shown to be acceptably accurate (by comparing the solution to the two limiting cases of "complete soil support" and "no soil support") and can be implemented very conveniently using an Excel spread sheet.

4.1.3 Parametric Study of Washout Length and Location

Results presented in this section assume a soil modulus, k = 30psi/in, standard loads (self-weight of slab, lane load and design tandem (more critical than truck load)), 12" slab strip width, and slab length of 25'. Results from various combinations of washout length from 0' (completely soil supported) to 25' (no soil support) and washout locations to produce maximum internal forces have been analyzed exhaustively. Figure 4-3 shows the influence of washout parameters, L and b, on the maximum moment in the slab due to the most critical combinations of self-weight, lane load, truck load, and design tandem. The plot shows the maximum design moment required for various washout lengths (L) from 0' (complete soil support) to 24' (near complete washout or no soil support) as the washout location, b, is varied. When, L = 0', the moment required is independent of the washout location, as expected, and is identical to the BAS-ES design moment (~200 k-in). When L =25', the maximum moment (959 k-in) is identical to that obtained for a simply supported slab with no soil support. For L

values in the 0’ < L < 25’ range, the plot shows variations of the maximum moment and the location in 2’ increments of the washout length. Each such plot starts at a “b” value of 0’ and is terminated at a “b” value of (25’ – L)/2 reflecting exhaustive variation in this parameter as the property of symmetry can be effectively used to establish maximum internal forces for all combinations of b and L.

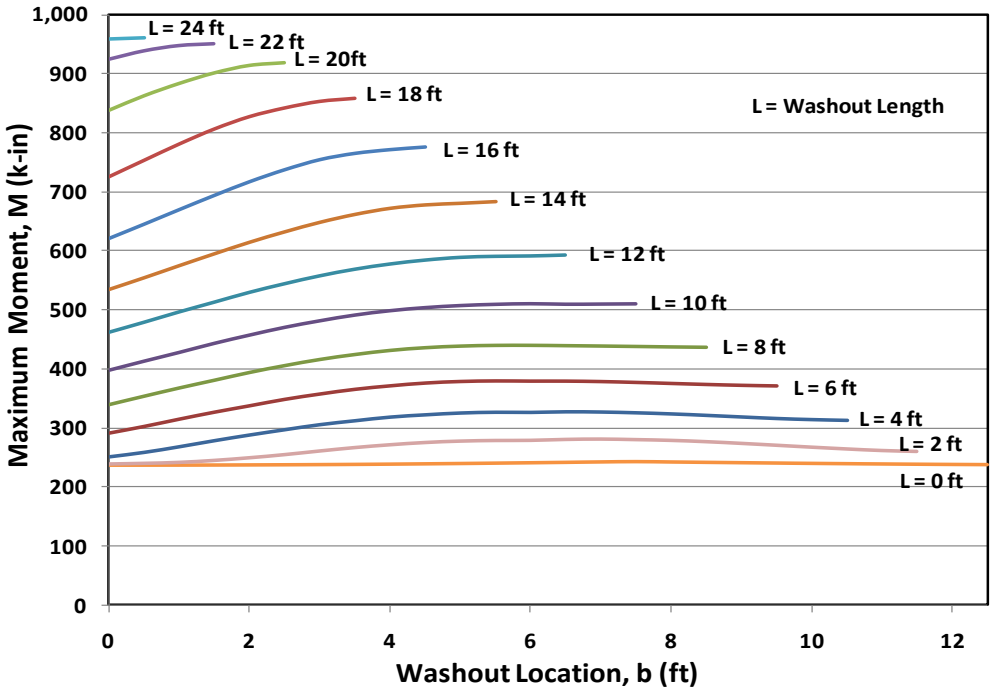

Figure 4-3 Maximum moment vs washout location for various washout lengths

As the washout length gets larger, the maximum moment approaches the maximum moment for a simply supported slab. Even if one assumes a washout length of 20% of the slab length (5 ft., representing quite significant void formation under the BAS), it is observed that the maximum moment is only 35% of the maximum moment calculated assuming simply supported design (i.e. no soil support). Figure 4-4 shows a plot of composite moment diagram (critical combination of all bridge loads) as a 5’ washout region moves along the span. Three cases of washout are shown (L = 5’, with b = 0’, 5’

and 10') along with the two limiting cases of no washout and complete washout (L = 0', b = 12.5' - no washout representing complete soil support, and L = 25', b = 0' – complete washout representing no soil support, same as being simply supported). It can be observed from the parametric study that washout regions closer to the midspan cause maximum moments in the slab. In addition to showing that if elastic soil support is considered in BAS designs, even fairly large washout lengths provide for significant reductions in maximum moment from that for a simply supported BAS. Figure 4-4 also highlights that washouts at locations closer to the abutment exhibit lower magnitudes of maximum moment compared to washouts closer to the midspan. Field observations of voids under the BAS have typically been observed to be closer to bridge abutments resulting from poor drainage and differential movement than closer to midspan of the BAS. It is hence reassuring that when BAS designs using elastic soil support are considered, the influence of potential washouts are relatively small. Even if design moments from BAS-ES are increased by multipliers to incorporate the influence of potential washout, significant savings can still be realized compared to the current standard MoDOT BAS design that relies on a simply supported assumptions with no soil support.

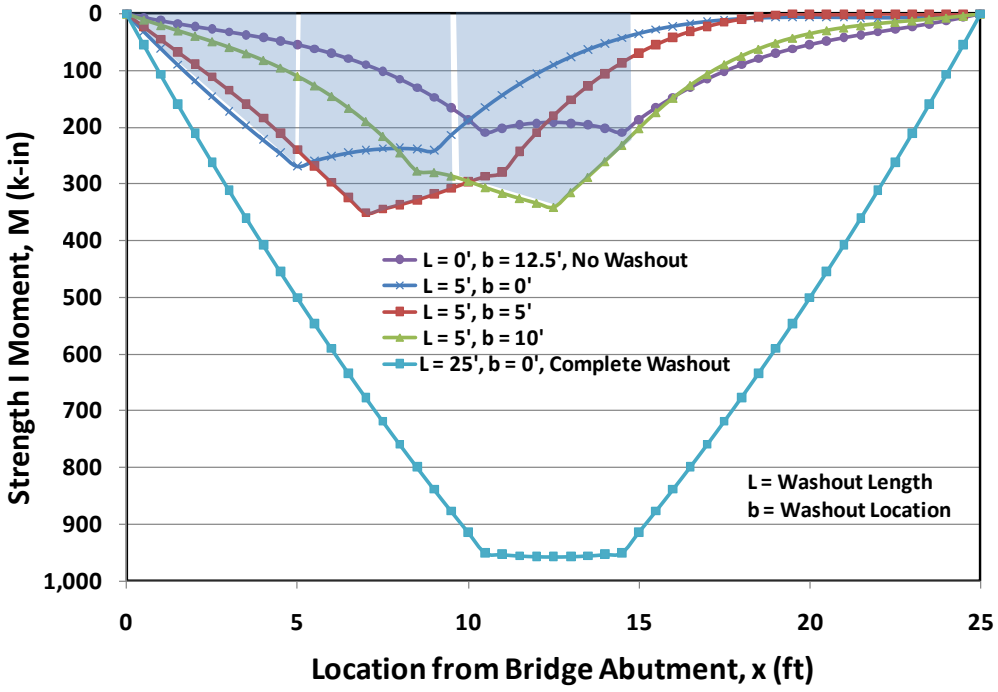

Figure 4-4 Moment diagrams for different locations of 5 ft soil washout length

Figure 4-5 shows plots similar to Figure 4-3 for variations in the shear force along the length of the slab from the parametric study of washout lengths and locations. It is interesting to observe that washout locations closer to midspan result in smaller maximum shear forces compared to locations closer to the supports. This is, as expected, because shear forces are typically larger near the supports in common single-span flexural configurations. For the flexural design of BAS, as shown later in the design example in Appendix A, the geometries and material strengths typically used make it a moment critical, and not a shear critical, design problem. Design shear capacities almost always far exceed ultimate shear force requirements. Hence even with increased shear forces, potential washout does not influence shear design requirements.

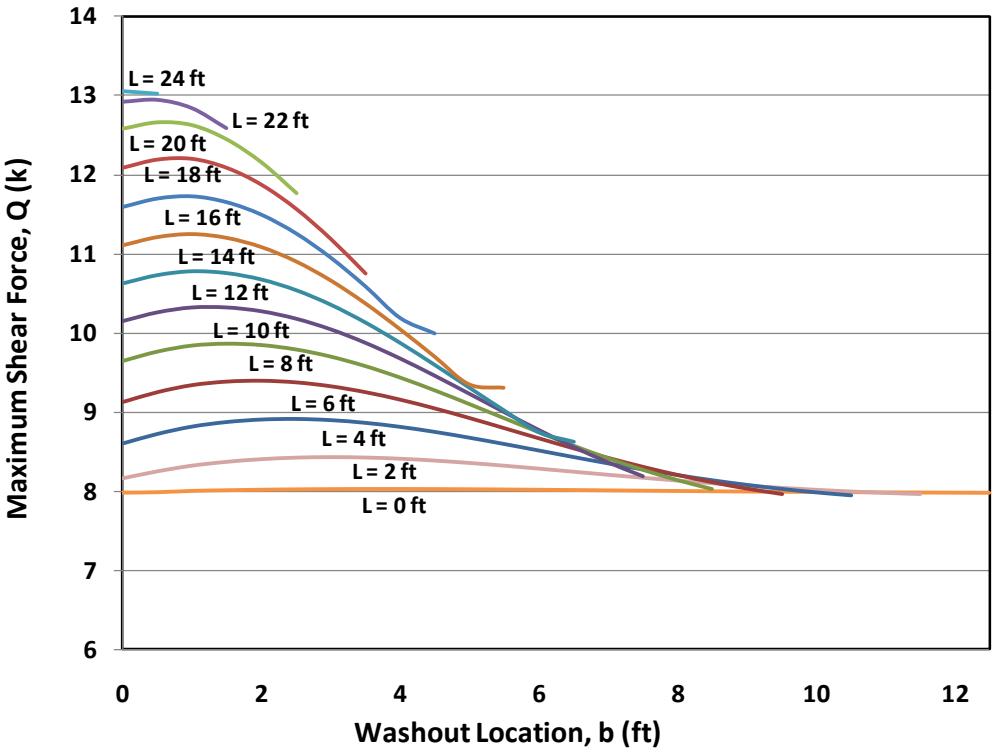

Figure 4-5 Maximum shear force vs washout location for various washout lengths

4.1.4 Washout and Soil Stiffness

Fig. 4-6 shows a plot of maximum moment reduction factor, M_R, versus washout length, L, for three different soil modulus values, k, ranging from k = 30 psi/in to k = 500 psi/in. The limiting values of the washout length of 0' and 25' represent the cases of "complete soil support" (BAS-ES design) and "no soil support" (standard MoDOT BAS design), respectively. M_R is the nondimensional moment representing the ratio of the maximum moment of an elastically soil supported BAS with partial washout (placed to produce maximum internal forces), M_e, to the maximum moment from a simply supported slab with no soil support (standard MoDOT BAS design), M_s).

$$M_R = M_e / M_s \qquad \text{(Eqn.4-7)}$$

M_R values less than one represent reductions in design moment required. For example, with k = 30 psi/in, the BAS-ES design with no washout can reduce the design moment to 25% of that of a simply supported BAS with no soil support. Even assuming a 5' washout anywhere along the length of the slab, the moment reduction is still significant at 37%. For k = 500 psi/in, the BAS-ES design with no washout can reduce the design moment to 9% from that of a simply supported BAS with no soil support. Even assuming a 5' washout anywhere along the length of the slab, the moment reduction is still large at 19%.

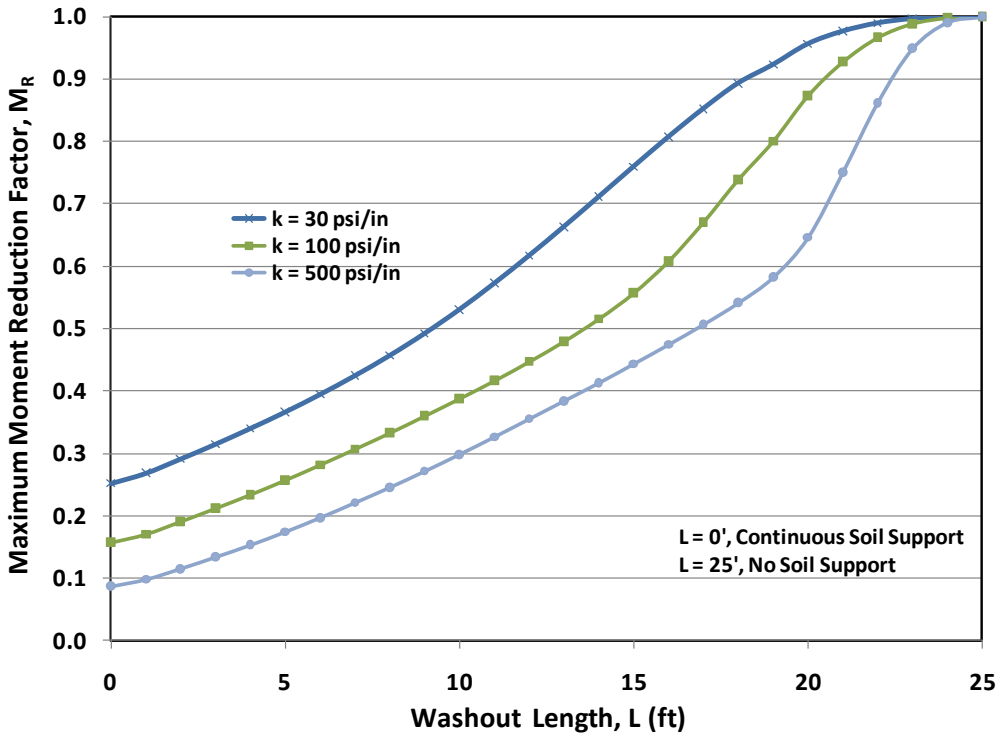

Figure 4-6 Moment reduction factor versus washout length for various soil moduli

Figure 4-7 shows a plot of maximum shear reduction factor, Q_R, versus washout length, L, for different soil modulus values, k. Q_R is the nondimensional shear reduction factor representing the ratio of the maximum shear of an elastically soil supported BAS with

partial washout (placed to produce maximum internal forces), Q_R to the maximum shear force from a simply supported slab with no soil support (standard MoDOT BAS design), Q_s.

$$Q_R = {Q_e}/{Q_s} \qquad \text{(Eqn.4-8)}$$

Assuming a weak embankment with soil modulus k = 30 psi/in and a 10 ft long soil washout, maximum shear force is reducted 20% from simply supported slab. However, the shear deduction response for very stiff soil k = 500 psi/in was observed to fluctuate when more than half of the soil is washed away, which is possibly because of numerical issues with the relatively small shear force magnitudes.

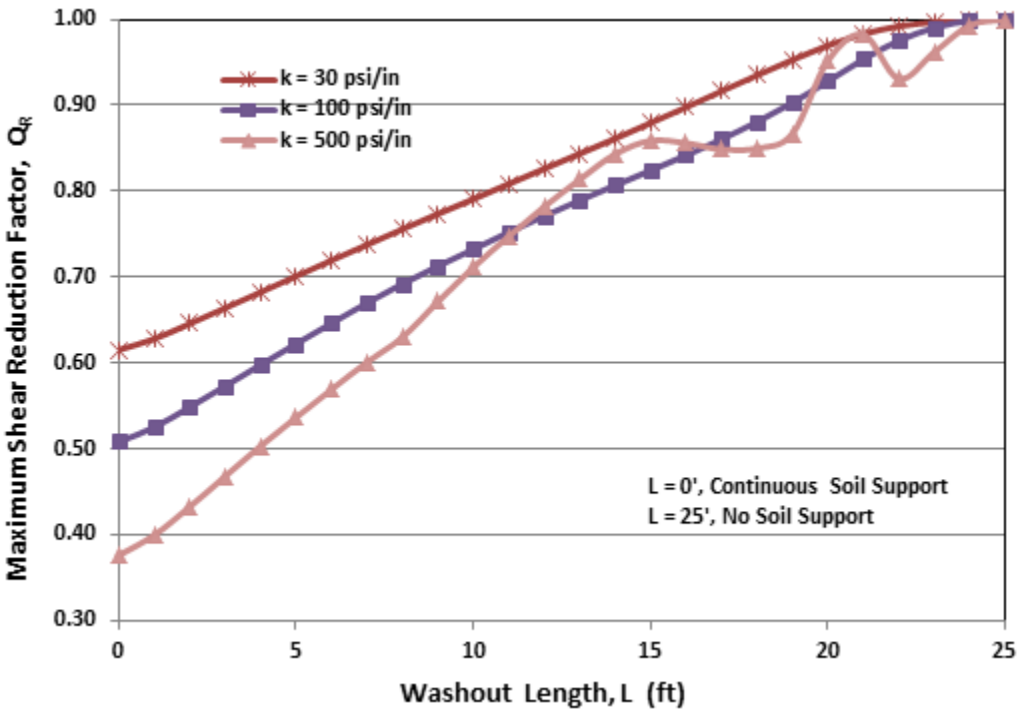

Figure 4-7 Shear reduction factor versus washout length for various soil moduli

4.1.5 Yielding and Nonyielding Pavement End Support

The common measure taken in field to minimize settlement of bridge approach at pavement end is to construct a cast-in-place concrete sleeper slab. In Missouri, sleeper slab with a depth of 18" and a span of 3 ft, is placed directly below the approach slab.

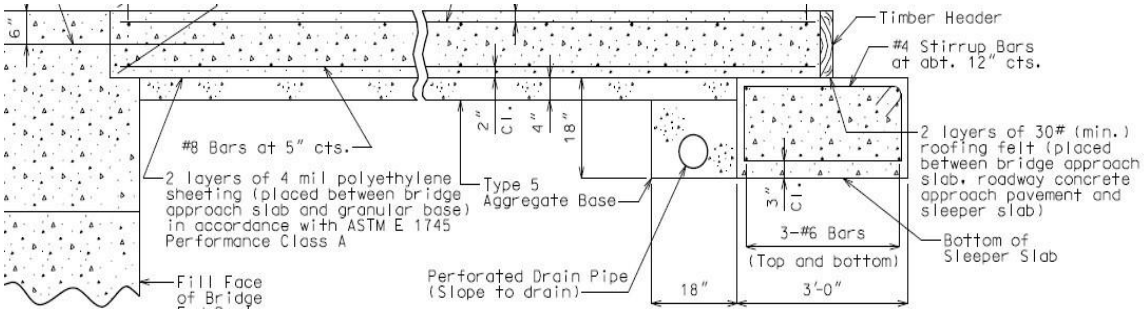

Figure 4-8 Section View of bridge Approach Slab and Sleeper Slab

This relatively rigid concrete beam is supposed to provide stiff support to approach slab. However, conventional design assumes no settlement of the sleeper slab, which is just supported on the embankment soil just like the BAS. Hence it would be more realistic to assume that sleeper slabs also yield (settle) under normal service. The effect of yielding support at the sleeper slab is investigated using a "finite difference model" to compute internal forces and sab deflections under such conditions.

For the nonyielding pavement end support, approach slab is simulated as simple supported at ends in longitudinal direction and is soil supported on the edges in transverse directions. While for yielding case, approach slab has three soil supported edges and one simple supported edge. In both cases, weight of sleeper slab is ignored because it's beneath the approach slab support system and soil support is assumed to be continuous throughout the span of slab, which simplifies the modeling effort.

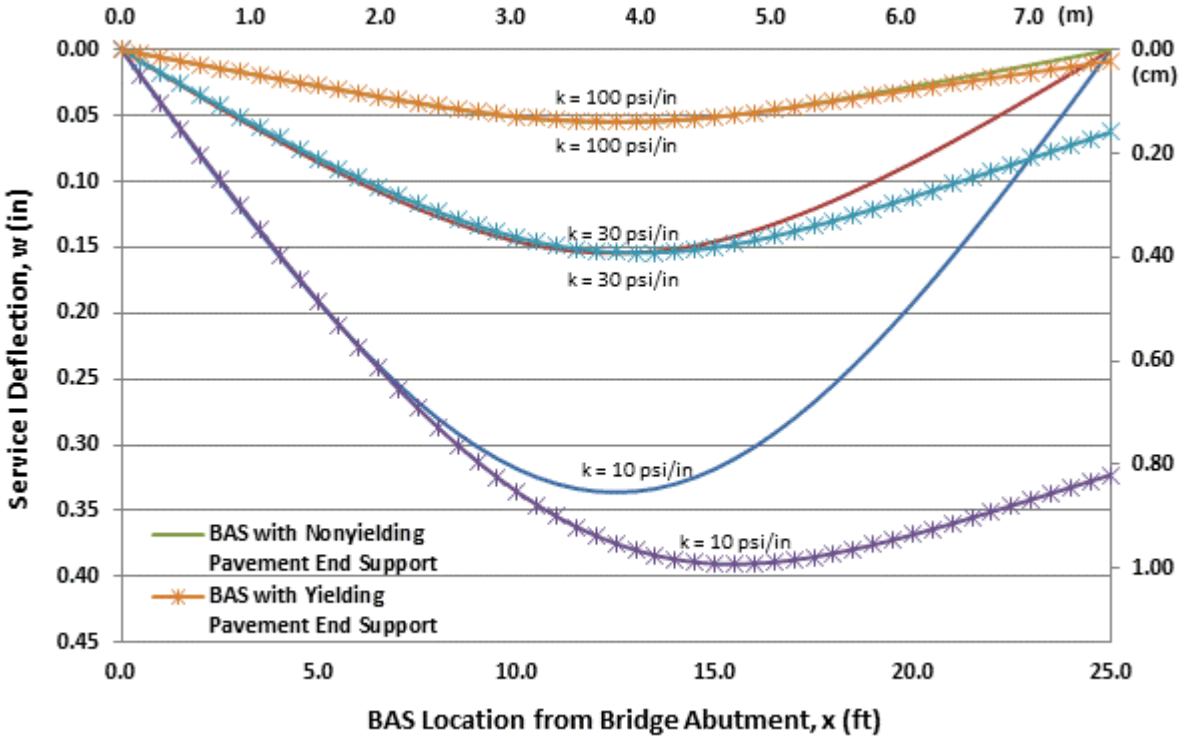

Figure 4-9 Comparison of Service I deflections of BAS with yielding and nonyielding sleeper slab (pavement end support)

Figure 4-9 illustrates the deflection profile for BAS with yielding as well as nonyielding pavement end support. No washout is considered for the solutions reported in Figure 4-9. When the soil is very soft, deflection of bridge approach slab at the pavement end can reach 0.6 inch. The maximum deflection is observed slightly off the middle span for the yielding end supports and is more than twice of the maximum deflection observed for the nonyielding support. This represents the field conditions more accurately. The figure also demonstrates that the soil stiffness significantly influences the maximum deflection for the case of a yielding end support. The maximum deflection decreases to less than 0.3 inch and deflection at pavement end to 0.1 inch for an elastic soil support of 30 psi/in.

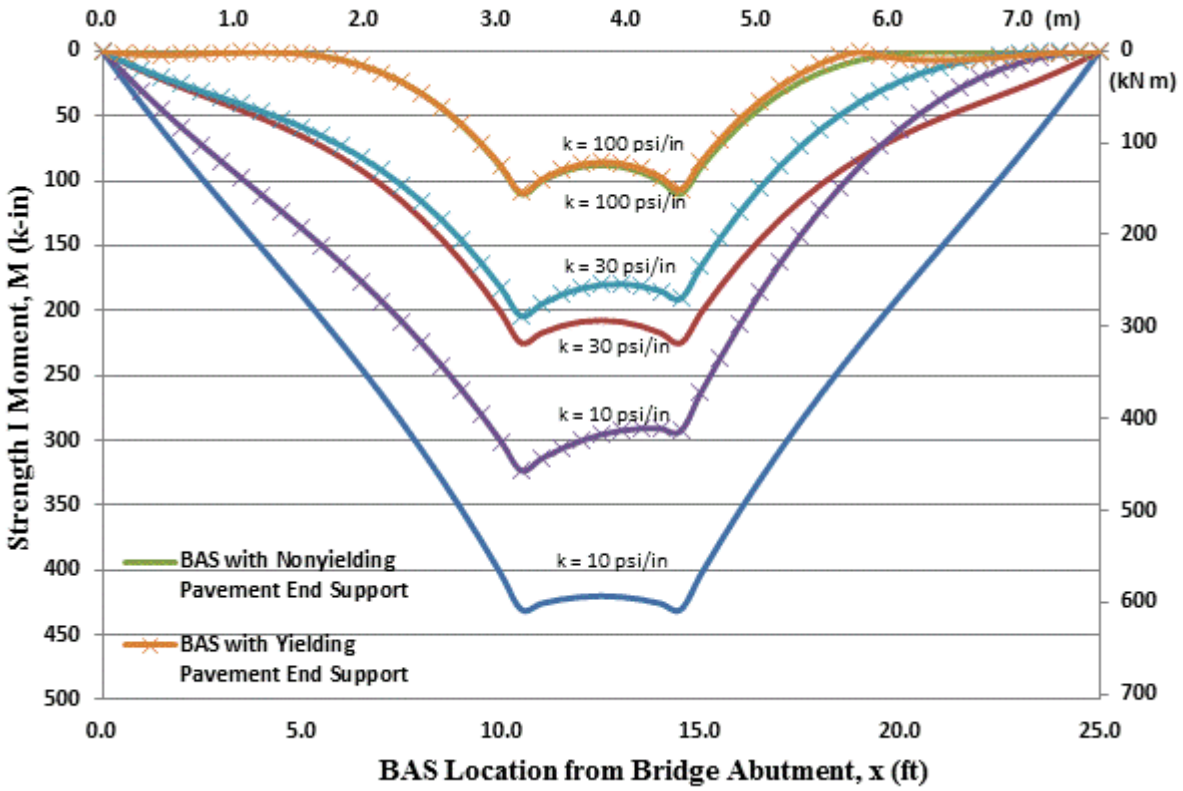

Figure 4-10 Comparison of strength I moments of BAS with yielding and nonyielding sleeper slab (pavement end support)

While deflections increase with settlement of the sleeper slab, more soil support is provided with the larger deflections. Figure 4-10 comparing solutions for moment profiles from yielding and nonyielding support highlights that moments computed for nonyielding support are higher than those for yielding support cases (deflections being larger for yielding cases result in increased soil support). The difference between maximum moments of nonyielding and yielding cases is less for higher soil moduli.

4.2 Biaxial Bending Solutions

Bridge approach slabs in most states have typically been designed as a simply supported beam using a strip of unit width under uniaxial bending. Behavior of approach slab needs to be analyzed as a biaxial bending problem particularly if localized voids (voids that are not along the entire width) are present. Available literature report of cracks both along longitudinal and transverse directions suggests biaxial flexural action of BAS. According to AASHTO specification, the amount of transverse steel is set as default for bridges. A biaxial bending model could validate the default transverse reinforcement requirements per AASHTO. A comprehensive study of the overall performance of a bridge approach slab is conducted by applying finite difference method on a soil supported plate. Results from the biaxial bending model with arbitrary voids representing potential asymmetric soil washout are discussed later. The potential use of the simplified uniaxial bending for conservative estimate of design moments is also discussed by comparing results from the uniaxial and biaxial models.

4.2.1 Theory and Principle

Compared to uniaxial bending, bending in both directions is considered which allows studies of internal forces due to arbitrary voids (that are not along the entire width). The moment in x direction involves the curvature in x and also the curvature in y direction while using the plate bending theory for biaxial bending. Thus, in finite difference solution, the fourth derivative of displacement for the node under

consideration is dependent in displacement on displacement of 12 nodes in its vicinity both along the x and y directions (Figure 4-11) as highlighted in Eqn. 4-7.

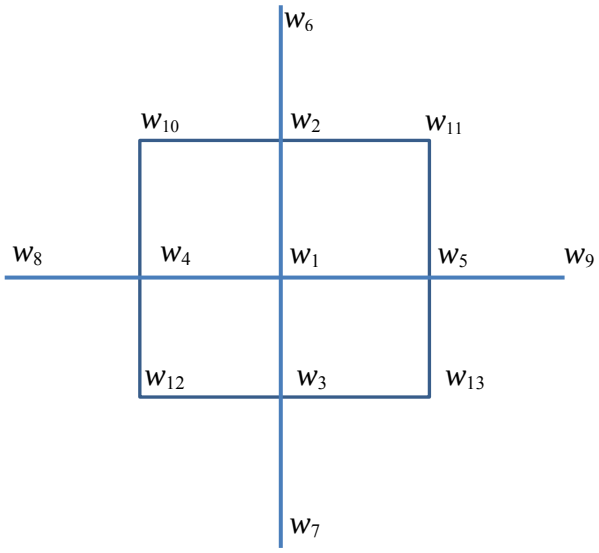

Figure 4-11 Biharmonic finite difference operator applied at w_1

$$\nabla^2(\nabla^2 w) = \frac{\partial^4 w}{\partial x^4} + 2\frac{\partial^4 w}{\partial x^2 \partial y^2} + \frac{\partial^4 w}{\partial x^4}$$
$$= 20w_1 - 8w_2 - 8w_3 - 8w_4 - 8w_5 + w_6 + w_7 + w_8 + w_9 + 2w_{10} + 2w_{11} + 2w_{12} + 2w_{13}$$

(Eqn. 4-7)

Governing differential equation for the BAS treated as a plate is given by Eqn. 4-8:

$$-D \cdot \nabla^2(\nabla^2 w) = q - kw \qquad \text{(Eqn. 4-8)}$$

The BAS is modeled as a plate is 38 ft wide and 25 ft long, and is discretized into 0.5 ft by 0.5 ft elements. X axis is in the longitudinal traffic direction and y axis is in the transverse direction. The size of element is consistent with that used in the uniaxial analysis. External uniform load and soil support is applied at nodal loads using the elemental tributary areas. External concentrated forces are converted to equivalent nodal loads applied as the vertices of the element under consideration.

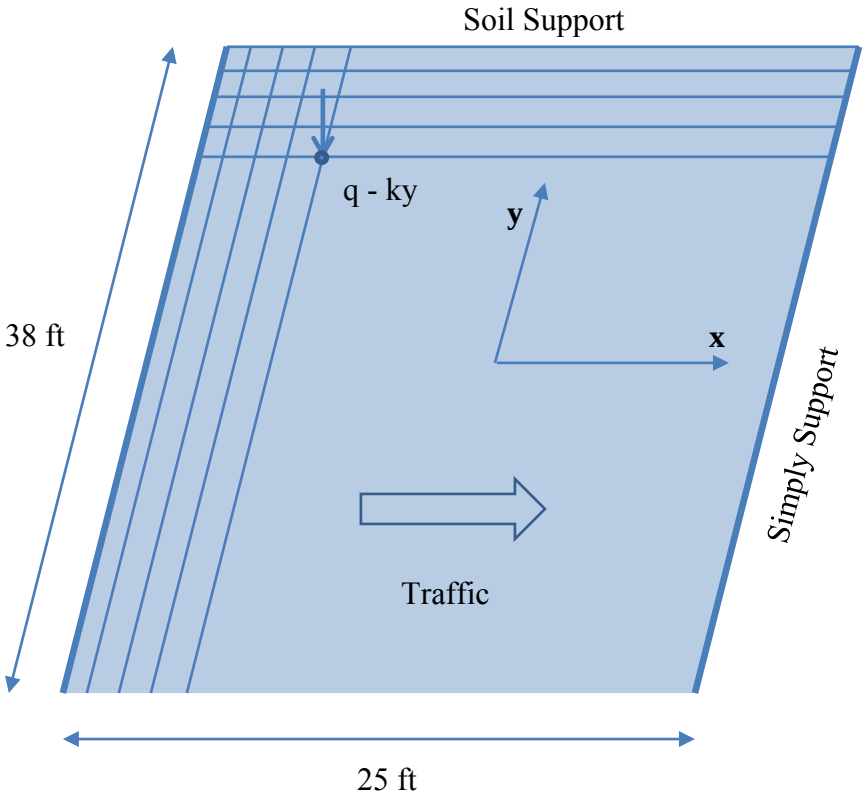

Figure 4-12 Schematic illustration of the biaxial finite difference model of the BAS

The two longitudinal edges are soil supported (free to displace and rotate in the x, y and z direction). Displacements of internal nodes of the plate, which are two rows inside from every edge, are used to apply appropriate edge boundary conditions as described in Appendix D.

Boundary conditions are used to develop operators along the edges and in its vicinity. For simple supported edge, bending moment perpendicular to the edge and displacement are zero; for soil supported edge, bending moment and shear are zero; for corner nodes, twisting moment is zero. Nodes on the simple supported edge are not included in the formulation of the stiffness matrix because these nodes have prescribed displacement of zero. Detailed derivations of the relations between nodal

displacements along all edges are presented for the various edge and corner boundary conditions in Appendix D.

4.2.2 Modeling of AASHTO Loading Conditions

AASHTO specification about loading comprises lane load (of 0.64 kips/ft/lane), design truck (HL93 with axle loads of 8k, 32k, 32k respectively) and design tandem (axle loads of 25k, 25k). The most critical loading condition for the 25 ft long slab is due to a combination of lane load and tandem load. The distance between front wheel and rear wheel of tandem is 4 ft, and that between right and left wheel is 6 ft. Therefore, in the finite difference model, tandem is simulated as four point concentrated loading, the amount of each loading is 12.5 kips. 38 ft wide slab has two lanes, so two tandems are included in this finite difference model. Based on the results from uniaxial bending, for both ends simple supported, tandem located at the mid span will result in the maximum design bending moment; for one end simple supported the other soil supported, tandem need to be located near the abutment end to produce maximum design moments in the BAS. The location is also a parameter in the biaxial bending model in order to check the consistency with uniaxial bending.

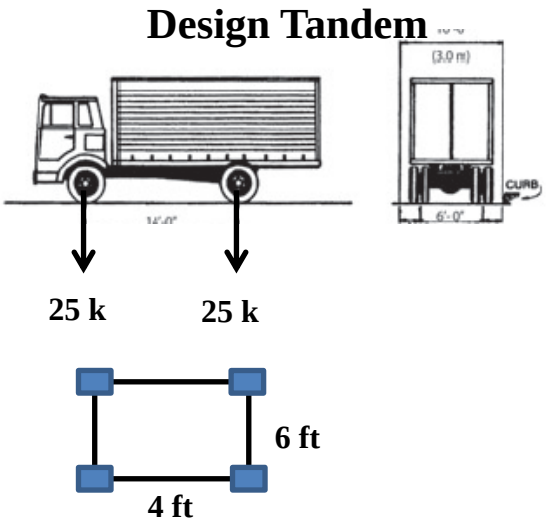

Figure 4-13 Design tandem loading per AASHTO specification

4.2.3 Modeling of Soil Washout

Different from the beam problem, there are many possibilities of soil washout in the biaxial plate problem. In the investigation, two kinds of washout are employed to explore the effect of voids location and the size. Strip washout simulates a strip through the width of the slab (equivalent to the beam problem). Circular washout simulates localized voids, which have been observed under normal service conditions at many BAS sites. The parameters related to washout are programmed in MATLAB so that users can set arbitrary voids size at user-selected locations. The critical tandem location for slab with partial soil support will change from the original location for fully soil supported slab. It becomes very complicated for biaxial bending problem to find the critical location, so critical tandem location from the uniaxial problem will be used as guides for obtaining comparable solutions for the biaxial model of the BAS.

4.2.4 Detailed Cases Studies and Observations

Based on the theory developed in the previous sections, the biaxial finite difference model for BAS-ES is developed using MATLAB. Six cases including different pavement end supports, different tandem loading patterns and different washout patterns are studied as a part of the biaxial bending BAS model. Table 4-1 provides highlights of the parameters used in each of the case studies and Figure 4-14 provides plan schematics of the different loading cases.

Table 4-1 Details of the finite difference biaxial model cases studied

Cases No.		1	2	3	4	5	6
End Support		Nonyielding	Yielding	Nonyielding	Yielding	Yielding	Yielding
Washout	Type	Strip	Strip	Strip	Circle	Circle	Circle
	Location (ft)	Left edge at x = 0	Left edge at x = 0	Left edge at x = 0	Center at x = 8 y = 8	Center at x = 8 y = 19	Center at x= 12.5 y = 19
	Size (ft)	L = 5	L = 5	L = 5	D = 15	D = 15	D = 15
Tandem location*		x1 =12.5 x2 = 12.5	x1 =12.5 x2 = 12.5	x1 = 8 x2 = 15	x1 =12.5 x2 = 12.5	x1 =12.5 x2 = 12.5	x1 =12.5 x2 = 12.5

**Tandem location in the transverse direction for every case is at the center of each lane.*

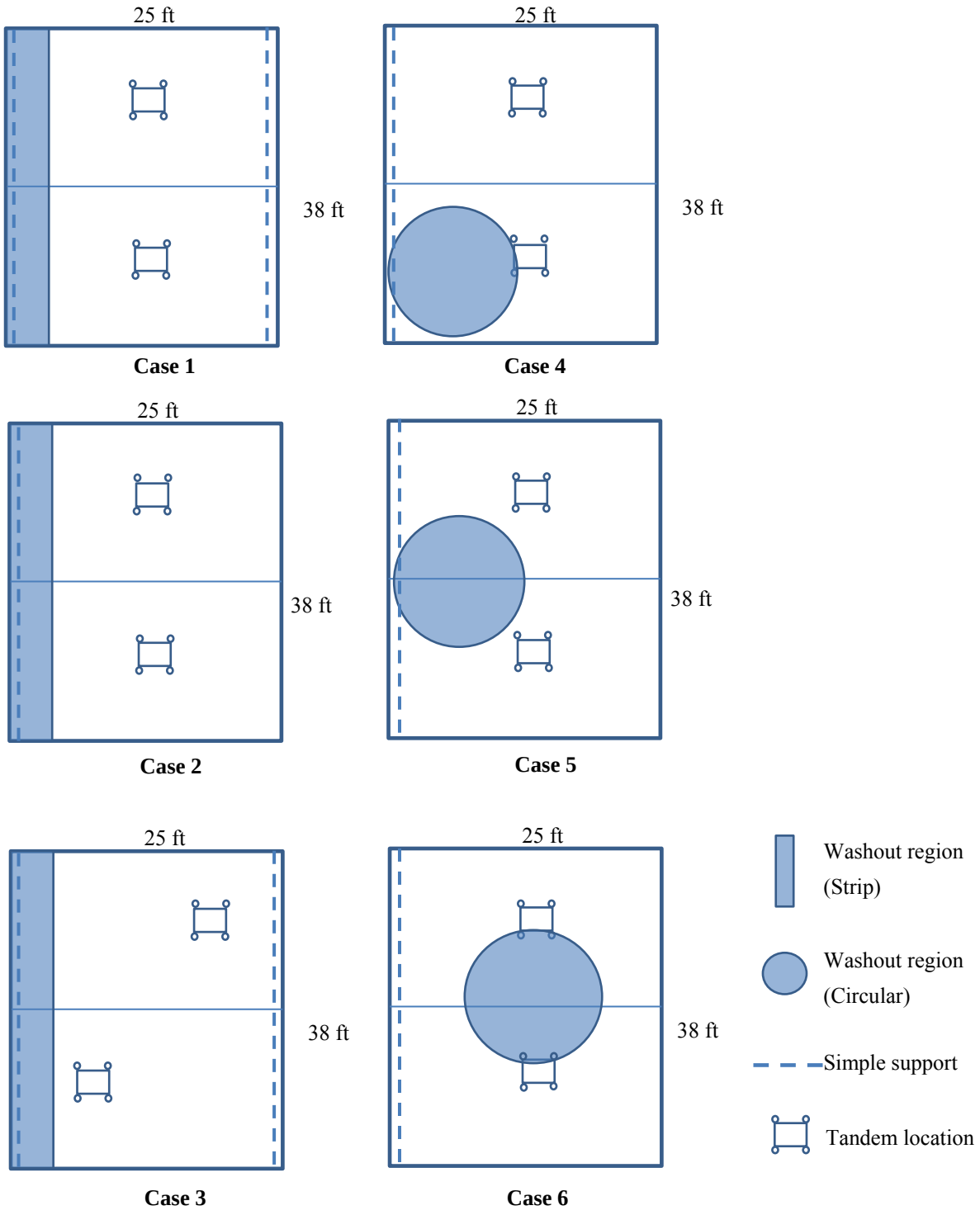

Figure 4-14 Plan views of BAS Cases 1 to 6

Results for the six cases studied are summarized in Table 4-2.

Table 4-2 Maximum moments and deflection from biaxial solutions for six cases

Cases No.	1	2	3	4	5	6
Service I w_{max} (in)	0.26	0.31	0.25	0.41	0.36	0.42
Strength I $M_{x,max}$ (k-in/ft)	396.9	303.4	395.2	439.0	368.9	378.8
Strength I $M_{y,max}$ (k-in/ft)	179.7	168.6	183.0	219.3	201.6	221.3

1. Influence of yielding and nonyielding pavement end support conditions.

Case 1 and Case 2 are compared here to demonstrate the effect of yielding versus nonyielding pavement end support on BAS. Deflection response and longitudinal moment diagram of BAS are presented in Figures 4-15 - 4-18 for the two cases. Maximum deflection of nonyielding support (Case 1) occurs at the middle span of BAS, which is smaller than the maximum deflection of BAS with yielding support (Case 2) at the pavement end. Meanwhile, maximum longitudinal moment of BAS with nonyielding support is larger compared to that of BAS with yielding support. It can be observed, due to the larger deformation and hence increased soil support, biaxial bending model of BAS with yielding pavement end support generates smaller

internal forces (moment and shear).

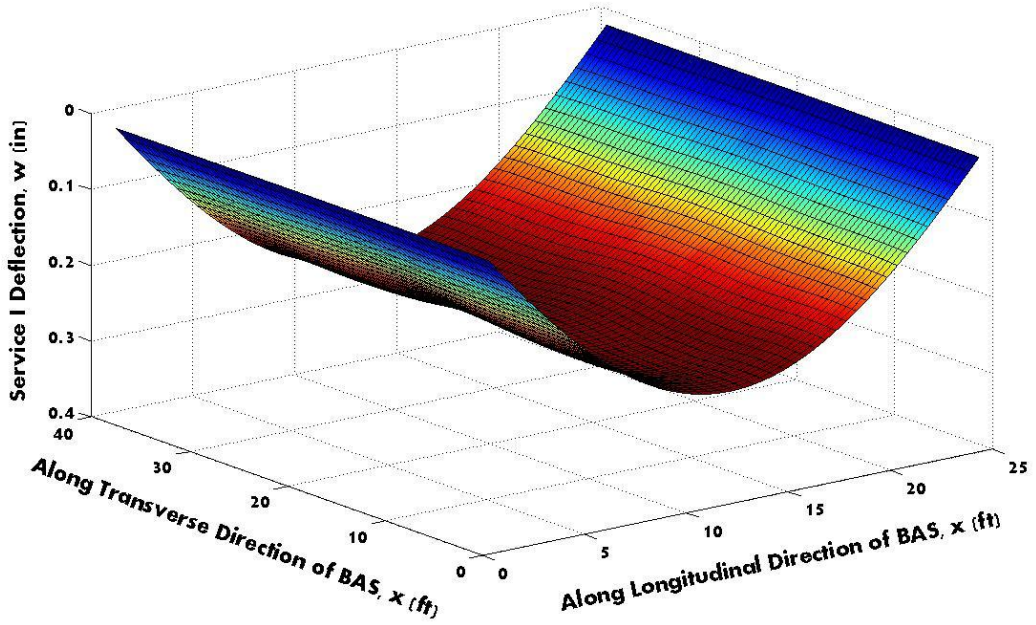

Figure 4-15 Service I deflection (w) response for Case 1

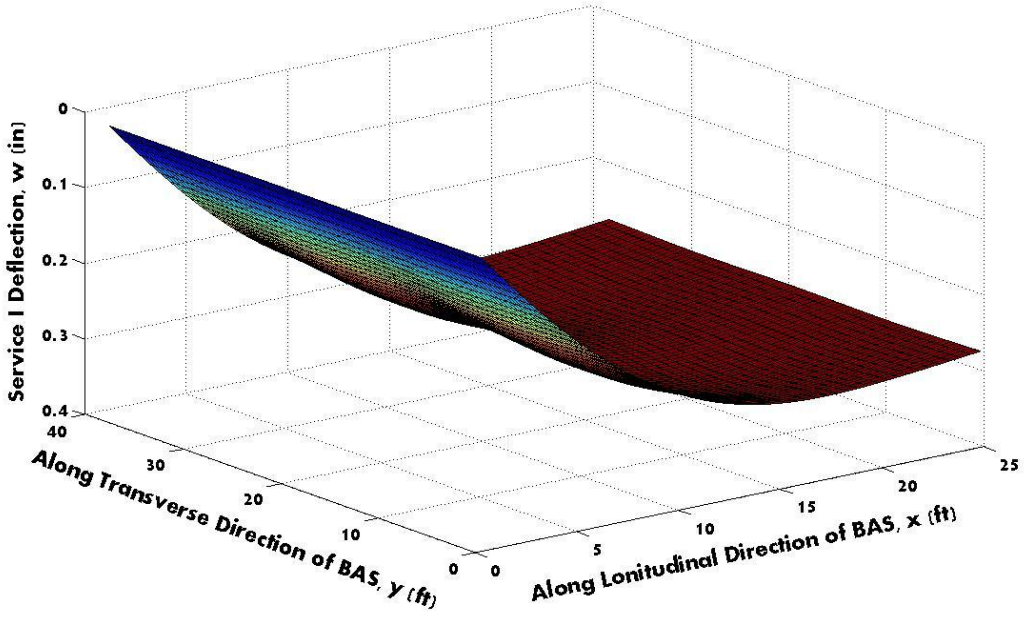

Figure 4-16 Service I deflection (w) response for Case 2

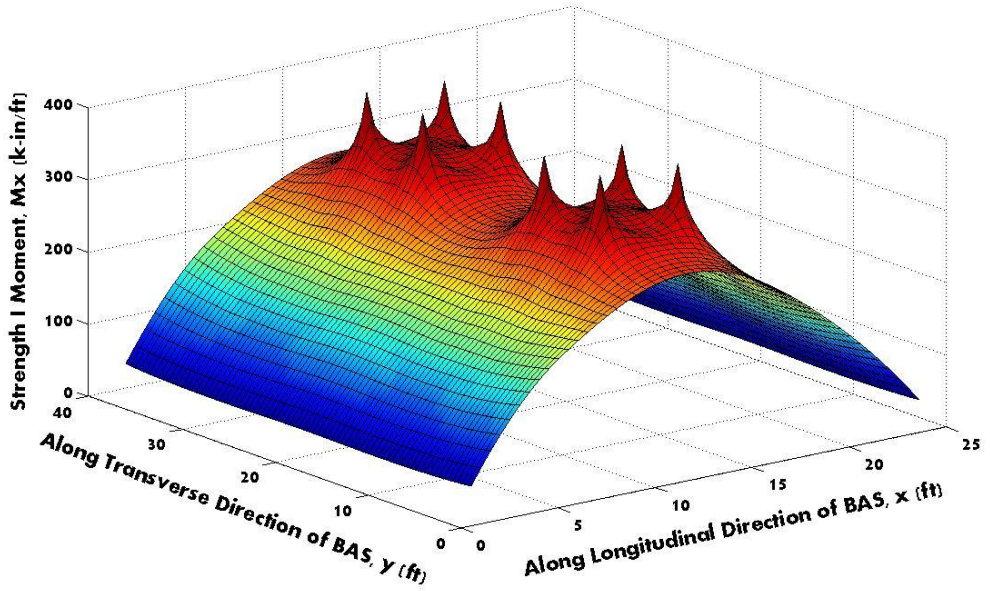

Figure 4-17 Strength I moment (M_x) diagram for Case 1

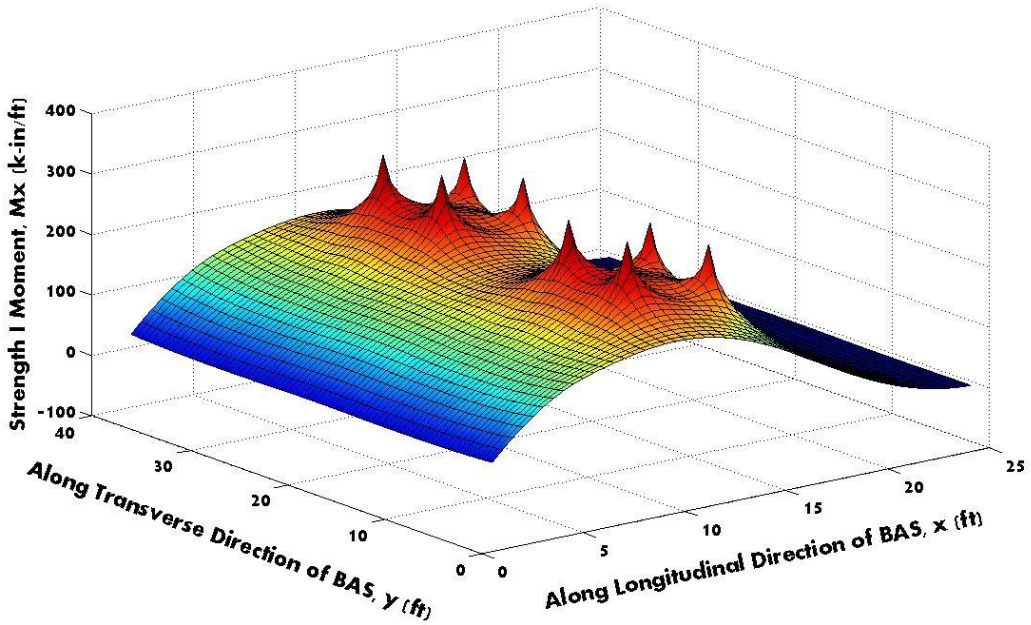

Figure 4-18 Strength I moment ($M_{x)}$ diagram for Case 2

2. Effect of unsymmetrical tandem loading

Deflection response and transverse moment diagram of Cases 1 and 3 are shown in Figures 4-19 - 4-21. BAS loaded unsymmetrically with two design tandems (case 3) has slighter smaller maximum deflection and maximum longitudinal moment compared to a BAS with symmetric tandem loading (case 1) for same washout geometry and pavement end support conditions. It can be observed from these figures that the tandem location does not make much difference on the internal forces in the BAS most likely due to the dominant effect of the uniform lane load and slab self-weight. The slightly greater transverse moment in Case 3 compared to Case 1 indicates the torsional effect due to the asymmetrical loading of the tandem.

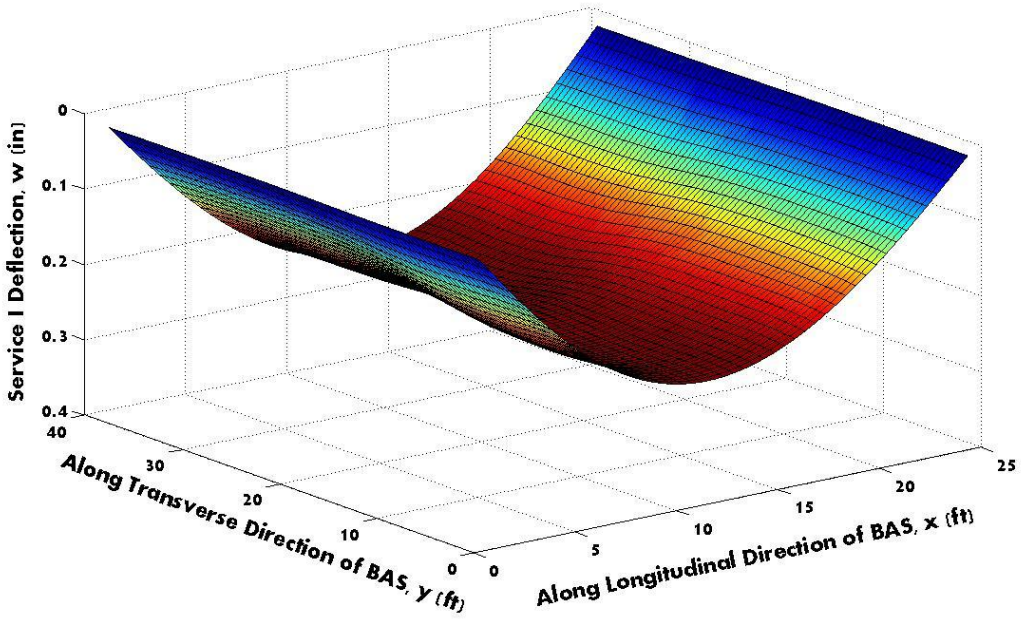

Figure 4-19 Service I deflection (w) response for Case 3

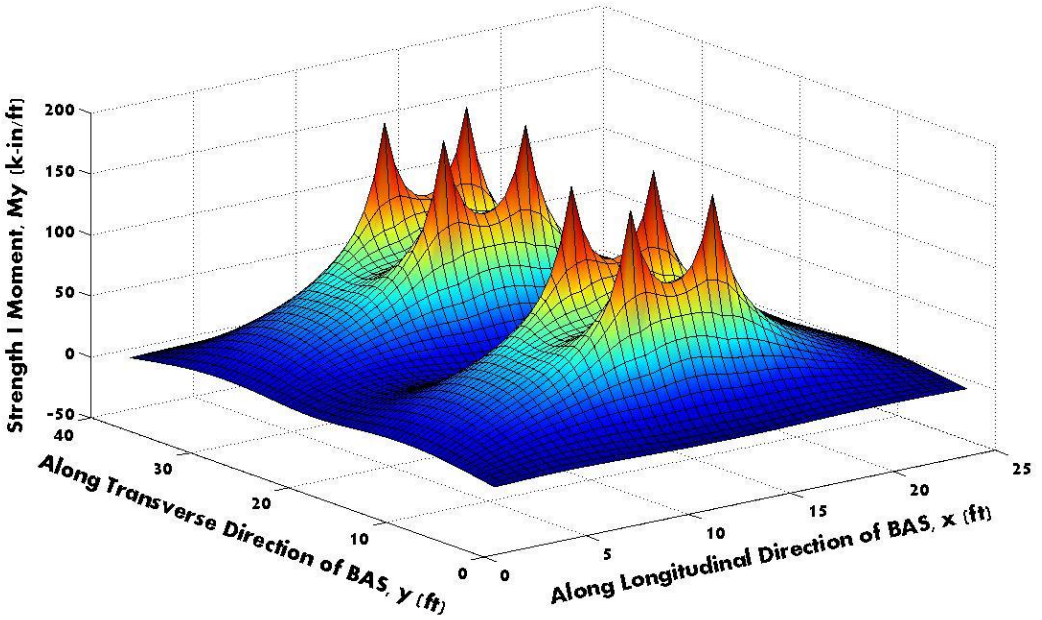

Figure 4-20 Strength I moment (M_y) diagram for Case 1

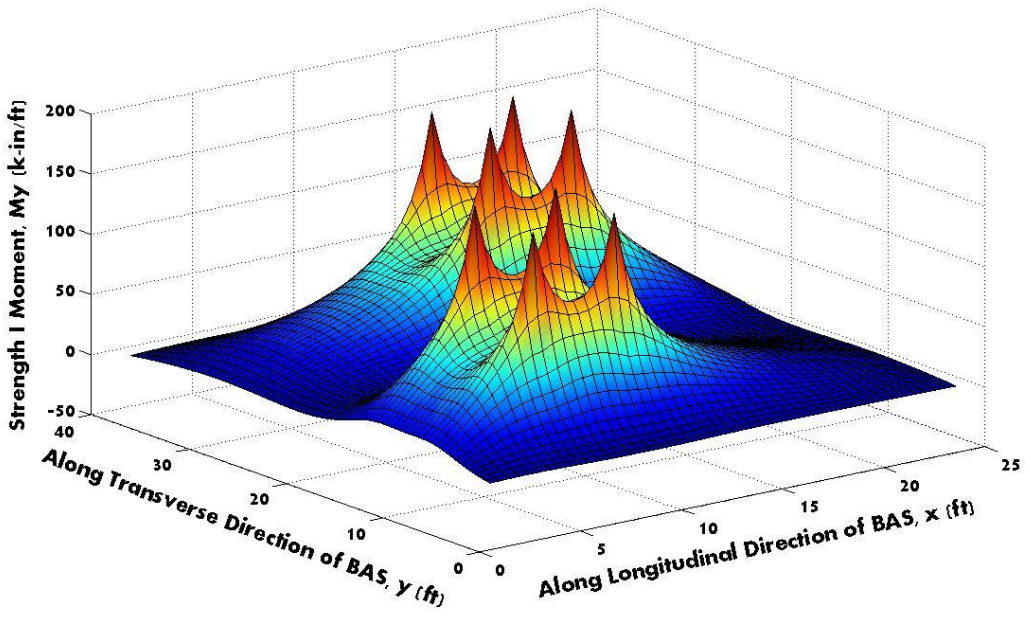

Figure 4-21 Strength I moment (M_y) diagram for Case 3

3. Effect of location of circular washout.

Figures 4-22 - Figure 4-24 show the longitudinal moment diagrams for Cases 4 - 6, respectively. In the three cases, the size circular washout is identical while the locations are different (see Figure 4-14). The peak moment occurs at the location of tandem in all three cases. Case 4 has the largest longitudinal moment as observed in Table 4-2, revealing that less support from the slab in the vicinity can be gained because the washout is located near the BAS edge in the transverse direction. Case 5 generates the smallest internal forces in the BAS due to the location of circular washout (the middle of slab from transverse direction and near the abutment longitudinally). Although same as Case 5 in the transverse direction, circular washout in Case 6 at the midspan of the slab results in larger moment and deflection just like Case 4, which indicates the BAS with tandem loading in the region of soil washout generates the large internal forces.

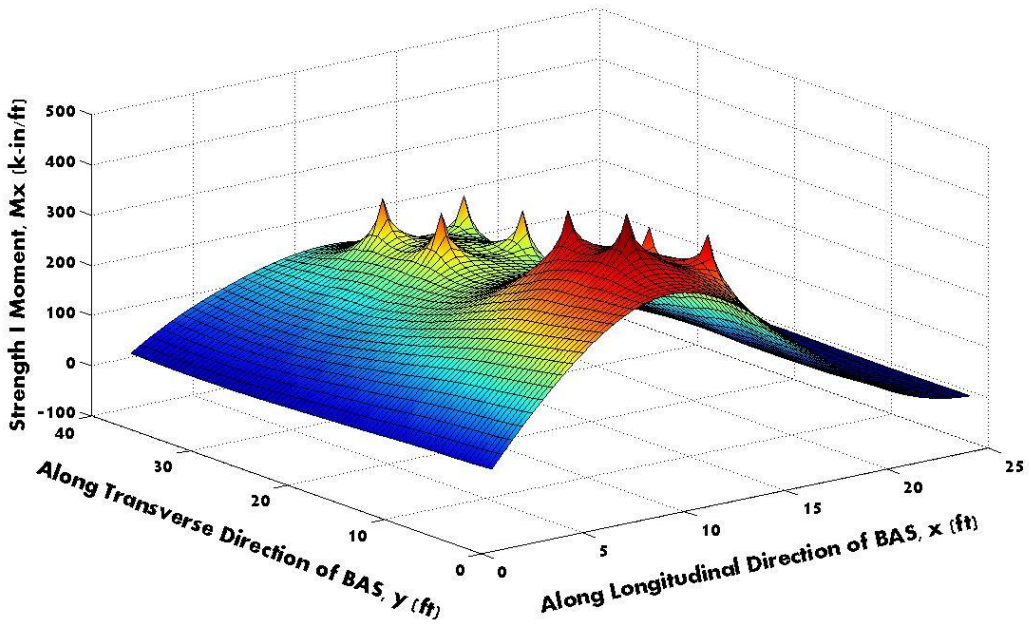

Figure 4-22 Strength I moment (M_x) diagram for Case 4

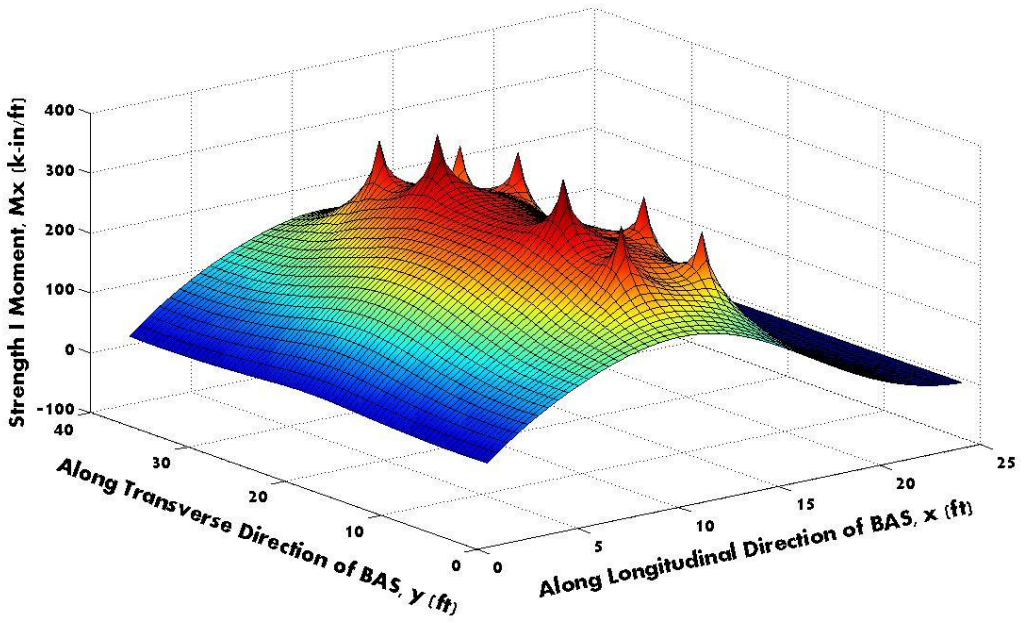

Figure 4-23 Strength I moment (M_x) diagram for Case 5

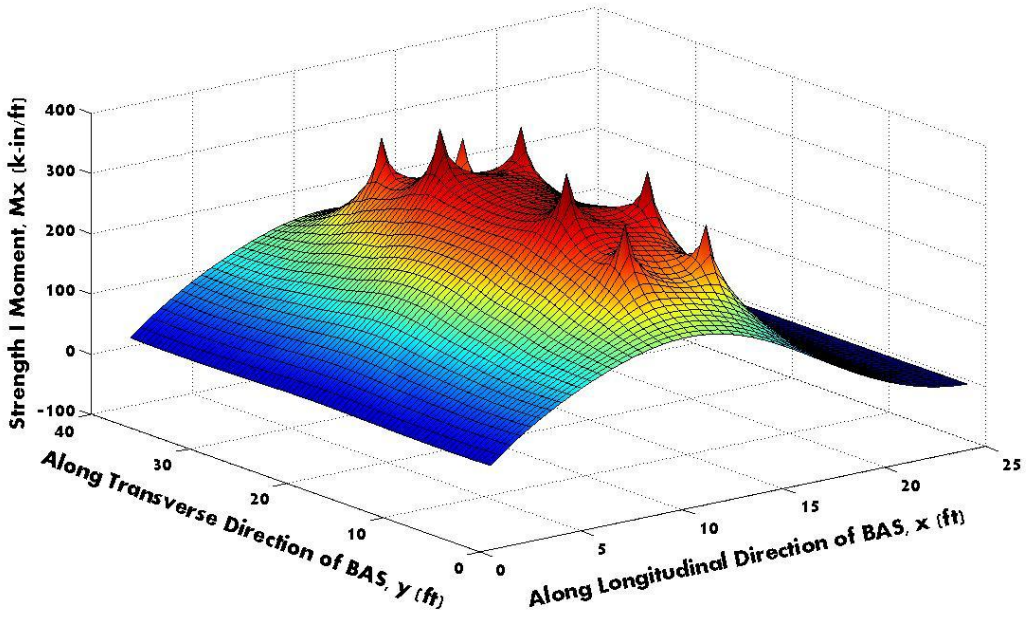

Figure 4-24 Strength I moment (M_x) diagram for Case 6

4. Influence of the strip washout compared to circular washout

Case 2 and Case 5 are compared to the influence of strip washout and circular washout, given comparable washout area, soil and support conditions. Figure 4-25 and Figure 4-26 show the transverse moment diagrams from these two cases. From the figures, it can be seen that moments at the outside axle of tandem are at the same level of moments at the inner axle of tandem for BAS with strip washout. While for BAS with circular washout, moments at inner axle of tandem are larger because the circle washout is at the center in the transverse direction. From the statistics provided in Table 4-2, circular washout leads to more deflection, larger longitudinal and transverse moment of BAS compared to strip washout. Thus the localized circular washout appears to generate more internal forces compared to strip washout.

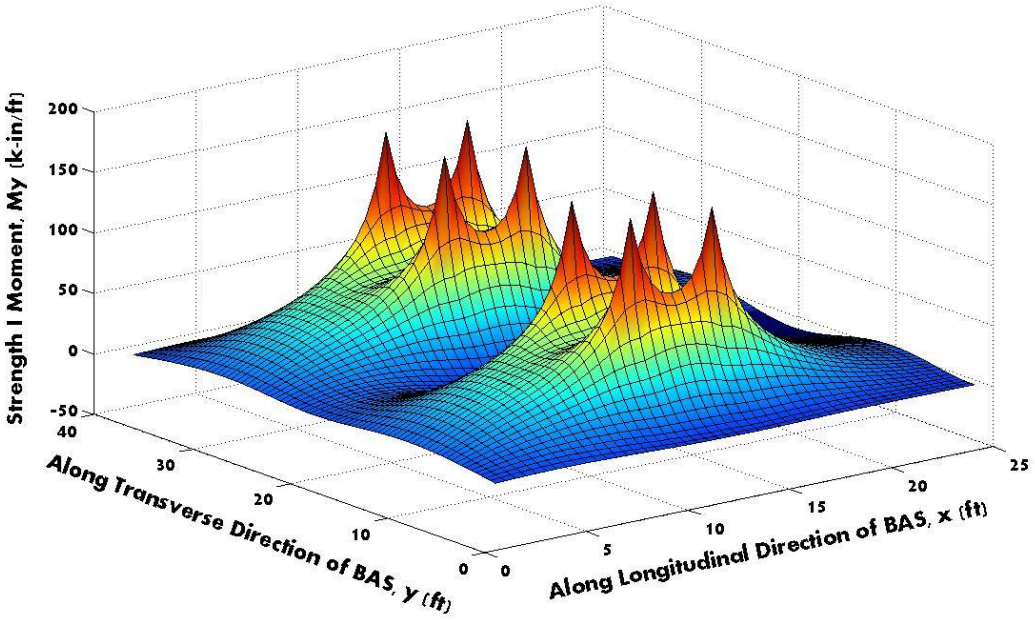

Figure 4-25 Strength I moment (M_y) diagram for Case 2

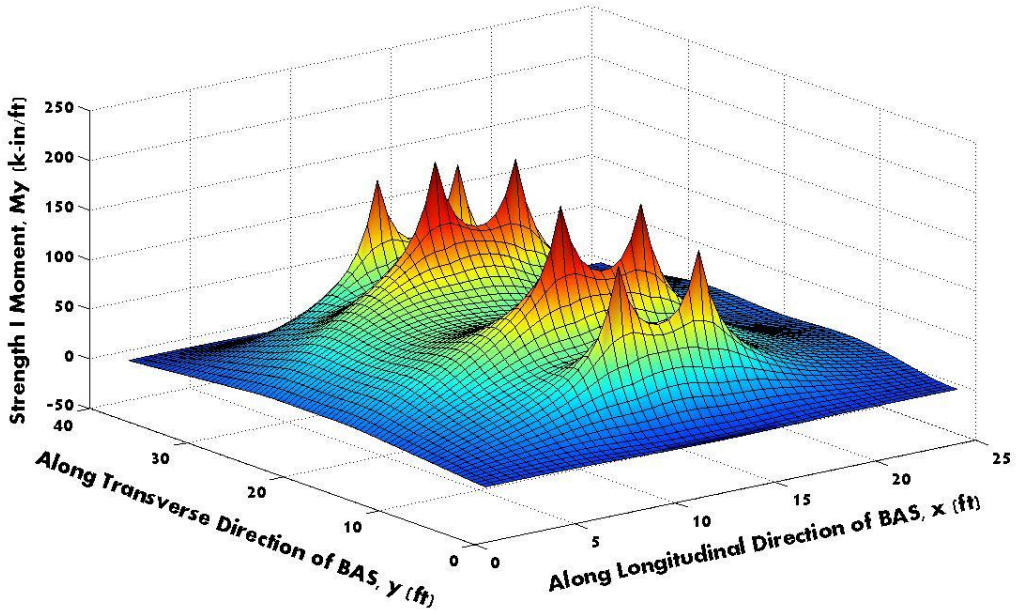

Figure 4-26 Strength I moment (M_y) diagram for Case 5

4.3 Comparison of Results from Uniaxial and Biaxial Bending Models

4.3.1 Comparison of Simply Supported BAS-ES with Continuous Soil Support in Uniaxial and Biaxial Models

Strength I moments and Service I deflections from uniaxial and biaxial models are compared in the Figure 4-27. The solutions are for the cases of continuous soil support (no washout) and a nonyielding pavement end. The primary vertical axis represents the maximum Strength I moment and the secondary vertical axis represents the maximum Service I deflection. These two parameters are plotted with respect to the soil modulus on the abscissa using a logarithmic scale.

The figure shows that all of the curves are descending with the increase of soil modulus. Deflection of biaxial model is always smaller than that of uniaxial model

regardless of soil stiffness, and the difference decreases to zero when soil modulus increases to 500 psi/in. When the soil modulus is below 20 psi/in representing loose sand, uniaxial model predicts a higher moment than biaxial model, with a maximum difference of approximately 200 kips-in/ft. However, the result reverses when soil modulus exceeds 20 psi/in, with the maximum difference of 60 kip-in/ft at dense sand of 500 psi/in. It can be observed that the uniaxial model is conservative when being employed to solve for deflection of BAS-ES for all soil stiffness and for Strength I moment for weak soil (soil stiffness20 psi/in or smaller).

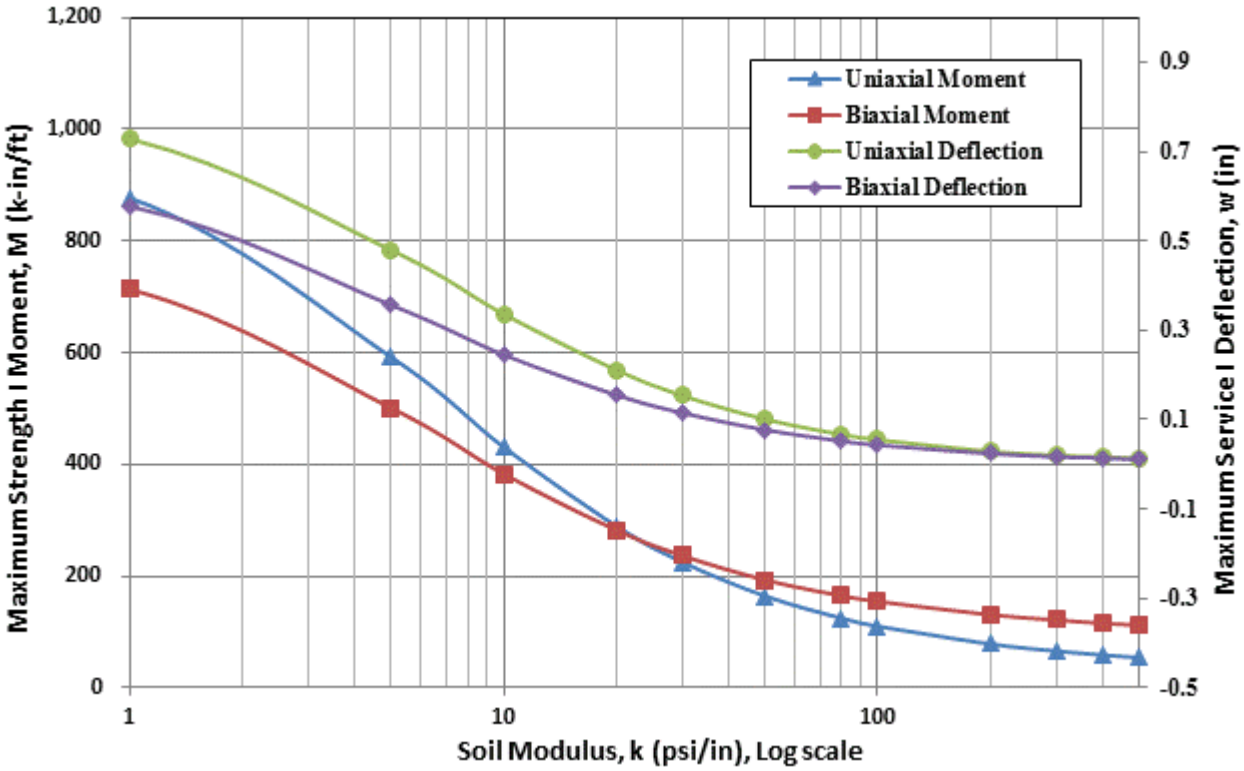

Figure 4-27 Comparison of maximum moment and maximum deflection completed using uniaxial and biaxial models of BAS.

4.3.2 Comparison of BAS-ES with Partial Soil Support in Uniaxial and Biaxial Models

The bar charts included in Figure 4-28 show results from uniaxial bending and biaxial bending solutions for BAS with partial soil support (includes washout) and nonyielding pavement end support. There are three sets of data corresponding to soil moduli of 10 psi /in, 30 psi /in and 100 psi/in which represent very loose sand, loose sand and medium stiffness sand respectively. The hatched bars represent results from uniaxial bending solution while solid bars represent results from biaxial bending solution. For each type of soil (very loose sand, loose sand and medium stiffness sand respectively), washout length from 0 to 25 ft in increments of 5 ft have been denoted on the figure)

With very few exceptions the maximum moments from biaxial solutions are smaller than that of uniaxial solutions, typically ranging from 80 percent to 100 percent. For example, the cases of 0 to 25 ft washout for a 10 psi/in soil modulus, 5 to 25 ft washout for a 30 psi/in soil modulus and 10 to 25 ft washout for a 100 psi/in soil modulus. It can be concluded that maximum moments predicted using the biaxial model are smaller when soil modulus is low and there is significant washout (i.e., weak soil support). However, for more substantial soil support (little or no washout) and stiff soil modulus, maximum moment predictions using the biaxial model are marginally larger than those from the uniaxial model. Maximum moment predictions for uniaxial bending model hence can be routinely used for BAS-ES design as it is conservative, particularly for weak soils and larger washout lengths.

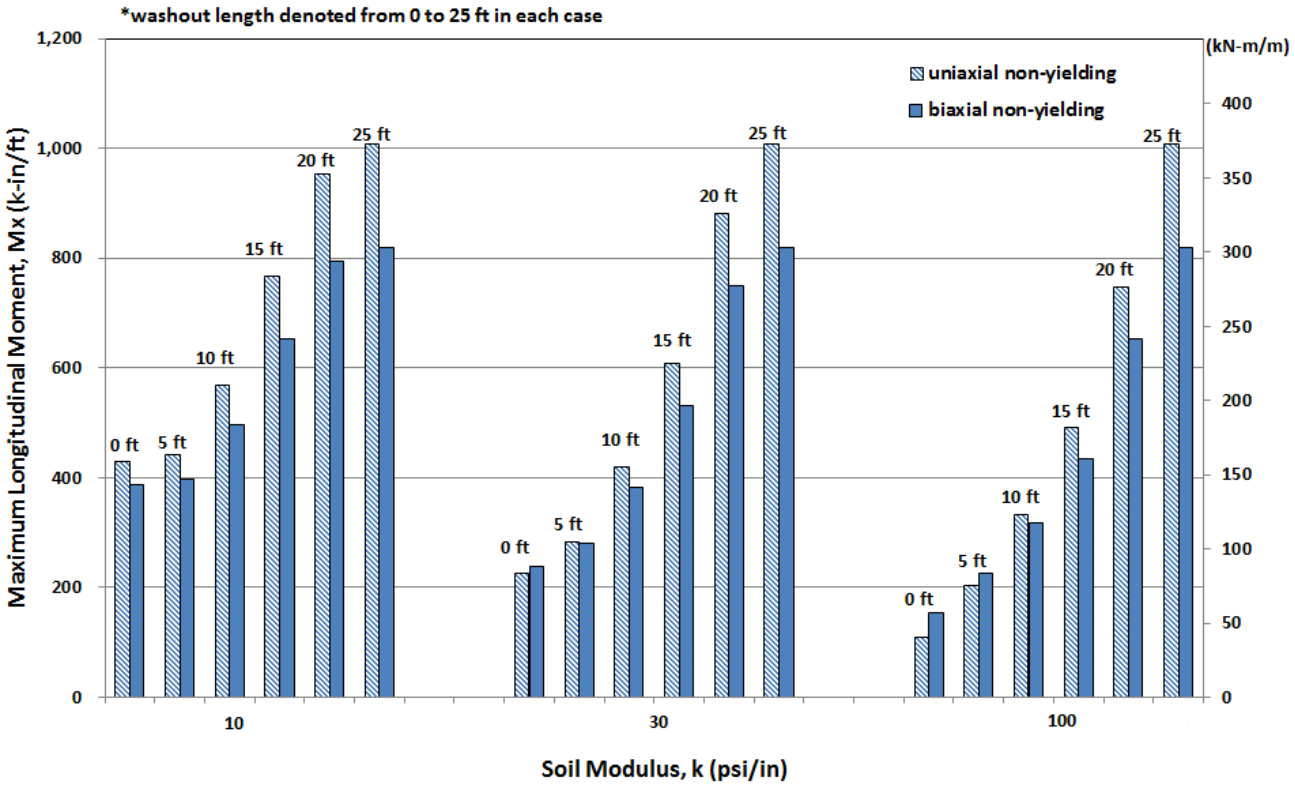

Figure 4-28 Comparison of maximum moments from uniaxial bending and biaxial bending models assuming non-yielding pavement end support, insert values indicating washout lengths from 0 to 25 ft, in increments of 5 ft.

4.3.3 Comparison of Uniaxial and Biaxial Models of BAS-ES with Yielding Pavement End Support

The bar charts included in Figure 4-29 show the results from uniaxial bending and biaxial bending models with partial soil support and yielding pavement end support. The hatched bars represent results from uniaxial beam bending solutions while solid bars represent results from from biaxial plate bending solutions. For every soil moduli shown in the figure, the bars are in order of washout length rom0 ft to 25 ft (in 5 ft increments).

Like for the non-yielding solutions discovered in Section 4.4.2, maximum moment predictions from the uniaxial bending model are conservative, particularly for weak soil and larger washout lengths and hence can be conveniently used in BAS in BAS-ES design (instead of the more complex biaxial bending model).

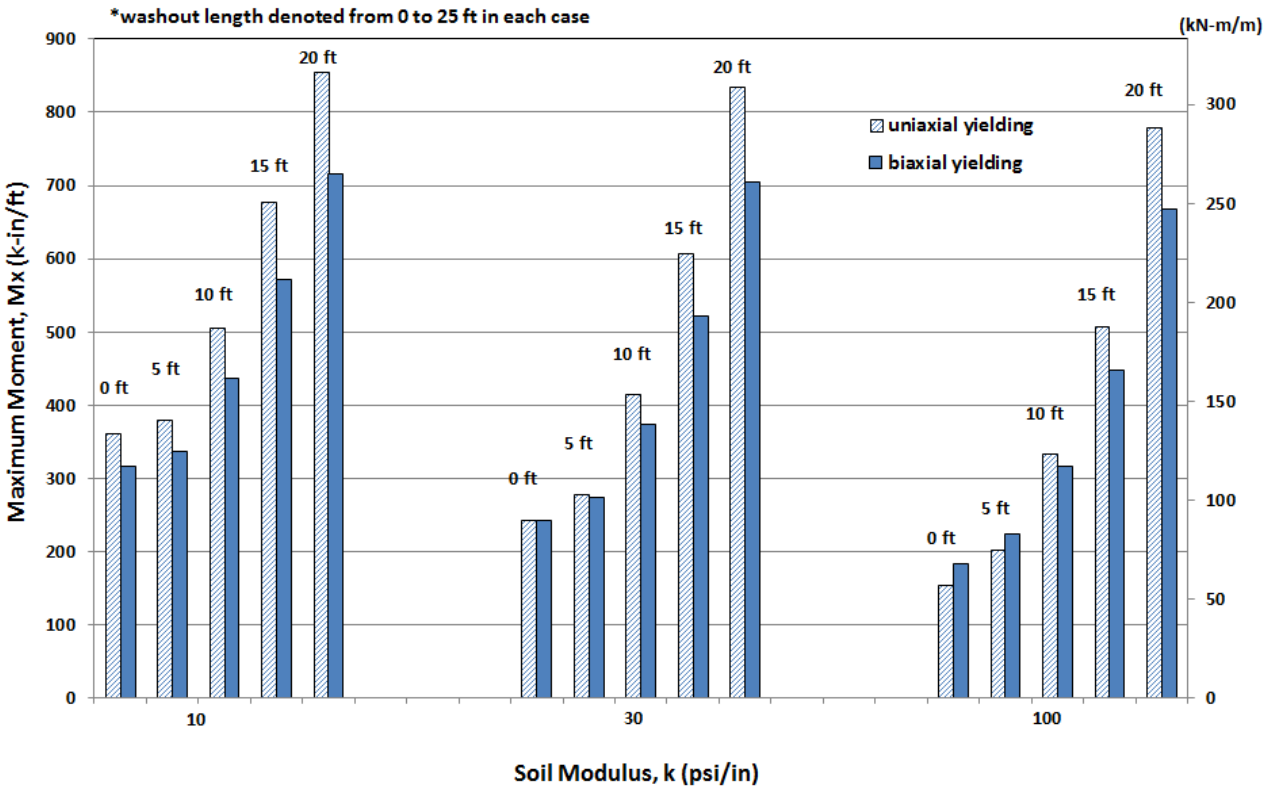

Figure 4-29 Comparison of maximum moments from uniaxial bending and biaxial bending models assuming yielding pavement end support, insert values indicating washout lengths from 0 to 25 ft, with increments of 5 ft.

4.3.4 Summary Results

Moment Reduction Factor

Table 4-3 summarizes the Moment Reduction Factor for various soil moduli, washout lengths and end support conditions for the uniaxial and biaxial bending models. It can be simply used as a reference of practical design. Internal moment can be predicted by

multiplying easy computed moment of simply support slab with the moment reduction factor, which is selected based on soil conditions, pavement end support and preferred models of uniaxial or biaxial bending.

Table 4.3-3 Moment Reduction Factor

	Uniaxial		Biaxial	
Washout Length, ft	Nonyielding Pavement End Support	Yielding Pavement End Support	Nonyielding Pavement End Support	Yielding Pavement End Support
k = 10 psi/in				
0	0.43	0.36	0.38	0.32
5	0.44	0.38	0.39	0.33
10	0.56	0.50	0.49	0.43
15	0.76	0.67	0.65	0.57
20	0.95	0.85	0.79	0.71
25	1.00		0.81	
k = 30 psi/in				
0	0.22	0.24	0.24	0.24
5	0.28	0.28	0.28	0.27
10	0.42	0.41	0.38	0.37
15	0.60	0.60	0.53	0.52
20	0.88	0.83	0.74	0.70
25	1.00		0.81	
k = 100 psi/in				
0	0.11	0.15	0.15	0.18
5	0.20	0.20	0.22	0.22
10	0.33	0.33	0.31	0.31
15	0.49	0.50	0.43	0.45
20	0.74	0.77	0.65	0.66
25	1.00		0.81	

End Reinforcement Detailing

Because the sleeper slab always yields, the use of it is not recommended per the BAS-ES design as the entire slab is designed assuming soil support. As a result, the use of a Type 4 rock ditch liner is recommended to contain and confine the Type 5

aggregate ditch holding the perforated drain pipe (see the highlighted rectangle in Fig. 17). Also, to allow for some two-way flexural action at the end of the slab (the end opposite to the bridge abutment), simulating the effect of a sleeper slab, additional transverse reinforcement in the bottom layer (8 #4 bars at 3" centers in the end zone) is recommended. Stirrup reinforcement (#4 bars @ 12" centers) similar to those provided in the sleeper slab is also recommended for the end zone of the BAS-ES. The additional transverse reinforcement will provide post-cracking stiffness for transverse bending and limit widths of potential longitudinal cracks in end zone. The stirrup reinforcement will provide confinement for the concrete in the end zone, improving overall slab performance in transverse bending. Additional reinforcement details are illustrated in the highlighted portion of Fig. 17

Figure 4-30 End zone details of the BAS-ES design

CHAPTER 5 COST ANALYSIS

5.1 Initial Construction Cost

Providing a cost effective bridge approach slab is the essential objective of this research. Since the new BAS-ES design calls for reduced material with increased flexural stiffness and longer permissible slab lengths between expansion joints, it is very economical. Both initial construction cost as well as life cycle cost incorporating agency user cost have been computed and reported to demonstrate that the BAS-ES design alternate is cost effective.

Table 5-1 includes a comparison of reinforcements used in the standard MoDOT BAS design with that used in BAS-ES. Soil condition, material and geometry of slabs are same. As can be observed, the main steel reinforcement designed to resist longitudinal flexure is greatly reduced. The sleeper slab function to ensure a two-way action of the plate has been fulfilled by the replaced end reinforcement detailing, which decreases the amount of concrete needed for the pavement end support for the BAS.

Table 5-1 Reinforcement details in the current and proposed BAS designs

Reinforcement	Standard MoDOT BAS Design	BAS-ES Design
Main Steel	Top #7 @ 12”	Top #5 @12”
	Bottom #8 @ 5”	Bottom #6 @ 8”
Distribution Steel	Top #4 @ 18”	Top #4 @ 12”
	Bottom #6 @ 15”	Bottom #4 @ 12”
Sleeper Slab	3’-0”×18”	Not used
	3 #6 Top and 3 #6 Bottom	
	Stirrup #4 @12”	
End Reinforcement	Not used	2’-0” ×12”
		8 #4 @ 3” Bottom Transverse
		Stirrup #4 @12”

Table 5-2 includes the cost estimates based on pay-item details provided by MoDOT. The primary reductions in cost for the BAS-ES design come from reduced reinforcement costs and the elimination of sleeper slabs. The estimated initial construction costs for the standard MoDOT BAS is $60,912 (including sleeper slabs) versus the new BAS-ES design proposed of $45,375. This represents a savings of approximately 25%. All cost estimates are for two approaches to the bridge, i.e. one at each end of the bridge.

Table 5-2 Comparison of initial construction cost in the current and proposed BAS designs

		Standard MoDOT BAS	BAS-ES Design
Base Preparation	Quantity yd^3	23	23
	Cost $	2,051	2,051
Form Approach Slab	Quantity ft^2	176*	176
	Cost $	4,256	4,256
Set Steel	Quantity lb	20,310	9,730
	Cost $	21,683	10,508
Pour Approach Slab	Quantity yd^3	83	70
	Cost $	33,706	28,561
Total Cost $		60,912	45,375

**It is assumed that the sleeper slabs are poured after excavation per MoDOT practice without specifically forming them.*

5.2 Life Cycle Cost Analysis

Life Cycle Cost Analysis (LCCA) is used to evaluate several bridge approach slab alternatives considering initial construction, service life, rehab method and user cost. As a part of this project, LCCA as it relates to BAS is well defined in master thesis of Balu, G. (2011) and report of MoDOT (2010). Important conclusions relating to this research are made:

1. Based on a discount rate, expenditures that related to the use of approach slab in a life cycle are converted into present value of approach slab for four design alternatives, which are Standard MoDOT BAS Design, BAS-ES Design, Fully Precast Prestressed BAS Design and CIP Topped PC Prestressed BAS Design
2. Considering only of initial construction cost, BAS-ES is economically superior to other alternatives.

3. BAS-ES has the lowest life cycle cost among the four alternatives while only agency cost are considered.
4. Even when user cost is incorporated, BAS-ES has the lowest life cycle cost for low volume traffic areas as rural bridges. Only when user costs are considered for urban bridges (high volume traffic), does the precast prestressed BAS options become less expensive than BAS-ES.

CHAPTER 6 SUMMARY AND CONCLUSIONS

6.1 Summary Conclusions

It has been demonstrated through analytical modeling that incorporation of elastic soil support significantly reduces the design moments required for the bridge approach slab. This design is referenced in this thesis as BAS-ES (as Bridge Approach Slab incorporating Elastic Soil Support). The "elastic soil support" assumption not only leads a a cost effective design of the BAS, but also represents more realistically the physical mechanisms of support of these slabs under normal service. Numerical extension of the uniaxial model to systematically study potential washout of soil using the finite difference method indicates that significant reductions in design moments can still be conservatively assumed even with as much as 20% washout of soil support. Results from the further extension of the BAS-ES design to include the effect of biaxial bending (plate on elastic support) validate all the observations from the uniaxial model. Results from the biaxial model also demonstrates that with very few exceptions (very stiff soil, very little washout, or very localized washout near BAS edges), the uniaxial bending model results in conservative design moment predictions and hence the user-friendly Excel-based Visual Basic application for uniaxial BAS-ES design can be used effectively for implementing BAS-ES design in almost all practical situations. More specific conclusions from various aspects of this research are discussed in detail in the following sections of this chapter.

6.2 Conclusions from the Parametric Studies

Conclusions from exhaustive parametric studies conducted using the analytical as well as finite difference uniaxial bending models are summarized in this section. The parameters include: soil stiffness, washout length and location, thickness of the BAS, and conditions of support at the pavement end of the BAS (yielding or nonyielding support at the sleeper slab, which is itself resting on deforming soil).

6.2.1 Soil Stiffness

Internal forces of the bridge approach slab are very much dependent on the stiffness of supporting soil, an aspect ignored by most conventional BAS design practices, including the analysis used in the Standard MoDOT BAS design (BAS treated as a simply supported beam). Increasing soil modulus of the supporting soil from 0 psi/in to 500 psi/in allows the design moment to drop from 1,000 kip-in/ft (the design moment for a simply supported BAS with no soil support) to almost negligible magnitudes. The model also predicts that small improvements to stiffness of loose sand (like improving stiffness from 10 psi/in to 20 psi/in through treatments like fly ash stabilization) can be very helpful in reducing design moments significantly. The investigation also confirmed that shear capacities of BAS significantly exceed shear force demands and typically do not govern BAS design (unlike design moments). Deflections predicted in the BAS-ES models are understandably lower than those computed in conventional simply supported analysis of BAS.

6.2.2 Soil Washout and Associate Parameters

Length and location of soil washout investigated in both uniaxial and biaxial analysis resulted in similar findings with regard to the influence of washout of soil beneath the BAS on the design moments. Larger soil washout (more soil area washed out) results in more severe demands on design moment capacity as well as in larger deflections of the BAS. Soil washout at or near the middle span of the approach slab can result in the maximum design moment. Design shear force is relatively less affected by soil washout when the washout is near midspan than when the washout is closer to the bridge abutment. The influence of localized washout (in the biaxial bending model) versus strip washout (washout of a rectangular strip along the entire width of the BAS) in the numerical models is discussed in a layer section.

6.2.3 Thickness of Approach Slab

Standard MoDOT BAS as well as BAS-ES designs proposed here are 12” deep. The main difference in the BAS-ES design is that it requires less reinforcing steel due to the reduced design moments resulting from soil support. The interesting observation on BAS-ES designs is that with more flexible slabs (slab thickness of 10” instead of the standard 12”), there is a reduction in design moment. This is attributed to increased deflections in the more flexible slab thereby enhancing the soil support. Although an advantage from a flexural design perspective, the increased deflections may make very flexible slabs impractical from a functional standpoint. AASHTO deflection limits need to be met to ensure good ride quality in flexible BAS.

6.2.4 Pavement End Support Conditions: Yielding versus Nonyielding support

Standard BAS designs are typically supported at the pavement end on sleeper slabs which are assumed to be nonyielding (assumed to not deflecet vertically). This is not representative of their in-service performance, as the sleeper slabs themselves are supported on elastic soil that may additionally consolidate due to age and movement of moisture. It was observed from this study that yielding pavement end support for BAS resulted in increased deflections and smaller design moments compared to pavement end supports that were treated as nonyielding (rigid with no vertical displacements). Again the smaller design moment is attributed to increased deflection resulting in larger soil support.

6.3 Conclusions

6.3.1 Shear Force, Bending Moment and Deflections

Analysis of 12” bridge approach slab under standard AASHTO loading shows that the dominating factor in design is the bending moment capacity rather than shear force capacity, regardless of whether the BAS is analyzed conventionally as a simply supported beam or using the BAS-ES design approach where elastic soil support is incorporated. As a result much of the results and discussions are focused on the flexural moment capacity and not the design shear capacity. Reinforcements are governed by

Strength 1 checks. Maximum deflections are computed for Service 1 loads to ensure the requirement of AASHTO deflection limits (limited to span/200).

6.3.2 Analytical Model

The analytical model developed facilitates closed-form solutions of internal forces and slab deflections for finite sized BAS subjected to uniaxial bending, symmetric loading and uniform soil support. This model can be readily implemented in a Excel based user-friendly application. The ease of design of BAS-ES using this application allows significant cost savings as demonstrated earlier. The closed-form solution however cannot be used to study unsymmetrical loading such as those required for soil washout investigation. However the analytical model was extended using finite difference implementation to facilitate solutions for unsymmetrical loading from unsymmetrical soil washout.

6.3.3 Finite Difference Method

Finite difference method is effective in BAS problem solving as an advanced analysis method to deal with unsymmetrical cases and washout situations in addition to analytical solution. Nodal displacements of the BAS are the primary variables employed in this method. Soil washout was successfully described using length of washout and washout location from bridge abutment. Customized load cases were analyzed successfully including automation to allow critical placement of washout parameters and design tandem loads to produce maximum design moments. In addition,

the numerical implementation also allowed study of pavement end support conditions (nonyielding or constrained from vertical displacement versus yielding or unconstrained for vertical displacement).

6.3.4 Uniaxial and Biaxial Bending

Strip model assuming uniaxial bending of beam is a simplified analysis technique typically used for designing bridge approach slabs. The BAS-ES design also uses such uniaxial bending models because of their relative simplicity and adequacy for most practical designs of BAS. In order to validate this more simplistic approach of BAS design, a biaxial bending model using plate theory wassuccessfully developed with free edges (no displacement boundary conditions) at approach slab shoulder and a simple supported edge at longitudinal ends. Comparisons between uniaxial and biaxial bending models show that internal forces from uniaxial solutions are more conservative with very few exceptions as discussed earlier. Thus, uniaxial beding solutions can be used instead of the more complicated biaxial bending solutions for all practical designs.

6.3.5 End Reinforcement Detail

End reinforcement detail is proposed for use with BAS-ES as an alternative to the use of sleeper slabs at the pavement ends. This provides for increased transverse stiffness and two-way bending action that is normally provided by the sleeper slab. This design

modification greatly reduces initial construction cost and also makes the transition from the pavement to the BAS a smoother one.

6.3.6 Cost Analysis of BAS-ES

It has been shown that BAS-ES can save as much as 25% in initial construction cost. BAS-ES is also the most cost-effective as far as life cycle costs are concerned among four design options studied (Standard MoDOT BAS design, BAS-ES design, Fully Precast Prestressed BAS design and CIP Concrete Topped PC Prestressed BAS design) if only agency costs are included. Even when users costs are also considered, BAS-ES still remains the most cost-effective design alternate for low traffic demands (like rural bridges). Only when user costs for high traffic corridors are considered (like urban bridges), the precast prestressed designs become more competitive than BAS-ES.

6.3.7 Implementation of BAS-ES and BAS Washout Solutions

An Excel file embedded with Visual Basic Application that emphasizes a user-friendly interface was generated in this project for practical use by engineers. Parameters for soil condition and loading scenario can be input based on experience to get deflection profile as well as moment and shear diagrams of approach slab. Furthermore, reinforcement can be calculated according to strength and service checks from AASHTO. A VBA program is also available to generate cases systematically for better understanding of the relation between soil stiffness, washout, loads and behavior of approach slab.

6.4 Future Work

Theoretical work to predict internal forces of bridge approach slab given supporting soil and loading conditions has been completed as a part of the project to optimize approach slab design. Geotechnical and hydraulic research needs to be performed to guarantee desired soil stiffness and limit amount of soil to that can potentially wash away. Field experiment is expected in the future that can compare the recorded experimental data with theoretical results based on appropriate assumptions.

In general, this thesis has provided a way to design approach slab cost effectively considering soil support. With savings realized in initial construction cost saved from use of BAS-ES design, it is possible to support cost increases to improve soil support through many currently available soil treatments (such as fly ash stabilization etc.). Long-term service performance of BAS-ES designs in urban and rural traffic corridors will also be useful to validating the theoretical life-cycle cost estimates generated here.

REFERENCE

American Association of State Highway and Transportation Officials (AASHTO), 2004, *LRFD Bridge Design Specifications*, Washington, D.C.

American Concrete Institute (ACI), 318-08, "Building Code Requirements for Structural Concrete and Commentary", 2008.

Missouri Department of Transportation, *Bridge Design Manual, Online Version*, 2010

Abu- Hejleh, N., Hanneman, D., White, D.J., Wang, T. and Dsouri, I. (2006), "Flowfill and MSE bridge approaches: performance, cost, and recommendations for improvements", Colorado Department of Transportation, Report No. CDOT-DTD-R-2006-2, February, 2006.

Bakeer, R. M., Shutt, M. A., Zhong, J. Q., Das, S. C. and Morvant, M. (2005), "Performance of pile-supported bridge approach slabs", *Journal of Bridge Engineering*, Vol. 10, No. 2, March, 2005.

Balu, G., "Precast Prestressed Bridge Approach Slab - Cost Effective Designs", M.S. Thesis (Advisor: Prof. V. S. Gopalaratnam), Dept. of Civil and Environmental Engr., University of Missouri-Columbia, December 2011, 127 pp.

Briaud, Jean-Louis, James, Ray W and Hoffman, Stacey B. (1997), TRB, NCHRP Synthesis of Highway Practice 234: Settlement of Bridge Approaches "Bump at the End of the Bridge". National Academy Press, Washington, D.C., 1997.

Cai, C. S., Shi, X. M., Voyiadjis, G. Z. and Zhang Z. J. (2005), "Structural performance of bridge approach slabs under embankment settlement", *Journal of Bridge Engineering*, ASCE, Vol. 10, No. 4, July 2005.

Chai, Y. H., Chen, Y. T., Hung, H. J. and Rocha, G. N. (2009), "Service performance of bridge approach slabs and replacement alternatives", *Key Engineering Materials*, Vol. 400-402, pp 949-955, Trans Tech Publications, Switzerland, 2009.

Chen, D. H., Nazarian, S. and Bilyeu, J. (2006), " Failure analysis of a bridge embankment with cracked approach slabs and leaking sand", *Journal of Performance of Constructed Facilities*, ASCE, Vol. 21, No. 5, October, 2007.

Du, L. X., Arellano, M., Folliard, K. J., Nazarian, S. and Trejo, D. (2006), "Rapid-setting CLSM for bridge approach repair: a case study", *ACI Materials Journal*, ACI, Vol. 103, No. 5, September-October, 2006.

Dupont, B. and Allen, D. (2002), "Movements and settlements of highway bridge approaches", Kentucky Transportation Center, IHRB Project HR-1085, June, 2002

Ganesh, T, Gopalaratnam, V.S., Halmen, C., Ajgaonkar, S., Ma, S., Balu, G., and Chamarthi, R., (2010), "Bridge Approach Slabs for Missouri DOT Looking at Alternative and Cost Effective Approaches", Report TRyy0915 to Missouri Department of Transportation, August 2010, 249 pp.

Gopalaratnam, V., Balu, G., Ravi, S. Ch., (2011) "Life cycle cost analysis of bridge approach slab alternatives", Personal communication (draft paper -- to be submitted).

Groom, M. K. (1993), "Geotextile reinforced bridge approach embankment", Oregon Department of Transportation, March, 1993

Ha, H. S., Seo, J. and Briaud, J.L (2002), "Investigation of settlement at bridge approach slab expansion joint: survey and site investigations", Texas Department of Transportation, FHWA/TX-03/4147-1, Texas, August, 2002.

Hetenyi, M.(1967), *Beams on Elastic Foundation*, The University of Michigan Press.

Hoppe, E. J (1999), "Guidelines for the use, design and construction of bridge approach slabs", Virginia Transportation Research Council, Final Report VTRC 00-R4, November, 1999

James, R. W., Zhang, H. P., Zollinger, D. G., Thompson, L. J., Bruner, R. F. and Xin, D. P.(1990), " A study of bridge approach roughness", Texas Department of Transportation, FHWA/TX-91/1213-1F, November, 1990.

Kramer, S. L. and Sajer, P. (1991), " Bridge approach slab effectiveness", Washington State Department of Transportation, Report No. WA-RD 227.1, December, 1991.

Lenke, L. R. (2006), "Settlement issues-bridge approach slabs", New Mexico Department of Transportation, NM04MNT-02, December, 2006

Lin, K. Q. and Wong, I. H. (1999), "Use of deep cement mixing to reduce settlement at bridge approaches", *Journal of Geotechnical and Geoenvironmental Engineering*, ASEC, Vol. 125, No. 4, April, 1999.

Long, J. H., Olson, S. M., Stark, T. D. and Samara, E. A. (1998), "Differential movement at embank-bridge structure interface in Illinois", *Journal of the Transportation Research Board*, Page 53-60, January, 1998.

Ma, S. and Gopalaratnam, V. S. (2011), "Bridge approach slab analysis and design incorporating elastic soil support", Personal communication (draft paper -- to be submitted)

Mekkawy, M. M., White, D. J., Suleiman, M. T. and Sritharan, S. (2005), "Simple design alternatives to improve drainage and reduce erosion at bridge abutments", Proceedings of the 2005 Mid-Continent Transportation Research Symposium, Ames, Iowa, August, 2005

Merritt, D. K., Miron, A. J., Rogers, R. B. and Rasmussen, R. O. (2007), "Construction of the Iowa Highway 60 precast prestressed concrete pavement bridge approach slab demonstration project", Iowa Department of Transportation, IHRB Project HR-1085, Iowa, July, 2007.

Nassif, H., Abu-Amra T. and Shah N. (2003), " Finite element modeling of bridge approach and transition slabs", New Jersey Department of Transportation, FHWA NJ 2002-007, September, 2002.

Puppala, A. J., Saride, S., Archeewa, E. Hoyos, L. R. and Nazarian, S. (2008), "Recommendations for design, construction, and maintenance of bridge approach slabs: synthesis report", Texas Department of Transportation, FHWA/TX-09/0-6022-1, April, 2009.

Robinson, J. L. and Luna, R. (2004), "Deformation analysis of modeling of Missouri bridge approach embankments", ASCE GeoTRANS Conference, Los Angeles, 2004

Roman, E., Khodair, Y. and Hassiotis, S. (2002), "Design details of integral bridges", proceedings of the Engineering Mechanics Conference, New York, May, 2002

Roy, S. and Thiagarajan, G. (2007), " Nonlinear finite-element analysis of reinforced concrete bridge approach slab", *Journal of Bridge Engineering*, ASCE, Vol. 12, No. 6, November 2007.

Seo, J. B. (2002), "The bump at the end of the bridge: an investigation", A Doctoral Dissertation, Texas A&M University, December, 2003.

Shi, X. M., Cai, C. S., Voyiadjis, G. and Zhang, Z. J. (2005), " Design of ribbed concrete approach slab based on interaction with the embankment", *Transportation Research Record: Journal of the Transportation Research Board*, No. 1936, pp. 181-191, Washington, D. C., 2005.

Timoshenko, S. P. and Goodier, J. N.(1951), *Theory of Elasticity* , McGraw-Hill Book Company, 2nd Ed.

Timoshenko, S. P. and Woinowsky-Krieger, S.(1959), *Theory of Plates and Shells*, McGraw-Hill Book Company, 2nd Ed.

White, D. J., Mekkawy, M. M., Sritharan, S. and Suleiman, M. T. (2007), " "Underlying" causes for settlement of bridge approach pavement systems", *Journal of Performance of Constructed Facilities*, ASCE, Vol. 21, No. 4, August 2007.

Wong, H. K. W. and Small, J. C. (1994), "Effect of orientation of approach slabs on pavement deformation", *Journal of Transportation Engineering*, ASCE, Vol. 120, No. 4, July/August, 1994

Yeh, S. T. and Su, C. K. (1995), "EPS, flow fill and structural fill for bridge abutment backfill", Colorado Department of Transportation, Report No. CODT-R-SM-95-15, August, 1995

Zhang, H. L. and Hu C. S. (2007), "Determination of allowable differential settlement in bridge due to vehicle vibrations", *Journal of Bridge Engineering*, Vol.12, No. 2, March, 2007

APPENDIX A. DESIGN EXAMPLE OF BAS-ES

A reinforced concrete bridge approach slab 38 ft. wide (for 2-12 ft lanes of traffic, assuming 4 ft wide inside shoulder and 10 ft wide outside shoulder) and 25 ft span assuming continuous elastic soil support is designed. It is assumed that the soil support is provided by weak "soft clay" with a soil modulus parameter, k, of 30 psi/in. Concrete with f'c = 4,000 psi, Ec = 3,605 ksi and γc = 150 pcf is used. Grade 60 conventional reinforcing steel is used. A representative 12" width (b=12") of the slab is considered for computing all design parameters.

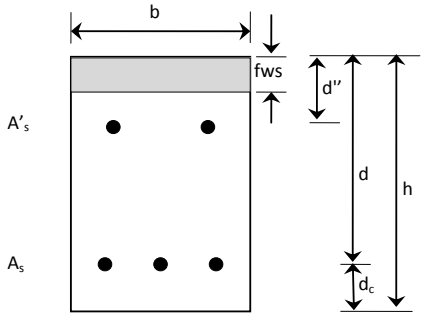

Figure A-1 One-ft-width strip of the BAS considered for the one-way flexural action

Geometric Parameters. The following geometric parameters are used:

$b = 12"$

$fws = 3'$

$d = 9'$

$d_c = 2"$

$h = fws + d + d_c = 14"$

$A_c = bh = 168 in^2 = 1.167\ ft^2$

$I_c = \frac{1}{12} bh^3 = 1728 in^4 = 0.0833\ ft^4$

The tension steel area A_s and the compression steel area $A_s^{'}$ are to be determined.

Loads Considered

Loads considered include dead load, HL-93 lane load, truck load or tandem load (in this case, tandem load dominates and hence is considered instead of the truck load)

The equivalent strip width is computed first.

For two wheels and lane load

$$E = (84 + 1.44\sqrt{L_1 W_1})/12 = (84 + 1.44\sqrt{25 \times 38}) = 10.7' < 12'$$

$$\frac{12W}{N_L} = \frac{38}{2} = 19' > E$$

$$\therefore E = 10.7'$$

Live load distribution factor $\frac{1}{E} = \frac{1}{10.7} lane/ft$

Therefore, for a width of b=12", the two wheel loads and lane loads should be applied and multiplied by the live load distribution factor

Dead Load

The self-weight of the slab is given by the uniformly distributed load, q_{DL}

$$q_{DL} = \gamma_c A_c = 150 \times 1.167 = 175 lb/ft = 0.175 kip/ft$$

Live Load

Lane load equals the uniformly distributed load, q_{La}

$$q_{La} = \frac{1}{10.7} \times 640 = 59.8 lb/ft = 0.0598 kip/ft$$

Tandem load, 2 F, consider impact factor 1.33, and a spacing , *a* of 4'

$$F = 1.33 \times \frac{25}{10.7} = 3.10 kips$$

Moment and Shear Computations

For the slab: $E_c I_c = 3{,}606 \times 1{,}728 in^4 = 43{,}260 kip - ft^2$

For the soil support $k = 30 psi/in \times 12 in = 0.36 ksi = 5.18 kip/ft$

Parameter $\lambda = \sqrt[4]{\frac{51.84}{4 \times 43260}} = 0.1316 ft^{-1}$

a. Moment and shear force under q_{DL} and q_{La}

Using the finite length slab with simple supports subjected to uniform load,

$q_{DL} = 0.175 kip/ft$

$$M_c = 2.0208 kip - ft$$

$$R_A = R_B = 0.7082 kips$$

For the uniform lane load, $q_{La} = 0.0598 kip/ft$

$M_c = 0.6908 kip - ft$

$R_A = R_B = 0.2421 kips$

b. Moment and shear force subjected to two concentrated tandem loads, F

Two equal forces F = 3.1 k spaced at a = 4ft.

$M_c = 7.2410 kip - ft$

$R_A = R_B = -0.0128 kips$

c. Combination loads to provide Strength I and Service I design parameters

Strength I - Factored Load

$$M_u = 1.25M_{c(DL)} + 1.75(M_{c(La)} + M_{c(Ta)})$$
$$= 1.25 \times 2.0208 + 1.75 \times (0.6908 + 7.2410)$$
$$= 16.4067 kip - ft = 196.88 kip - in$$

$$R_A = 1.25R_{A(DL)} + 1.75(R_{A(La)} + R_{A(Ta)})$$
$$= 1.25 \times 0.7082 + 1.75 \times (0.2421 - 0.0128)$$
$$V_u = 1.29 kips$$

Service I – Unfactored Service Loads

$$M_u = M_{c(DL)} + M_{c(La)} + M_{c(Ta)}$$
$$= 2.0208 + 0.6908 + 7.2410$$
$$= 9.9526 kip - ft = 119.43 kip - in$$

$$R_A = R_{A(DL)} + R_{A(La)} + R_{A(Ta)}$$
$$= 0.7082 + 0.2421 - 0.0128$$
$$V_u = 0.94 kips$$

Flexural Design of BAS

The BAS of unit width (b = 1’ = 12”) is designed as a singly reinforced beam,

$$C = T$$
$$0.85 f_c^{'} ba = A_s f_y$$
$$M_u \geq \varphi M_n = \varphi A_s f_y (d - \frac{a}{2})$$
$$\therefore \frac{f_y^2}{2 \times 0.85 f_c^{'} b} A_{s,required}^2 - (f_y d) A_{s,required} + \frac{M_u}{\varphi} = 0$$

In which,

$$\frac{f_y^2}{2\times 0.85 f_c' b} = \frac{60^2}{2\times 0.85\times 4\times 12} = 44.12$$

$$-f_y d = -60\times 9 = 540$$

$$\frac{M_u}{\varphi} = \frac{196.88}{0.9} = 218.75$$

Therefore,

$$A_{s,required} = \frac{540 - \sqrt{540^2 - 4\times 44.12\times 218.75}}{2\times 44.12} = 0.419 in^2$$

Using $A_s = \#6@8" = 0.663 in^2$

$$a = \frac{A_s f_y}{0.85 f_c' b} = \frac{0.663\times 60}{0.85\times 4\times 12} = 1.30 in$$

$$c = \frac{a}{\beta_1} = \frac{1.30}{0.85} = 1.53 in$$

$$\varepsilon_s = \frac{d-c}{c}0.003 = \frac{9-1.53}{1.53}\times 0.003 = 0.015 > \varepsilon_y$$

$$c/d = \frac{1.53}{9} = 0.17 < 0.42$$

$$\varphi M_n = \varphi A_s f_y (d - \frac{a}{2}) = 0.9\times 0.663\times 60\times (9 - \frac{1.30}{2}) = 298.8 kip - in$$

Check for Minimum Reinforcement Requirements

According to AASHTO 5.7.3.3.2, one of the following requirements should be satisfied:

$$\varphi M_n > 1.33 M_u$$

$$\varphi M_n > 1.2 M_{cr}$$

$$\varphi M_n = 298.8 kip - in > 1.33 M_u = 261.85 kip - in$$

$$\varphi M_n = 298.8 kip - in$$

$$> 1.2 M_{cr} = 1.2 f_r Z_b = 1.2\times 7.5\sqrt{f_c'}\times (\frac{1}{6} b h^2)$$

$$= 1.2\times (7.5\times \sqrt{4000}/1000)\times (\frac{1}{6}\times 12\times 11^2)$$

$$= 137.75 kip - in$$

Both checks for minimum reinforcement are okay

Check for Shear Capacity

The factored shear force at ultimate is

$V_u = 1.16\ kips$

V_n Should be the lesser of (per AASHTO 5.8.3.3)

$V_n = V_c + V_s,\ \ V_c = 0.0316\,\beta\sqrt{f_c'}b_v d_v$

$V_n = 0.25 f_c' b_v d_v$

for which,

$d_v = 9 - \frac{a}{2} = 9 - \frac{1.3}{2} = 8.35in$

$b_v = 12in$

Using a conservative value of $\beta = 2.0$

$\varphi V_n > \varphi V_c = 0.8 \times 0.0316 \times 2.0 \times \sqrt{4} \times 12 \times 8.35$

$= 10.13kips$

$> V_u = 1.29kips$

$\varphi V_n = \varphi(0.25 f_c' b_v d_v) = 0.8 \times (0.025 \times 4 \times 12 \times 8.35)$

$= 80.16kips$

$> V_u = 1.29kips$

Both shear capacity checks are okay.

Crack Check for Service I

According to AASHTO 5.7.3.4 the steel stress under Service 1 should satisfy the following requirement:

$$s \le \frac{700\gamma_e}{\beta_s f_s}$$

Where,

$$\beta_s = 1 + \frac{d_c}{0.7(h - d_c)} = 1 + \frac{2}{0.7 \times (11 - 2)} = 1.317$$

The service moment was obtained earlier as:

$$M_c = 119.43 kips - in$$

The longitudinal reinforcements used are listed below:
Top bar: $A_s' = \#5@12'' = 0.307 in^2, (n-1)A_s' = 7 \times 0.307 = 2.149 in^2$
Bottom bar: $A_s = \#6@8'' = 0.663 in^2, nA_s = 8 \times 0.663 = 5.304 in^2$

Transformed cracked elastic section analysis provides:

$$\frac{12c^2}{2} + 2.149(c - 2.3125) = 5.304(8.625 - c)$$

$$6c^2 + 7.453c - 50.72 = 0$$

$$c = 2.35 in$$

Moment of Inertia about N.A.

$$I_{cr} = \frac{12c^3}{3} + 2.149(c - 2.3125)^2 + 5.304(8.625 - c)^2$$

$$= \frac{12 \times 2.35^3}{3} + 2.149 \times (2.35 - 2.3125)^2 + 5.304 \times (8.625 - 2.35)^2$$

$$= 261 in^4$$

Stress in tension steel under Service I condition is given by:

$$f_s = n\frac{M_c}{I_{cr}} y = 8 \times \frac{119.43}{261} \times (8.625 - 2.35) = 22.97 ksi$$

Hence,

$$s = 12 \le \frac{700 \times 1.00}{1.317 \times 22.97} - 2 \times 2 = 19.0$$

Check for crack control is okay

Transverse Distribution Reinforcement

Transverse distribution reinforcement $= 100/\sqrt{L} \le 50\%$ of the longitude reinforcement

when $L = 25 ft$, $100/\sqrt{25} = 20\%$

$$20\% A_s = 0.133 in^2, \quad 20\% A_s' = 0.06 in^2$$

Use $\#4@12''(A_s = 0.196 in^2)$ as bottom and top reinforcement.

Temperature and Shrinkage Reinforcement

Per AASHTO 5.10.8.2, the temperature/shrinkage reinforcement is given by:

$$A_s \geq 0.11 A_g / f_y$$

$$A_s \geq 0.11 \times (12 \times 12)/60 = 0.264 in^2$$

Both A_s and A_s' are larger than $0.264 in^2$. The reinforcement provided is adequate.

APPENDIX B. DETAIL COST OF APPROACH SLAB INCORPORATING ELASTIC SOIL SUPPORT

1. Base preparation cost

Span: 25 ft Width: 38 ft

Productivity	=	25	cub yard /day
Quantity of base preparation	=	23	cub yard /day
Estimated time	=	0.92	days

Base preparation cost is broken up into three items

1) Labor 2) Equipment 3) Material / supplies

1) Labor

	No	Days	Rate	Cost	
a) Operator	2	0.92	471.79	868.09	Unit rate = 37.01 $/ cub yard

2) Equipment

	No	Days	Rate	Cost	
a) Compactor	1	0.92	174.4	160.45	
b) Loader cat	1	0.92	312.74	287.72	
				448.17	Unit rate = 19.11 $/ cub yard

3) Material supplies

	Qty	Rate	Cost	
a) Type V Aggregates	23.5	18.15	417.45	
Adding 10% waste			459.2 $	Unit rate = 19.58 $/ cub yard

Total task cost = 868.09 + 448.17 + 459.2 = 1775.46 $
Overhead is 5% of total cost = 88.77 $
Profit is 10.5% of total cost = 186.42 $

Total cost = 2050.65 $ Unit rate = 87.42 $/ cub yard

2. Form Approach slab

Span: 25 ft Width : 38 ft
Form work Qty: 176 sq ft

Cost of form for BAS is broken down into

1) Labor 2) Equipment 3) Material / supplies

1) Labor

	No	Days	Rate	Cost
a) Foreman	1	1	437	437
b) Laborer	2	1	374.5	749
c) Operator	1	1	471.8	471.8
d) Carpenter	2	1	441.85	883.7
				2541.5 $

2) Equipment

	No	Days	Rate	Cost
a) Loader cat	1	1	312.8	312.8
b) Compressor	1	1	105.4	105.4
c) Generator cat 45 kw	1	1	114.6	114.6
d) Truck 2 ton flatbed	1	1	93.6	93.6
				626.4 $

3) Material supplies

Qty = span * width * 2/9

	Qty	Rate	Cost
a) Forms approach slab(sf)	176.00	1.01	177.76
b) Timber header - 3" x 10"(lf)	103.95	3.26	338.88
			516.64 $

Total cost for this task = 2541.5 + 626.4 + 516.64 = 3684.5 $
Overhead is 5% of total cost = 184.23 $
Profit is 10.5% of total cost = 386.88 $
Total cost = 4255.6 $

3. Set approach slab steel

Productivity = 20000 lbs/day
Quantity = 9730 lbs
Estimated time = 0.49 day

Cost of BAS steel is broken down into
1) Labor 2) Equipment 3) Material / supplies

1) Labor

	No	Days	Rate	Cost
a) Foreman	1	0.49	437.05	214.15
b) Laborer	2	0.49	374.55	367.06
c) Operator	1	0.49	471.59	231.08

d) Iron worker	2	0.49	503.92	493.84

1406.13$ Unit rate = 0.14 $/ lb

2) Equipment

	No	Days	Rate	Cost
a) Loader cat	1	0.49	312.84	153.29
b) Compressor	1	0.49	105.40	51.65
c) Generator cat 45 kw	1	0.49	114.66	56.18
d) Truck 2 ton flatbed	1	0.49	93.52	45.82

306.94 $ Unit rate = 0.03 $/ lb

2) Material supplies

	Qty	Rate	Cost
a) Forms approach slab	9730	0.69	6713.7

Adding 10% waste 7385.07 $ Unit rate = 0.76 $/ lb

Total cost for this task = 1406.13+306.94+7385.07 = 9098.14 $
Overhead is 5% of total cost = 454.9 $
Profit is 10.5% of total cost = 955.3$
Total cost = 10508$ Unit rate = 1.08 $/ lb

4. **Pour approach slab**

Span 25 ft Depth 12 in Width 38 ft

Cost of Pouring BAS is broken down into
1) Labor 2) Equipment 3) Material / supplies

1) Labor

	No	Days	Rate	Cost
a) Foreman	2	2.00	437	1748.00
b) Laborer	8	2.00	374.48	5991.68
c) Operator	2	2.00	471.78	1887.12
d) Carpenter	1	2.00	441.85	883.70
e) Finisher	2	2.00	480.55	1922.20

12432.7 $

2) Equipment

	No	Days	Rate	Cost
a) Loader cat	1	2.00	312.80	625.60
b) Compressor	1	2.00	105.40	210.80
c) Con. B.D.F.	1	2.00	156.00	312.00
d) Con. P.T.R.	1	2.00	982.00	1964.00

c) Generator cat 45

kw	1	2.00	114.60	229.20	
d) Truck 2 ton flatbed		1	2.00	93.60	187.20
e) Truck water		1	2.00	281.00	562.00
					4090.80 $

2) Material supplies

Qty = 2* L* B* D/27

	Qty	Rate	Cost
a) Con. 4000 psi	70.37	106	7459.3
Adding 10% waste			8205.2$

Total cost for this task = 12432.7 + 4090.8 + 8205.19 = 24728.7 $

Overhead is 5% of total cost = 1236.4 $

Profit is 10.5% of total cost = 2596.5 $

Total cost = 28561.6 $

Table B-1 Initial Construction Cost Detail of Standard MoDOT BAS Design and BAS-ES

		Standard MoDOT BAS Design	BAS-ES Design
Base Preparation	Quantity yd^3	23	23
	Cost $	2,051	2,051
Form Approach Slab	Quantity ft^2	176*	176
	Cost $	4,256	4,256
Set Steel	Quantity lb	20,310	9,730
	Cost $	21,683	10,508
Pour Approach Slab	Quantity yd^3	83	70
	Cost $	33,706	28,561
Total Cost $		60,912	45,375

APPENDIX C. BAS-ES SOIL WASHOUT SOLUTIONS

BAS-ES Soil Washout Solutions: Quick User's Guide

Vellore S. Gopalaratnam (Professor) and **Shuang Ma** (Graduate Student)

Department of Civil and Environmental Engineering

University of Missouri-Columbia

October 21, 2010

1. This Quick User's Guide is to accompany Macro-Enabled Excel files with names: ***20ft BAS-ES Soil Washout Solutions.xlsm*** and ***25ft BAS-ES Soil Washout Solutions.xlsm***. The two files are developed for analyzing the influence of soil washout from under BAS-ES (Bridge Approach Slab designed incorporating Elastic Soil Support). The first file is designed for a BAS spanning 20 ft, and the second for a BAS spanning 25 ft. The Excel files are based on a finite difference model detailed in [1]. The length of the "finite element" used in the model in both cases is 0.5 ft (6") so as to provide solutions of comparable resolution for the two span lengths. Visual Basic for Application (VBA) also commonly referred to as a Marco is embedded in these Excel files. Solutions can be obtained provided the user enables the Marco feature in Excel.
2. One can obtain the solutions for deflection, moment and shear-force diagrams along the span of an elastically soil supported BAS subjected to partial or complete washout of soil in one of two ways described below.

2.1 **Specific Solution:** If a specific solution for deflection, moment and shear-force profiles along the length of the BAS is desired for a given wash-out location, wash-out length and tandem location along the span, one can input appropriate geometry, material, washout parameters and tandem location (in the appropriate yellow cells of the first worksheet named ***General***), to get all the necessary solutions. The solutions are immediately computed and displayed in the same worksheet. Users don't need to review the other worksheets at all. The output parameters and plots of deflection, moment and shear-force are generated and displayed in the blue cells of the worksheet named ***General***.

2.2 **Parametric Washout Investigation:** If one requires to run a parametric study to obtain deflection, moment and shear-force solutions for an exhaustive range of washout lengths (fully soil supported to no soil support), wash out locations and for tandem locations that produce maximum moment and maximum shear force (remember that these are not at the same tandem locations), one needs to run the VBA program embedded in the Excel file. Prior to running the VBA application, the user needs to input the geometric and material properties in the ***General*** worksheet. Note: Unlike in the "Specific Solution" case, washout parameters and tandem location are automatically varied in the VBA application to perform exhaustive parametric studies and need not be input in the ***General*** worksheet. In order to run the VBA, users need to click on the ***Developer*** tab and select the ***Visual Basic*** option on the Developer toolbar (this opens another window which should show ***User Form 1***). If this form does not

readily show up, select ***User Form 1*** by double clicking it (in the ***Project Explorer*** window on the left, or by selecting the ***Project Explorer*** icon on the toolbar). Click anywhere on the ***User Form 1*** window and click "run" (triangle icon on the toolbar similar to the play button on a CD player). This will take the user to the ***General*** worksheet with a User Form 1 window and four individually selectable rectangular buttons: Strength I Moment, Service I Moment, Strength I Shear, and Service I Shear. Click on each of these four buttons in sequence to perform the named analysis each time. Each time, after performing the necessary computations, the program will return you to the original window (wait until each set of computations are completed before executing the next button). Once all four cases (Strength I Moment, Service I Moment, Strength I Shear, and Service I Shear) have been computed, the ***Results*** worksheet summarizes solutions of maximum moment and maximum shear force for all washout lengths and locations (based on tandem locations that produce maximum moment and maximum shear in each case).

3. Each Excel file contains nine worksheets, details of which are described below:

3.1 **General:** The yellow cells indicate that user can input basic information about the BAS in these cells of the sheet, including: geometry, material properties, washout length, washout location and tandem location. The blue cells present the resultant output, which include moment, shear and displacement for both Strength I and Service I limit states of loading. This sheet also generates plots of the deflection, moment and shear-force diagrams for the specific data input.

3.2 **Preprocess:** This sheet is not intended for the user. It comprises cells for which data is automatically generated based on the input provided in ***General*** worksheet. It includes data about the loads, slab rigidity, node numbers for the finite difference model including node numbers for washout segment and tandem load locations.

3.3 **Strength:** This sheet is not intended for the user. It is used to perform background matrix calculations for the case of "Strength I Loading". The red numbers starting from "2" and going on to 40 for 20 ft. Span BAS and to 50 for 25 ft Span BAS represent the node numbers used in the finite difference model. No user input needed on this worksheet. However it is possible for user to observe the moment, shear and displacement magnitudes on the bottom right of the sheet (blue cells). The sets of numbers marked as deflection, moment and shear are values at node, which are spaced at 0.5 feet from the left (abutment) end of the BAS.

3.4 **Service:** This sheet is not intended for the user. It is used to perform background matrix calculations for the case of "Service I Loading". The red numbers starting from "2" and going on to 40 for 20 ft. Span BAS and to 50 for 25 ft Span BAS represent the node numbers used in the finite difference model. No user input needed on this worksheet. However it is possible for user to observe the moment, shear and displacement magnitudes on the bottom right of the sheet (blue cells). The sets of numbers marked as deflection, moment and shear are values at node, which are spaced at 0.5 feet from the left (abutment) end of the BAS.

3.5 **Strength Moment:** This sheet stores results generated from the VBA for Strength I run for Moment and represents exhaustive investigation of different washout lengths, locations and tandem locations. Column “c” labeled “max” is for the maximum moment (when moving the tandem along the slab to produce maximum moment).

3.6 **Strength Shear:** This sheet stores results generated from the VBA for Strength I run for Shear-force and represents exhaustive investigation of different washout lengths, locations and tandem locations. Column “c” labeled “max” is for the maximum shear-force (when moving the tandem along the slab to produce maximum shear-force).

3.7 **Service Moment:** This sheet stores results generated from the VBA for Service I run for Moment and represents exhaustive investigation of different washout lengths, locations and tandem locations. Column “c” labeled “max” is for the maximum moment (when moving the tandem along the slab to produce maximum moment).

3.8 **Service Shear:** This sheet stores results generated from the VBA for Service I run for Shear-force and represents exhaustive investigation of different washout lengths, locations and tandem locations. Column “c” labeled “max” is for the maximum shear-force (when moving the tandem along the slab to produce maximum shear-force).

3.9 **Results:** Data from the previous four worksheets (Strength Moment, Strength Shear, Service Moment and Service Shear) has been collated to report only maximum values. User can observe where to place the washout patch to obtain maximum internal forces

in the slab. The row with red font numerals with a border below each table of results presents reductions in appropriate internal forces due to consideration of elastic soil support with washout compared to the same internal force based on a simply supported (end supported with no soil support like in Standard MoDOT BAS analysis).

B	C	D	E	F
Input geometry and material properties	width	B	38	ft
	lane	n	2	
	depth	d	12	in
	concrete compressive strength	fc'	4000	psi
	soil modulus	k	30	psi/in
Input tandem location and washout paramaters (THIS INPUT BOX NOT NECESSARY FOR PARAMETRIC INVESTIGATION)	dem load location (center to left e	a	7.5	ft
	washout length	L	0	ft
	out location (start point to left	b	0	ft
output (per 12" strip)	imum Factored Moment (strength lim	M	243.2	kip-in
	Maximum Factored Shear (strength limi	V	50.9	kips
	Maximum Deflection (strength limit)	w	0.219	in
	Maximum Factored Moment (service limi	M	145.0	kip-in
	Maximum Factored Shear (service limi	V	29.6	kips
	Maximum Deflection (service limit)	w	0.136	in

Figure C-1 Input and Output Interface of BAS-ES washout solutions

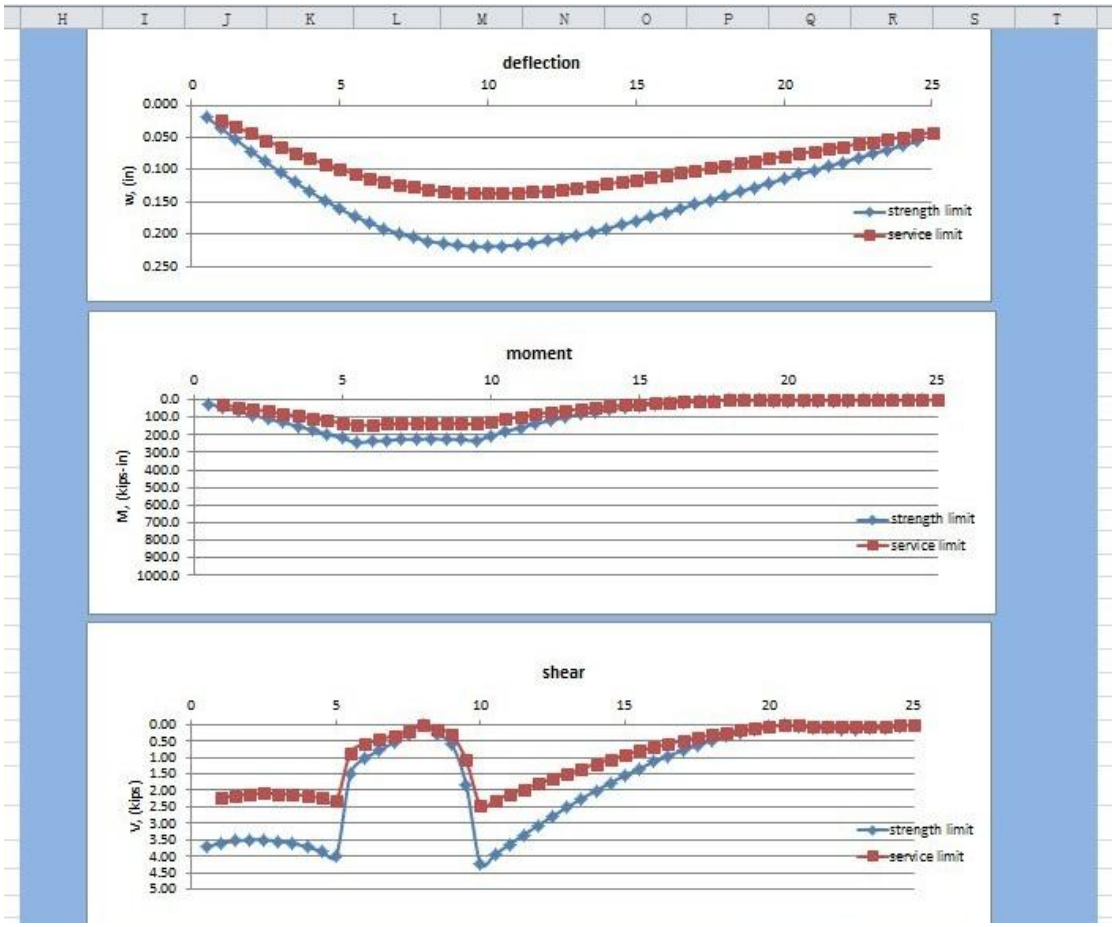

Figure C-2 Display of deflection and inner forces diagram of BAS-ES washout solutions

APPENDIX D. DETAILED DERIVATION PROCEDURE OF FINITE DIFFERENCE OPERATORS FOR BIAXIAL MODEL

1. Simple Supported:

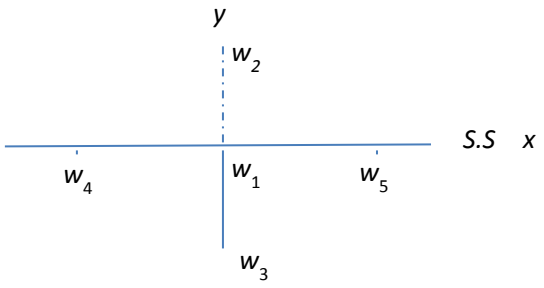

Node 1:

$$M_y = -D\left(\frac{\partial^2 w}{\partial y^2} + \gamma \frac{\partial^2 w}{\partial x^2}\right) = 0$$

$$\because w_4 = w_1 = w_5 = 0$$

$$\therefore \frac{\partial^2 w}{\partial y^2} = \frac{1}{h^2}(w_2 + w_3 - 2w_1) = 0$$

$$\therefore w_2 = -w_3$$

Finite Difference Operators:

1) nodes at inner part

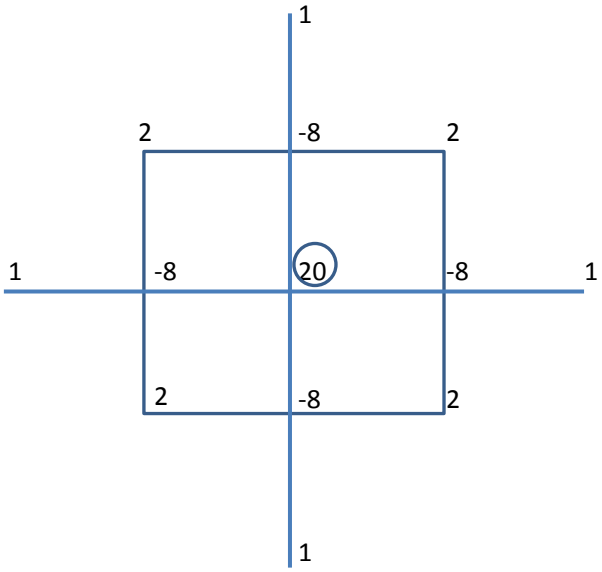

2) nodes near support-supported end

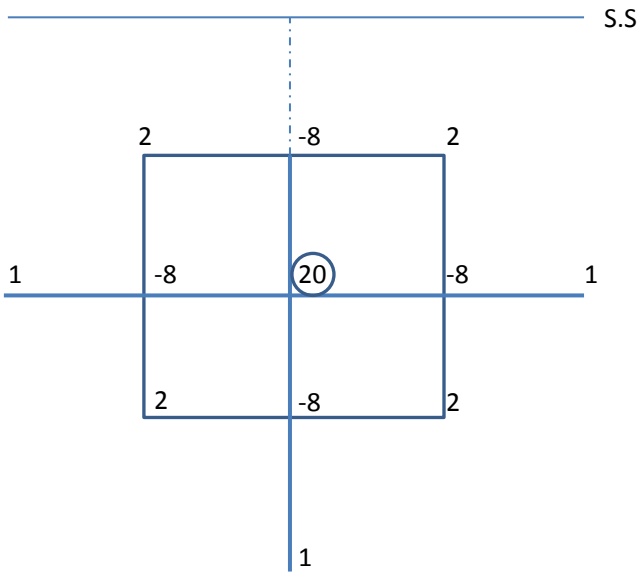

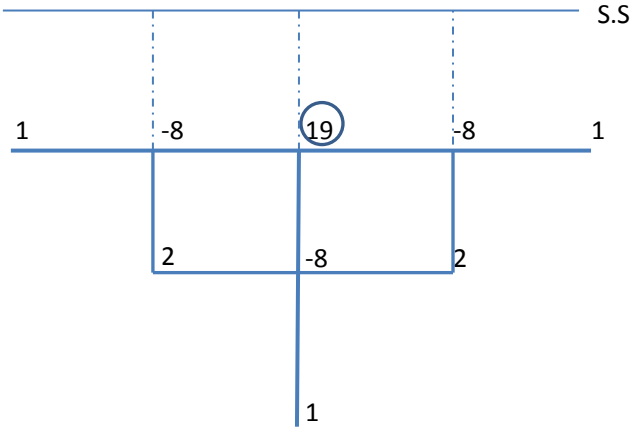

2. Free Edge:

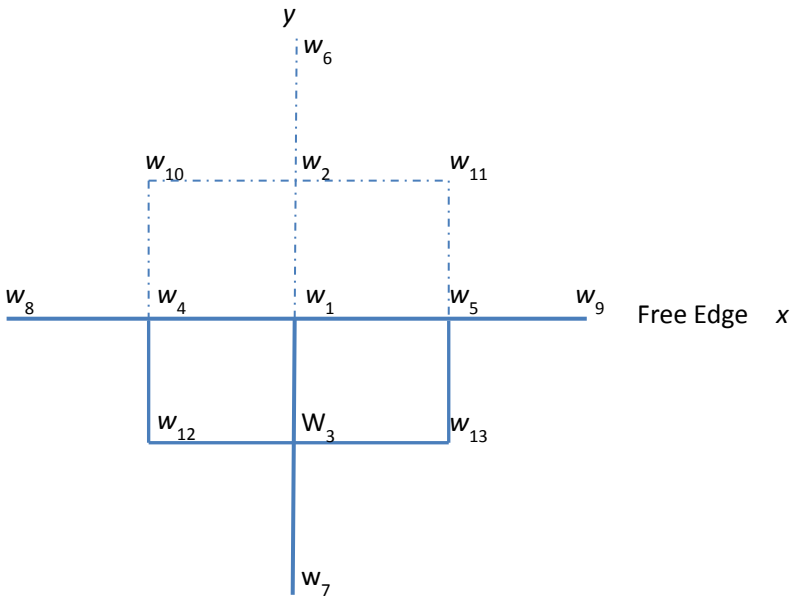

Node 1:

$$M_y = -D\left(\frac{\partial^2 w}{\partial y^2} + \gamma \frac{\partial^2 w}{\partial x^2}\right) = 0$$

$$\therefore \frac{1}{h^2}(w_2 + w_3 - 2w_1) + 0.2\frac{1}{h^2}(w_4 + w_5 - 2w_1) = 0$$

$$get,\ \ w_2 = 2.4w_1 - 0.2w_4 - 0.2w_5 - w_3$$

$$similarly,\ \ w_{10} = 2.4w_4 - 0.2w_1 - 0.2w_8 - w_{12}$$

$$w_{11} = 2.4w_5 - 0.2w_1 - 0.2w_9 - w_{13}$$

$$Q_y = -D\left(\frac{\partial^3 w}{\partial y^3} + \frac{\partial^3 w}{\partial x^2 \partial y}\right) = 0$$

$$\because \frac{\partial^3 w}{\partial y^3} = \frac{1}{2h^3}(w_6 - 2w_2 + 2w_3 - w_7)$$

$$\frac{\partial^3 w}{\partial x^2 \partial y} = \frac{1}{2h}(w_{xx,2} - w_{xx,3}) = \frac{1}{2h^3}((w_{10} + w_{11} - 2w_2) - (w_{12} + w_{13} - 2w_3))$$

$$\therefore w_6 - 4w_2 + 4w_3 - w_7 + w_{10} + w_{11} - w_{12} - w_{13} = 0$$

$$w_6 = 4w_2 - 4w_3 + w_7 - w_{10} - w_{11} + w_{12} + w_{13}$$

$$= 4\ (2.4w_1 - 0.2w_4 - 0.2w_5 - w_3) - 4w_3 + w_7 + w_{12} + w_{13}$$

$$-(2.4w_4 - 0.2w_1 - 0.2w_8 - w_{12}) - (2.4w_5 - 0.2w_1 - 0.2w_9 - w_{13})$$

$$\therefore w_6 = 10w_1 - 8w_3 - 3.2w_4 - 3.2w_5 + w_7 + 0.2w_8 + 0.2w_9 + 2w_{12} + 2w_{13}$$

Finite Difference Operators:

1) nodes near free edge end

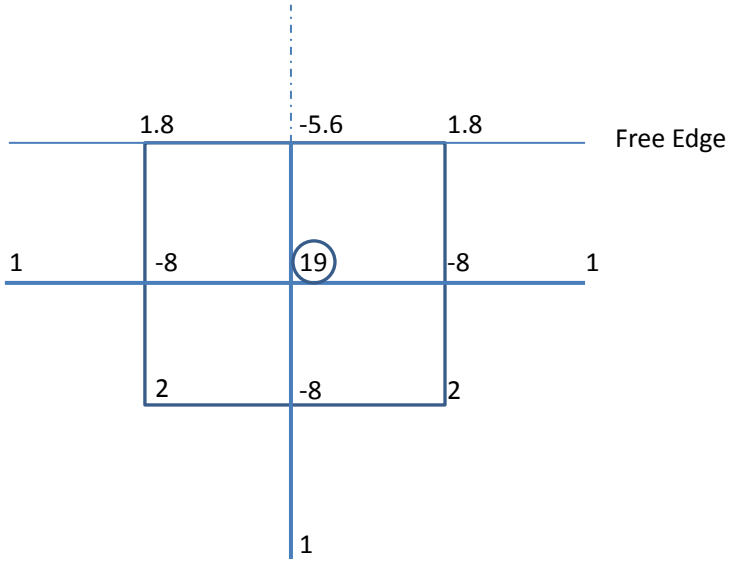

$$-5.6 = -8 + 2.4 * 1$$
$$1.8 = 2 + (-0.2) * 1$$
$$1.8 = 2 + (-0.2) * 1$$
$$19 = 20 - 1 * 1$$

2) nodes on free edge end

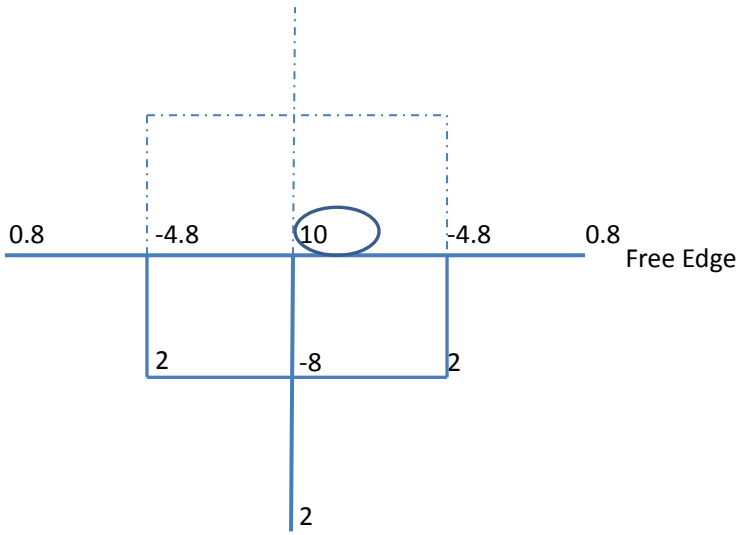

$$10 = 20 + (10)*1 + 2.4*(-8) + (-0.2)*2 + (-0.2)*2$$
$$-4.8 = -8 + (-3.2)*1 + (-0.2)*(-8) + 2.4*2 + 0*2$$
$$0.8 = 1 + (0.2)*1 + 0*(-8) + (-0.2)*2 + 0*2$$
$$2 = 2 + (2)*1 + 0*(-8) + (-1)*2 + 0*2$$
$$-8 = -8 + (-8)*1 + (-1)*(-8) + 0*2 + 0*2$$
$$2 = 1 + 1*1 + 0*(-8) + 0*2 + 0*2$$

3. Combined Boundaries:

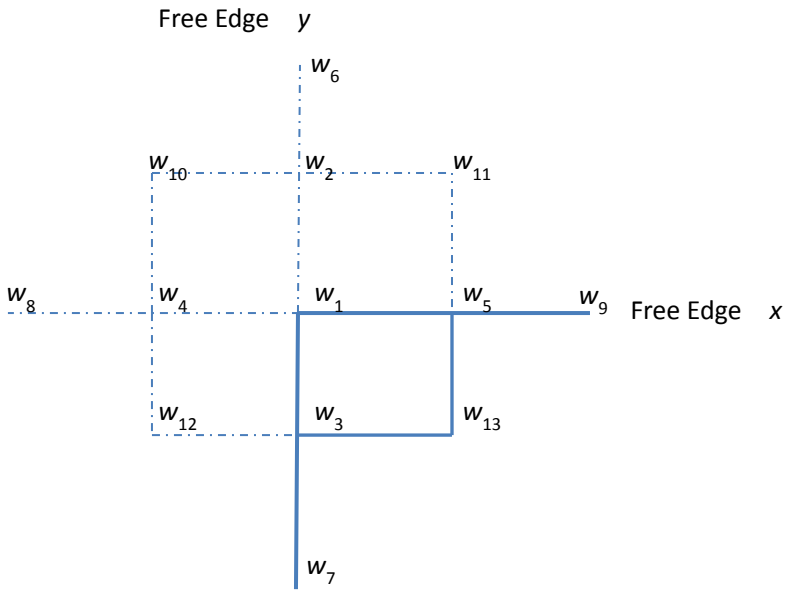

Known, $w_2 = 2.4w_1 - 0.2w_4 - 0.2w_5 - w_3 \ (i)$

$w_4 = 2.4w_1 - 0.2w_2 - 0.2w_3 - w_5 \ (ii)$

$(i) + (ii) \times 5,\ 4.8w_4 = 9.6w_1 - 4.8w_5, therefore\ w_4 = 2w_1 - w_5$

Also known,

$w_6 = 10w_1 - 8w_3 - 3.2w_4 - 3.2w_5 + w_7 + 0.2w_8 + 0.2w_9 + 2w_{12} + 2w_{13} (iii)$

similarly,

$$w_8 = 10w_1 - 8w_5 - 3.2w_2 - 3.2w_3 + w_9 + 0.2w_6 + 0.2w_7 + 2w_{11} + 2w_{13} \quad (iv)$$

$(iii) + (iv) \times 5,$

$$4.8w_8 = 60w_1 - 16w_2 - 24w_3 - 3.2w_4 - 43.2w_5 + 2w_7 + 5.2w_9 + 10w_{11} + 2w_{12} + 12w_{13}$$

$$= 60w_1 - 24w_3 - 43.2w_5 + 2w_7 + 5.2w_9 + 12w_{13} - 16\ (2w_1 - w_3)$$

$$-3.2\ (2w_1 - w_5) + 10\ (2.4w_5 - 0.2w_1 - 0.2w_9 - w_{13}) + 2\ (2.4w_3 - 0.2w_1 - 0.2w_7 - w_{13})$$

$$\therefore 4.8w_8 = 19.2w_1 - 3.2w_3 - 16w_5 + 1.6w_7 + 3.2w_9$$

$$w_8 = 4w_1 - 2/3w_3 - 10/3w_5 + 1/3w_7 + 2/3w_9$$

Use the boundary condition of corner nodes, that is twisting moment is zero.

$$\because M_{xy} = D(1-\nu)\frac{\partial^2 w}{\partial x \partial y} = 0$$

$$\therefore \frac{\partial^2 w}{\partial x \partial y} = 4w_1 - 2w_2 - 2w_3 - 2w_4 - 2w_5 + w_{10} + w_{11} + w_{12} + w_{13} = 0$$

So the expression of fourth derivative of displacement can be simplified as

$$\nabla^2(\nabla^2 w) = 12w_1 - 4w_2 - 4w_3 - 4w_4 - 4w_5 + w_6 + w_7 + w_8 + w_9$$

1) corner nodes: nodes on two free edges

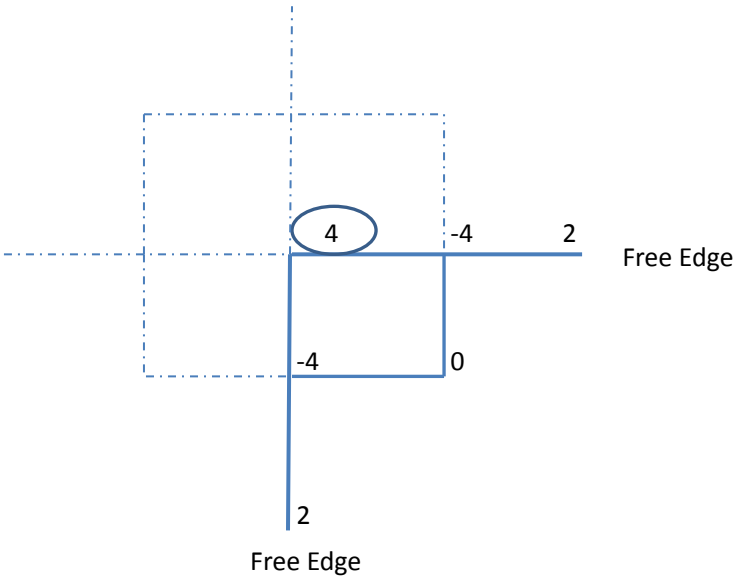

$$4 = 12 + 1*4 + 1*4 + (-4)*2 + (-4)*2$$

$$-4 = -4 + 1*(-2/3) + 1*(-10/3) + (-4)*(-1) + (-4)*0$$

$$2 = 1 + 1*(2/3) + 1*(1/3) + (-4)*0 + (-4)*0$$

APPENDIX E. DETAILED CASE STUDIES OF BIAXIAL MODELING

1. k=10psi/in, symmetric loading, tandem location 12.5ft from abutment, 5 ft wide strip washout from abutment, non-yielding pavement end support.

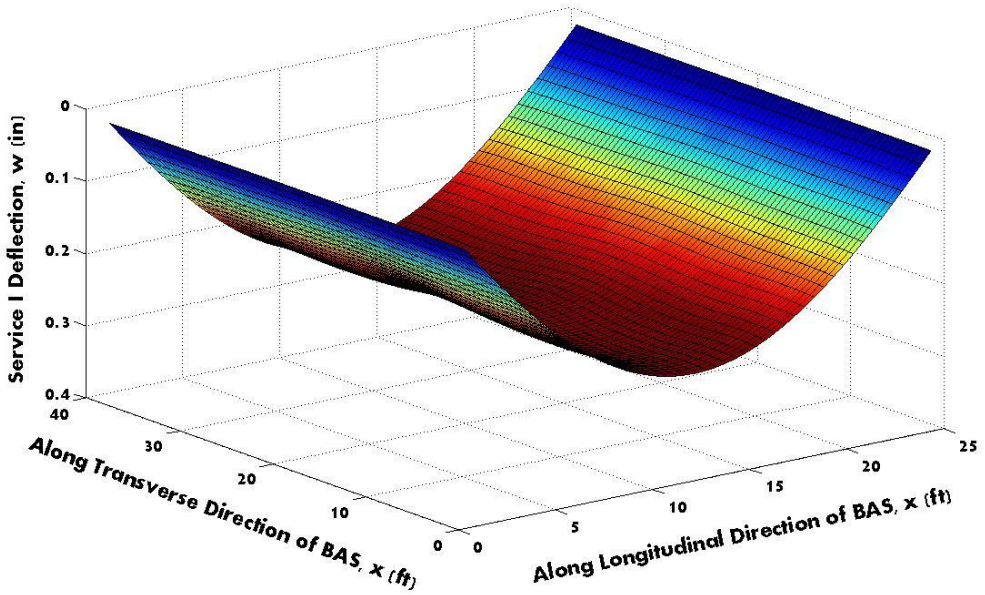

Figure E-1 Service I deflection (w) response for Case 1

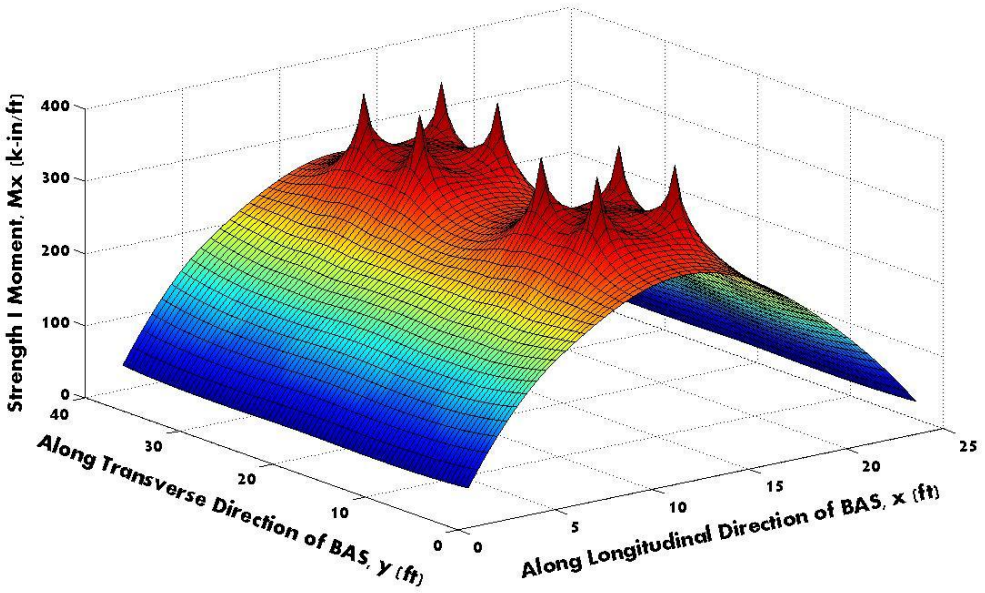

Figure E-2 Strength I moment (M_x) diagram for Case 1

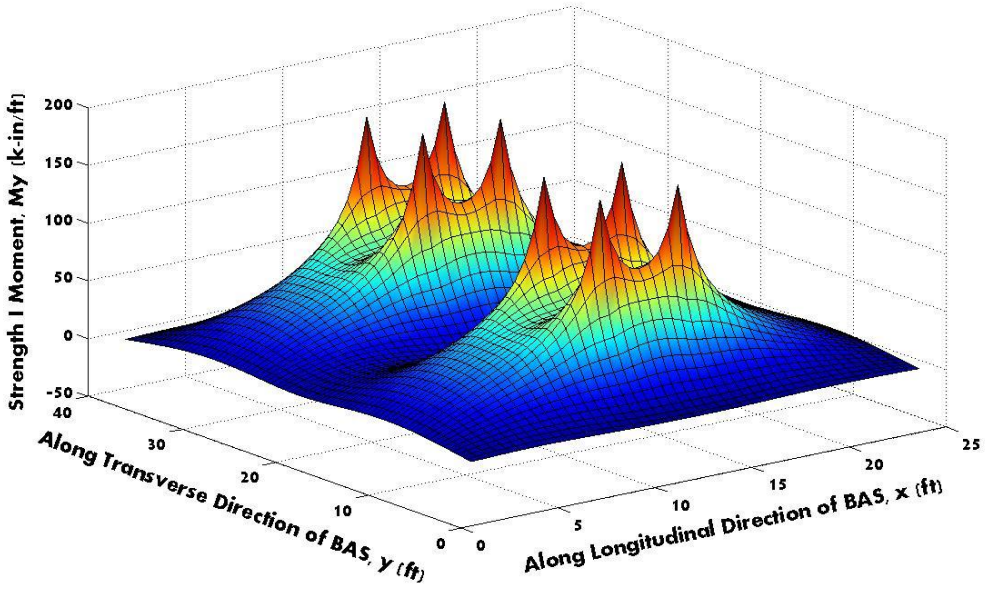

Figure E-3 Strength I moment (M_y) diagram for Case 1

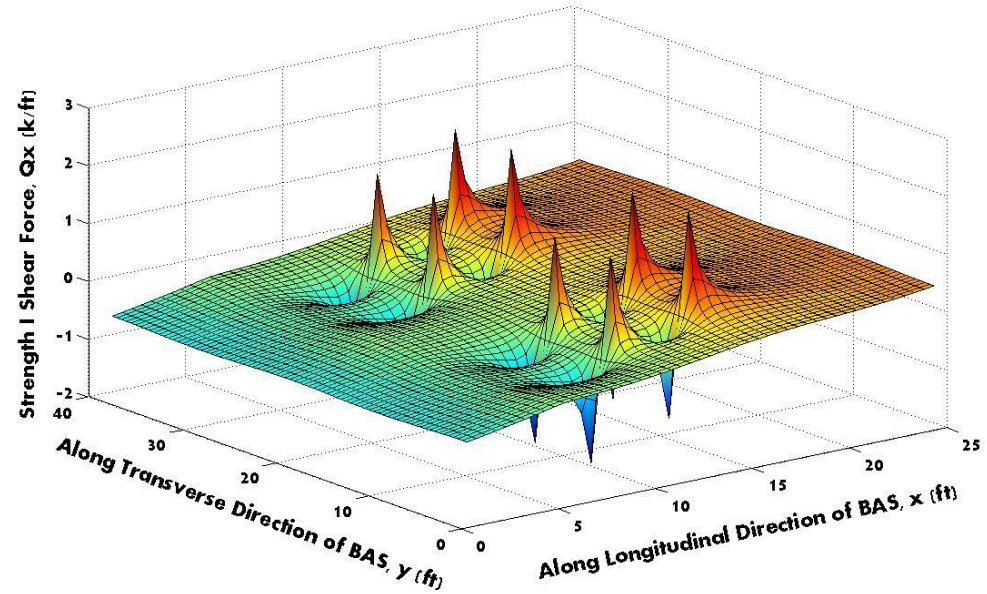

Figure E-4 Strength I shear force (Q_x) diagram for Case 1

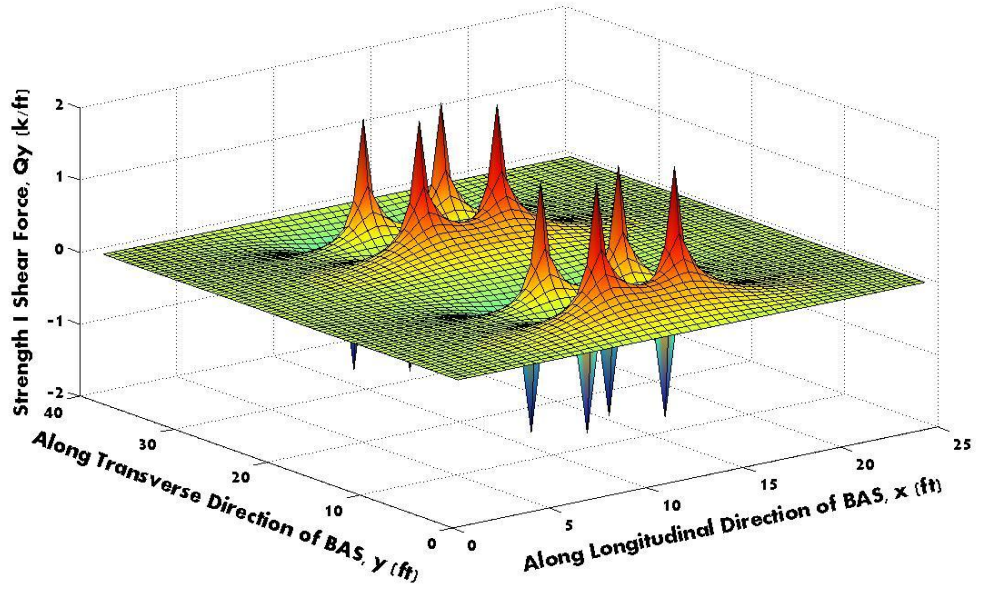

Figure E-5 Strength I shear force (Q_y) diagram for Case 1

2. k=10psi/in, unsymmetrical loading, 5 ft strip washout, tandem location 12.5 ft from abutment, yielding pavement end support.

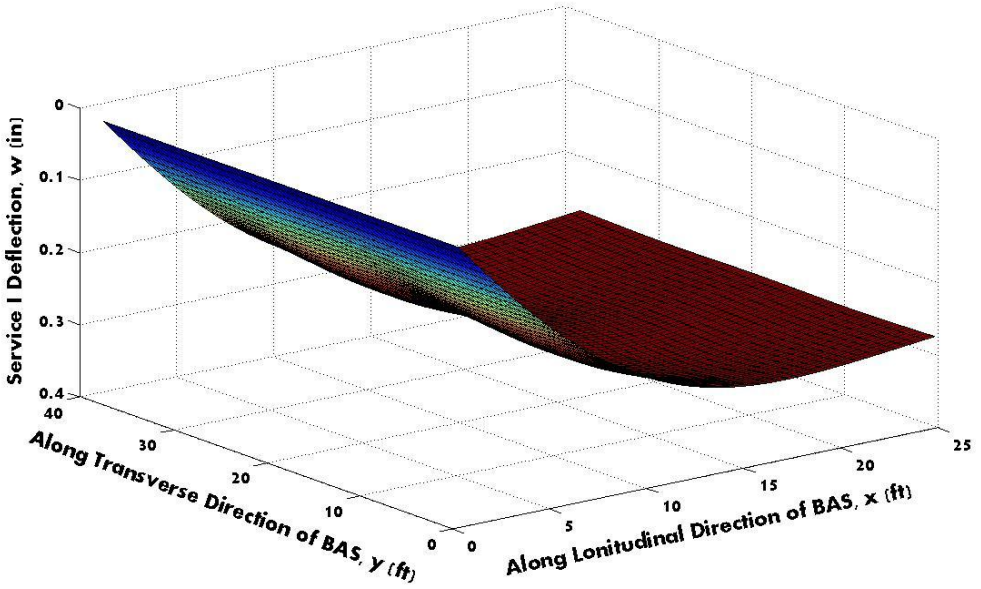

Figure E-6 Service I deflection (w) response for Case 2

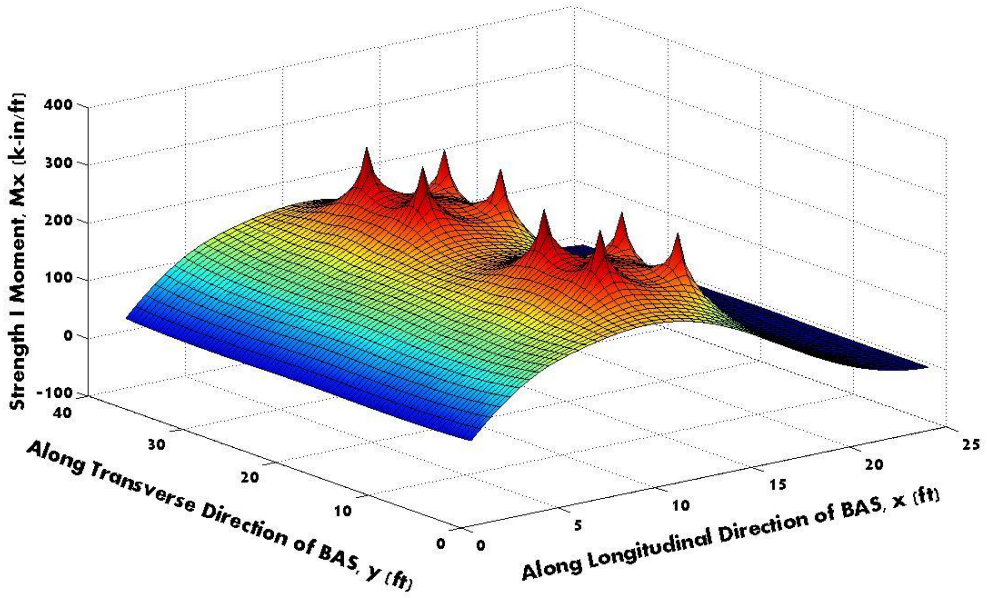

Figure E-7 Strength I moment (M_x) diagram for Case 2

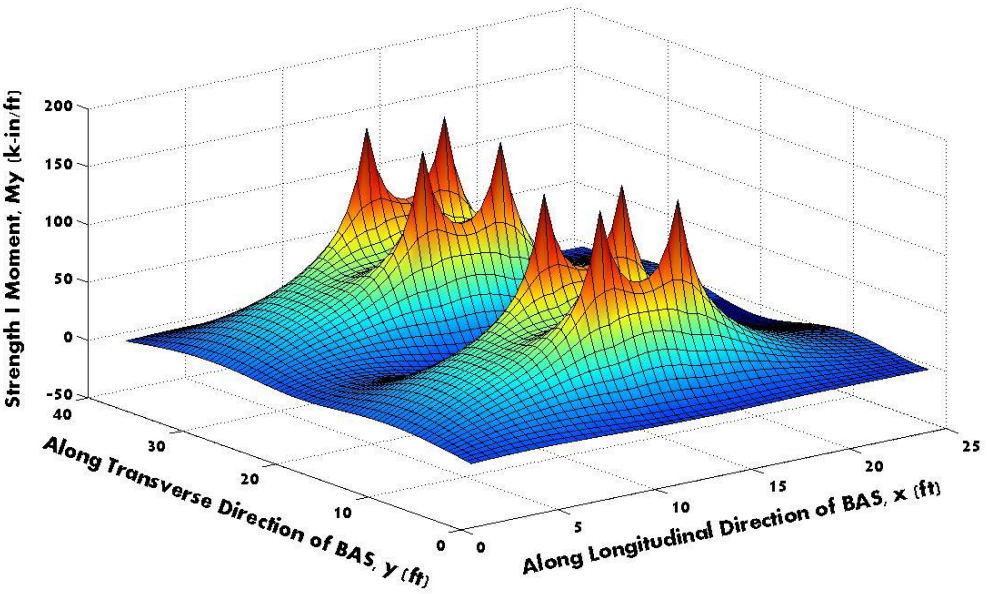

Figure E-8 Strength I moment (M_y) diagram for Case 2

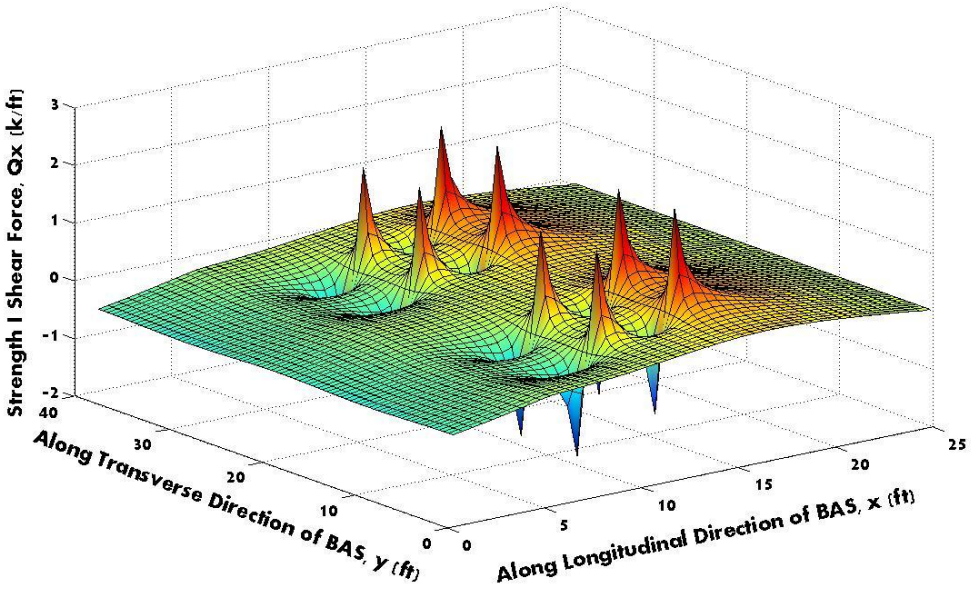

Figure E-9 Strength I shear force (Q_x) diagram for Case 2

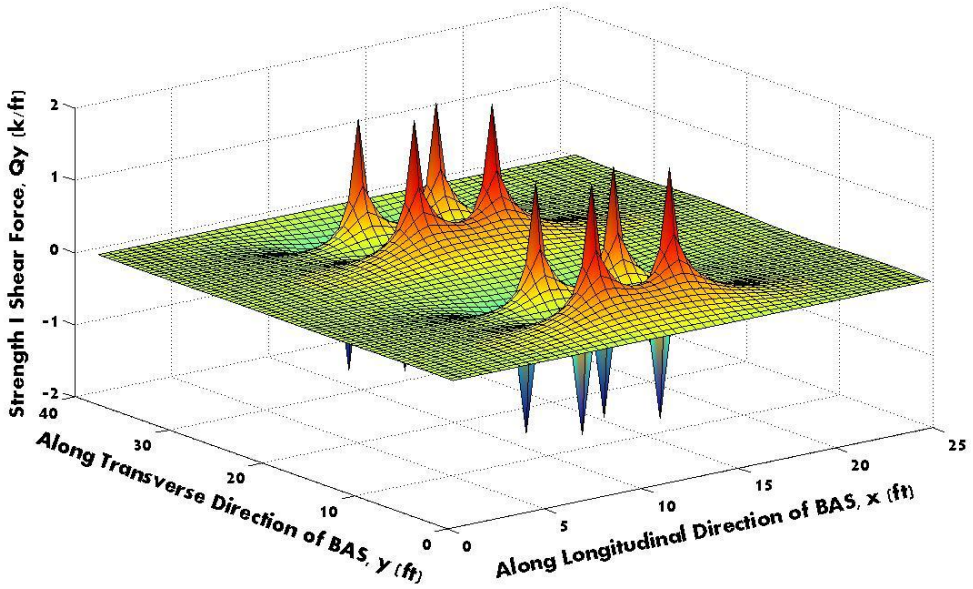

Figure E-10 Strength I shear force (Q_y) diagram for Case 2

3. k=10psi/in, asymmetric loading, 5 ft strip washout from abutment, tandem location 8 ft and 15 ft from abutment, nonyielding pavement end support.

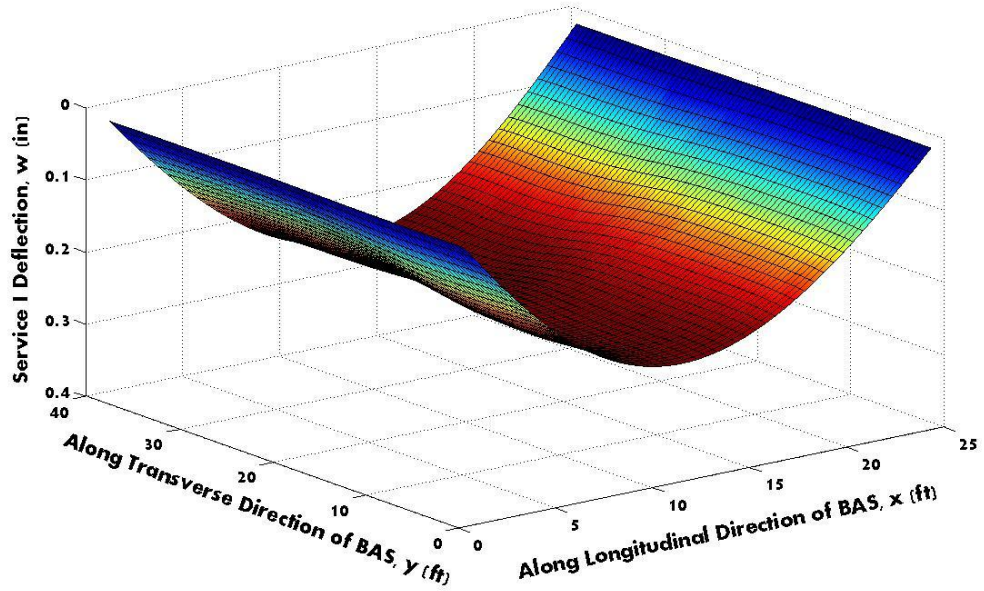

Figure E-11 Service I deflection (w) response for Case 3

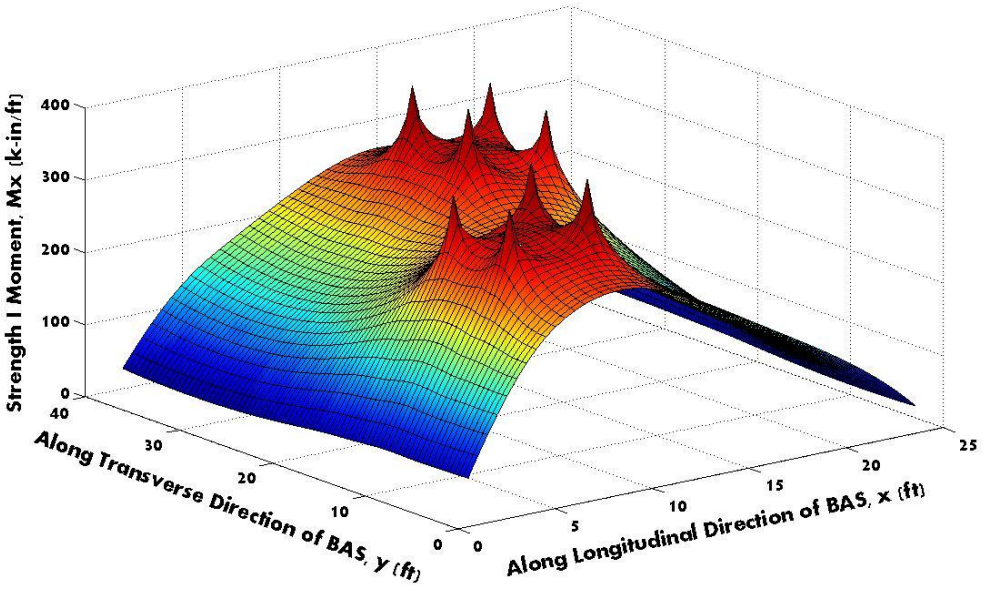

Figure E-12 Strength I moment (M_x) diagram for Case 3

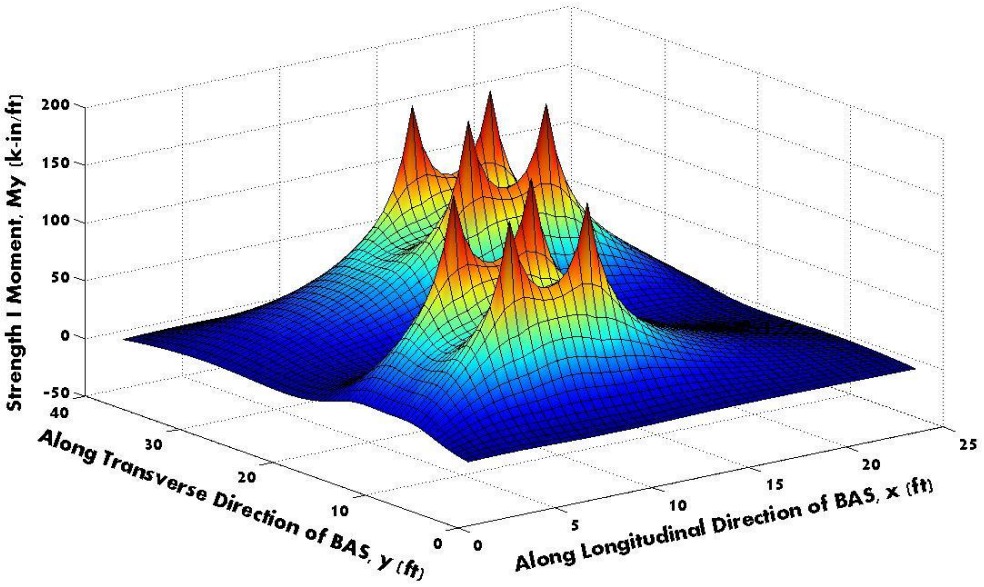

Figure E-13 Strength I moment (M_y) diagram for Case 3

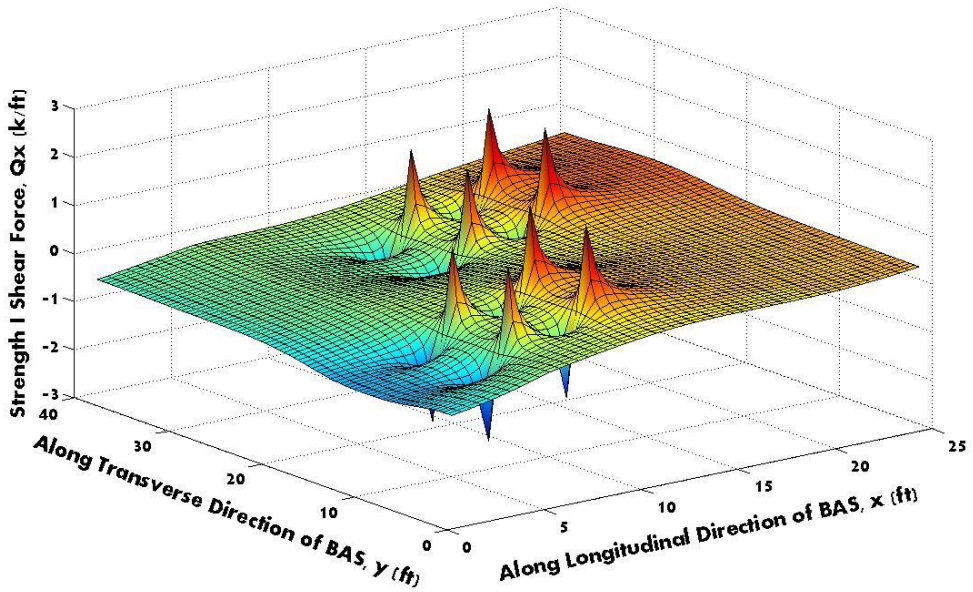

Figure E-14 Strength I shear force (Q_x) diagram for Case 3

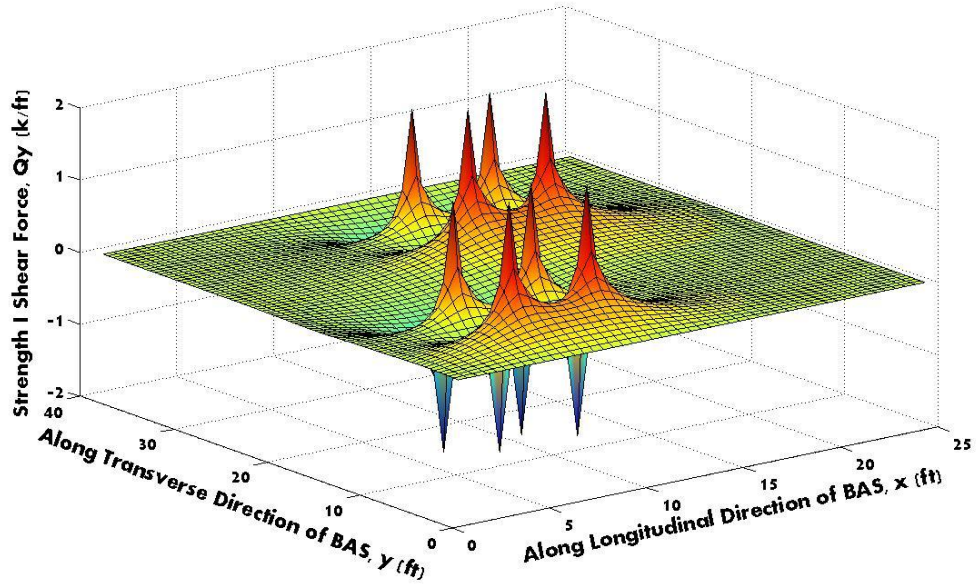

Figure E-15 Strength I shear force (Q_y) diagram for Case 3

4. k=10psi/in, symmetric loading, 15 ft circle washout (x=8 ft, y=8 ft), tandem location 12.5 ft from abutment, yielding pavement end support.

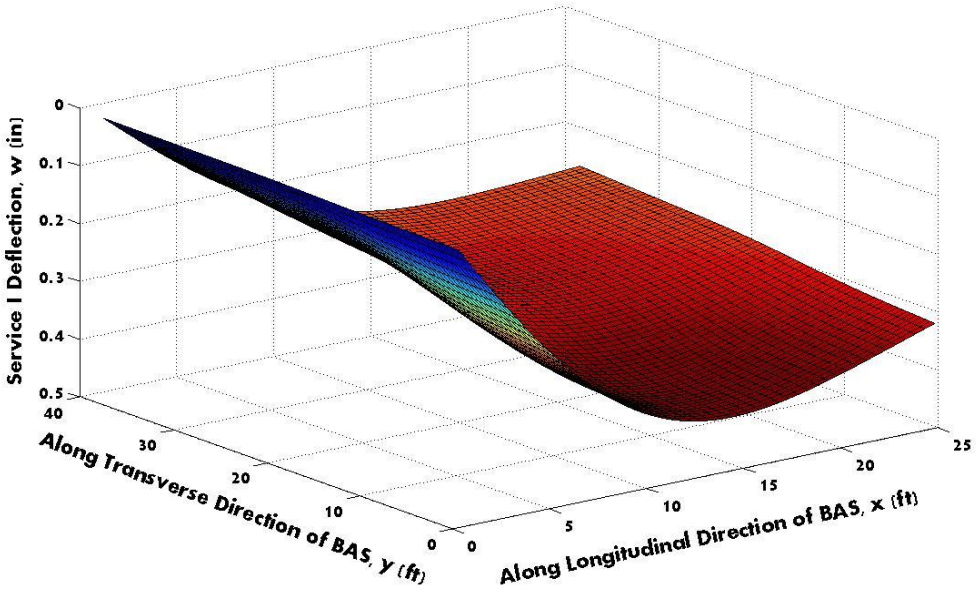

Figure E-16 Service I deflection (w) response for Case 4

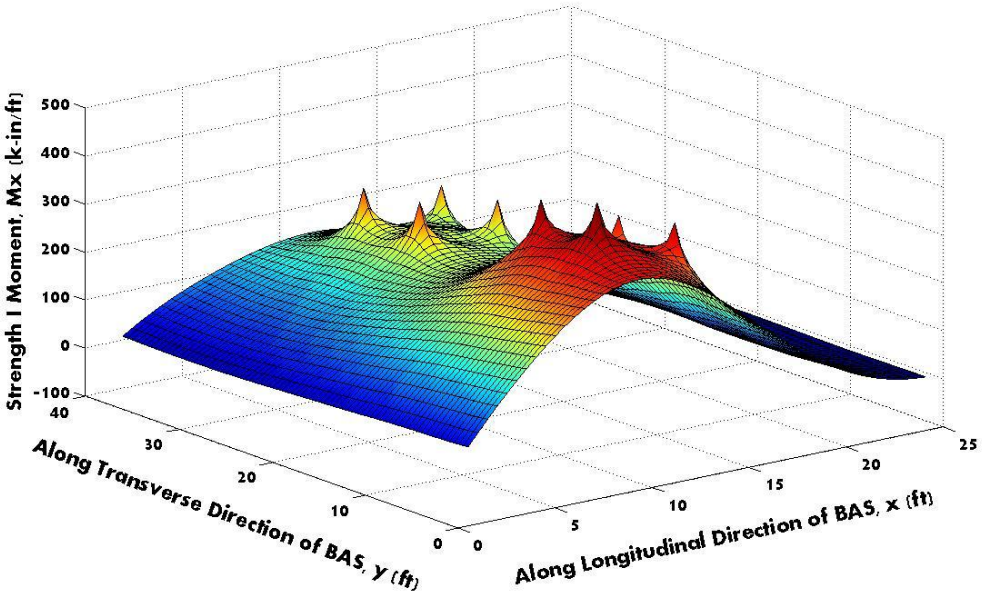

Figure E-17 Strength I moment (M_x) diagram for Case 4

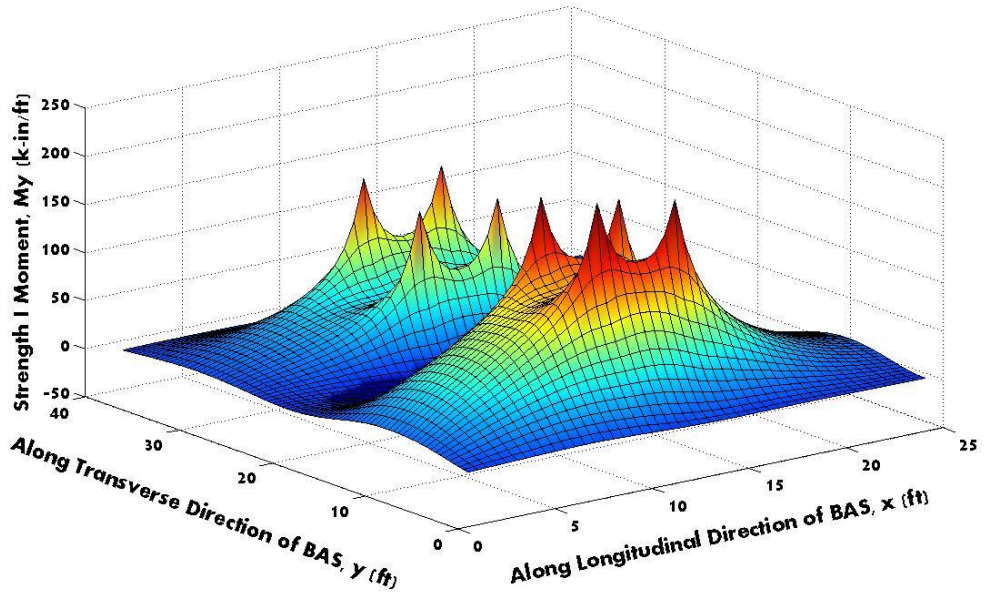

Figure E-18 Strength I moment (M_y) diagram for Case 4

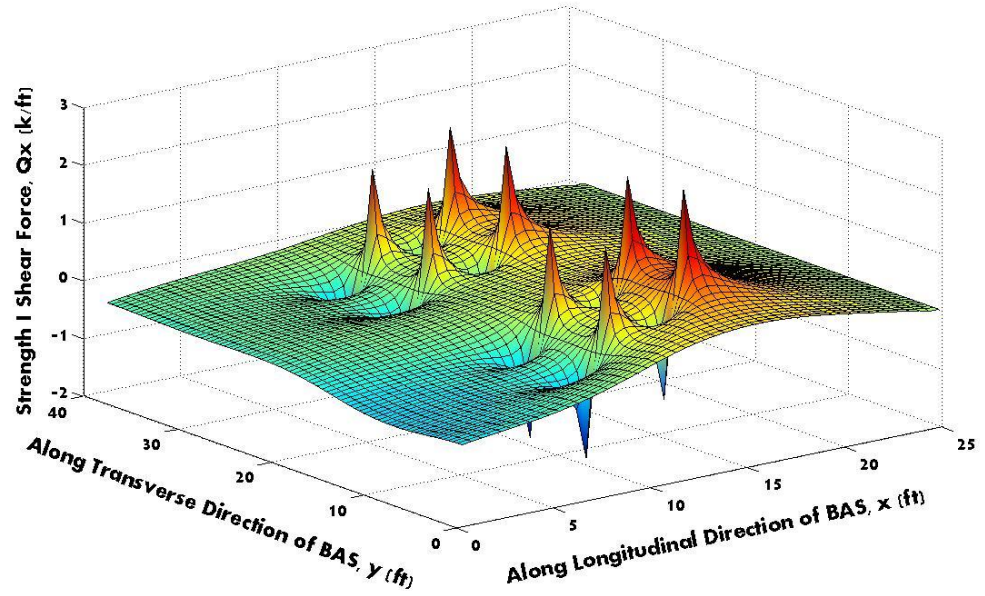

Figure E-19 Strength I shear force (Q_x) diagram for Case 4

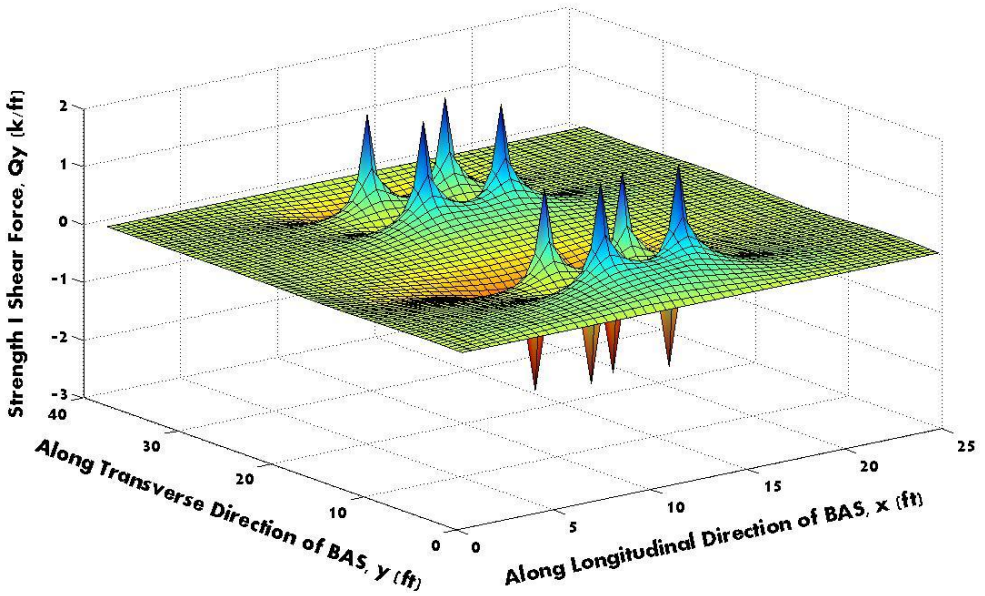

Figure E-20 Strength I shear force (Q_y) diagram for Case 4

5. k=10psi/in, symmetric loading, 15 ft circle washout (x=8 ft, y=19 ft), tandem location 12.5 ft from abutment, yielding pavement end support.

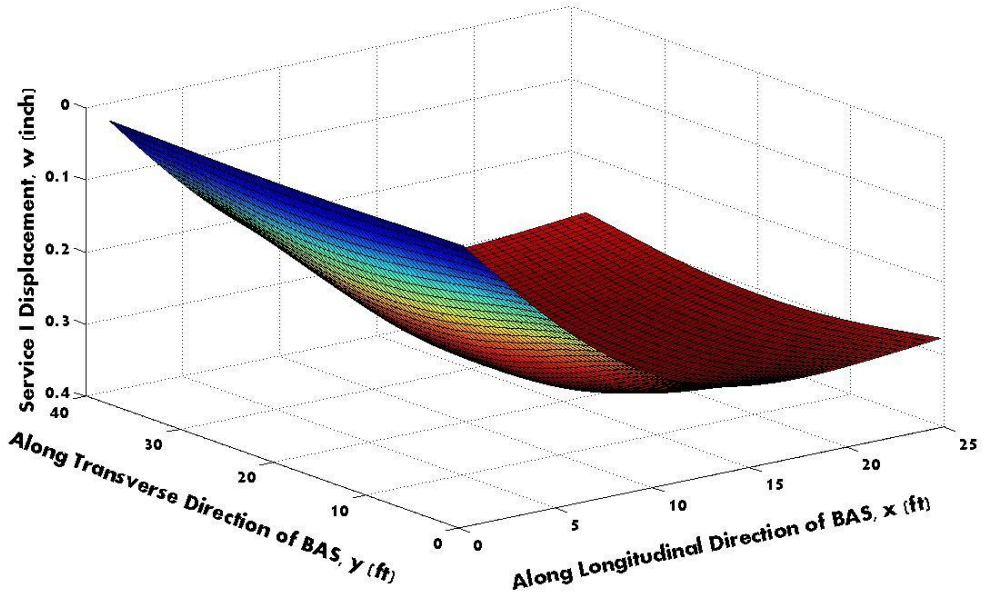

Figure E-21 Service I deflection (w) response for Case 5

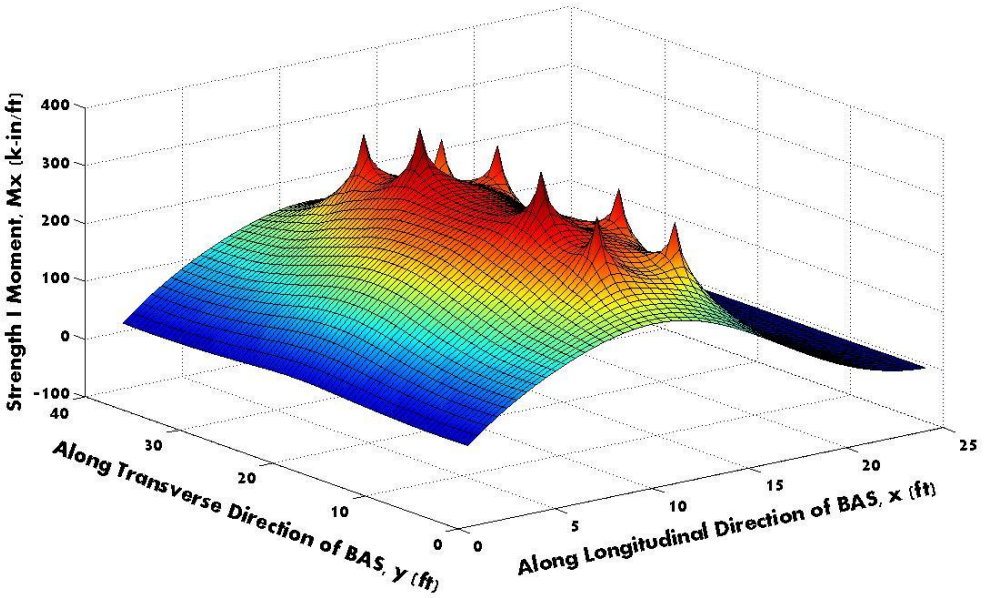

Figure E-22 Strength I moment (M_x) diagram for Case 5

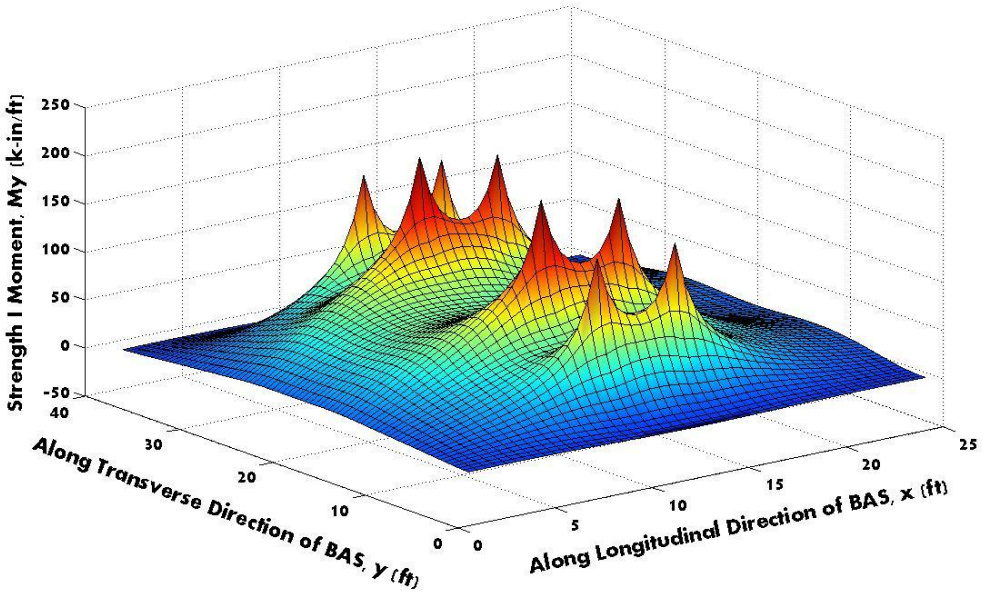

Figure E-23 Strength I moment (M_y) diagram for Case 5

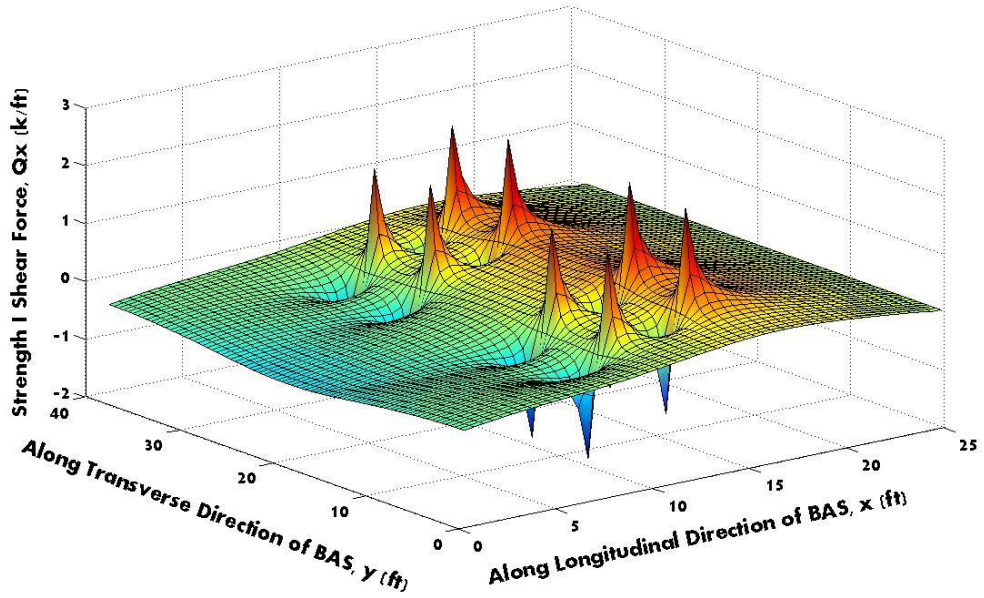

Figure E-24 Strength I shear force (Q_x) diagram for Case 5

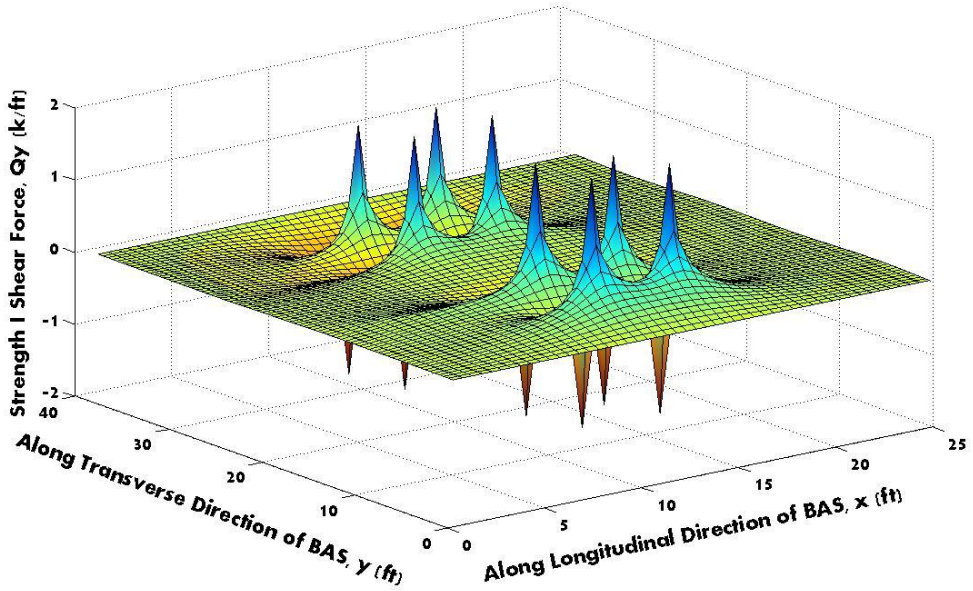

Figure E-25 Strength I shear force (Q_y) diagram for Case 5

6. k=10psi/in, symmetric loading, 15 ft circle washout (x=12.5 ft, y=19 ft), tandem location 12.5 ft from abutment, yielding pavement end support.

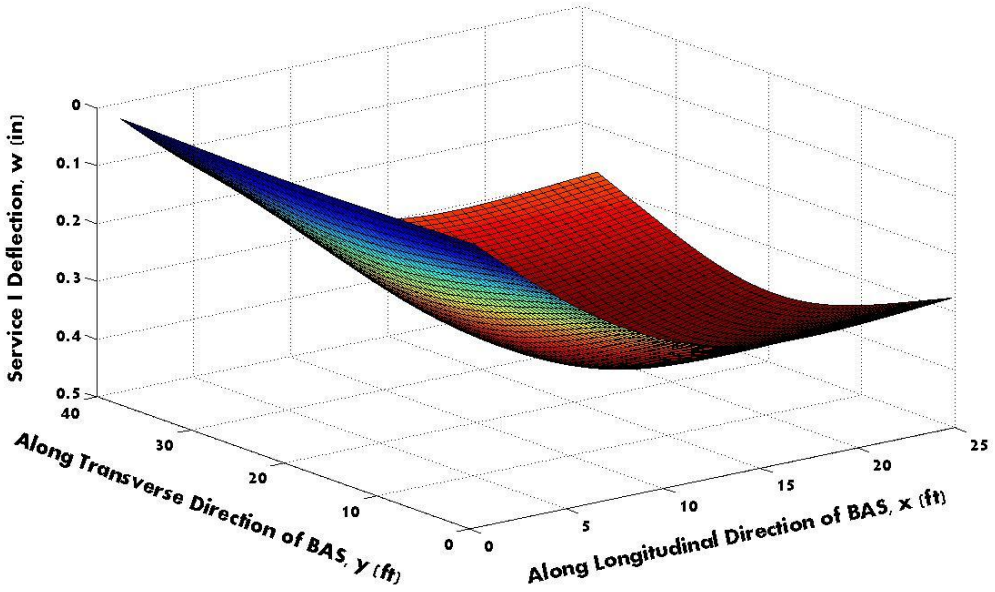

Figure E-26 Service I deflection (w) response for Case 6

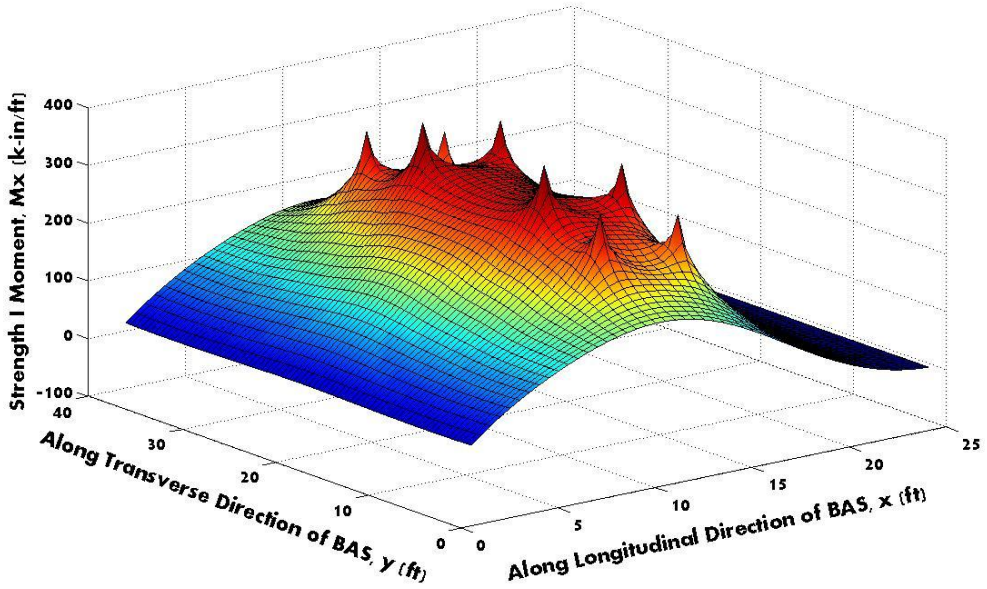

Figure E-27 Strength I moment (M_x) diagram for Case 6

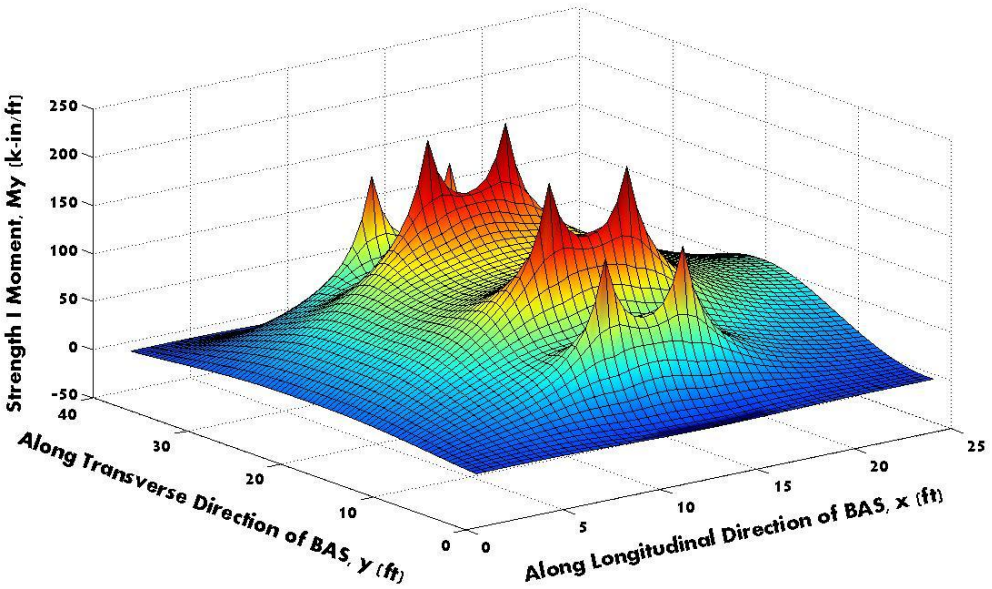

Figure E-28 Strength I moment (M_y) diagram for Case 6

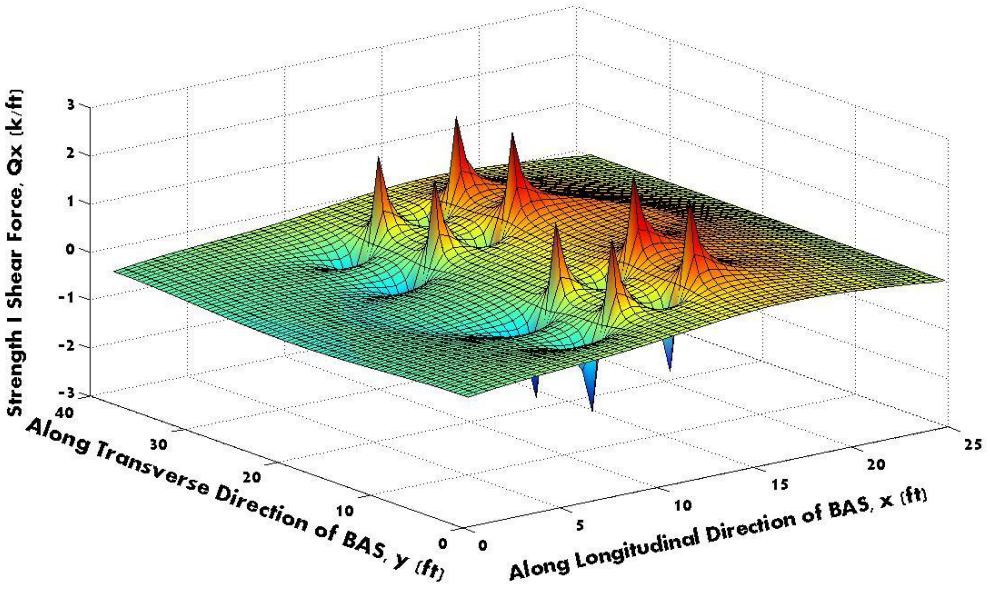

Figure E-29 Strength I shear force (Q_x) diagram for Case 6

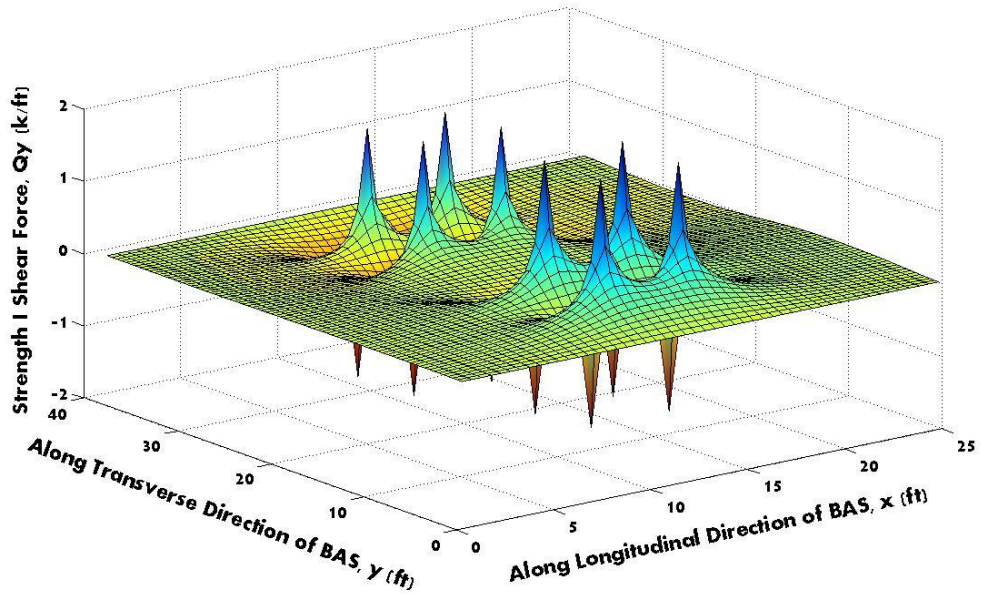

Figure E-30 Strength I shear force (Q_y) diagram for Case 6